Journal of Materials Chemistry A

ROYAL SOCIETY OF CHEMISTRY

REVIEW

View Article Online
View Journal | View Issue

Cite this: J. Mater. Chem. A, 2026, 14, 20009

Toward unified interphase engineering: the solid-electrolyte interphase in batteries and supercapacitors

Mehedi Hasan, *[a] Ishtiaq Murshed,[b] Khayrul Islam *[c] and A. K. M. Masud[d]

The development of next-generation electrochemical energy storage requires devices that synergistically combine the high energy density of batteries with the exceptional power capability and cycle life of supercapacitors, yet fundamental understanding of the interfacial phenomena governing performance across these platforms remains fragmented. While the solid-electrolyte interphase (SEI), a nanometer-scale passivation layer formed by electrolyte decomposition, has been extensively characterized in battery systems, analogous interfacial films in supercapacitors have received limited systematic investigation despite mounting experimental evidence for their existence and functional significance. This review advances the thesis that SEI formation constitutes a general electrochemical phenomenon arising whenever applied potentials drive electrode Fermi levels into electrolyte molecular orbitals beyond thermodynamic stability limits, independent of whether charge storage proceeds *via* faradaic redox or non-faradaic electrostatic mechanisms. Distinctions between battery SEIs (10–100 nm thickness, quasi-static evolution) and supercapacitor interphases (1–10 nm, dynamic reconstruction) reflect operational boundary conditions (potential range, cycling frequency, and ion flux) rather than fundamental mechanistic divergence. Quantitative analysis across reported studies indicates that interphase ionic resistivity (or fitted R_{SEI}) generally increases as the interphase becomes more inorganic-rich (*e.g.*, LiF/Li_2CO_3-dominated), although the reported ranges depend strongly on morphology/porosity, thickness, and the EIS fitting model and protocol Critically, rationally engineered interphases achieved through electrolyte additive optimization, atomic-layer-deposited protective coatings, or electrode surface functionalization substantially suppress parasitic leakage currents, maintain capacitance retention above 95% through tens of thousands of cycles, and enable stable operation exceeding 3.0 V in organic and ionic-liquid electrolytes. By establishing shared mechanistic principles and facilitating systematic knowledge transfer between battery and supercapacitor research communities, this unified framework enables predictive interphase engineering strategies that deliver battery-level energy density, capacitor-level power capability, and ultralong operational lifetimes for electrified transportation, renewable grid integration, and sustainable infrastructure.

Received 19th December 2025
Accepted 18th March 2026

DOI: 10.1039/d5ta10361d

rsc.li/materials-a

1 Introduction

The accelerating global transition toward electrification and renewable energy integration has driven the relentless pursuit of advanced electrochemical energy-storage technologies.[1–3] From smartphones and laptops to electric vehicles and grid-scale buffering, the demand for reliable, efficient, and sustainable energy-storage devices continues to rise.[4,5] At the core of this technological revolution lie two complementary families of systems: rechargeable batteries and supercapacitors, each occupying a distinct yet overlapping domain of the energy–power landscape.[6,7] Batteries, exemplified by lithium-ion and sodium-ion chemistries, deliver high energy density (100–300 Wh kg^{-1}) through bulk faradaic redox reactions, while supercapacitors, or electrochemical capacitors, provide rapid charge–discharge capability (up to 10 kW kg^{-1}) and ultralong cycle life (exceeding 10^6 cycles) through surface-controlled charge accumulation.[8–10] The synergistic coexistence of these devices forms the backbone of modern electrochemical energy storage, and the quest to merge their advantages has sparked immense scientific and industrial interest (Fig. 1 and 2).[11,12]

The concept of an interfacial passivation layer in electrochemical systems dates back to the pioneering work of Emanuel

[a]Department of Industrial and Production Engineering, Bangladesh University of Engineering and Technology, Dhaka–1000, Bangladesh. E-mail: mehedihasanbuet29@gmail.com

[b]Department of Chemical Engineering, Bangladesh University of Engineering and Technology, Dhaka–1000, Bangladesh

[c]Computational Engineering Department, Lawrence Livermore National Laboratory, Livermore, CA 94550, USA

[d]Department of Industrial and Production Engineering, Bangladesh University of Engineering and Technology, Dhaka, Bangladesh

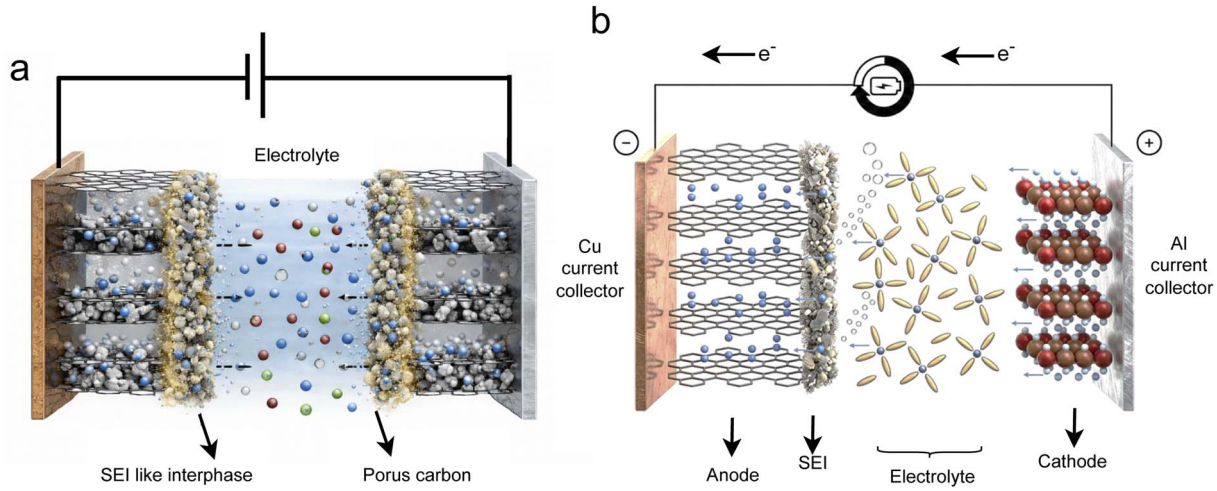

Fig. 1 Graphical abstract illustrating the unified interphase engineering framework bridging (a) super capacitors and (b) batteries.

Peled in 1979, who first described the solid-electrolyte interphase (SEI) on alkali-metal electrodes.[13] Peled observed that a spontaneously formed, nanometer-scale film (composed of electrolyte decomposition products) electronically insulates the electrode while permitting selective ion transport, thereby preventing continuous electrolyte breakdown.[14] This discovery revolutionized battery science, establishing the SEI as an indispensable component governing cycle life, coulombic efficiency, and safety in lithium-ion, sodium-ion, and lithium–metal batteries.[15–17]

Over the ensuing decades, intensive research effort has been directed toward elucidating SEI formation mechanisms, chemical composition, morphology, and dynamic evolution in rechargeable batteries.[18–20] Techniques such as X-ray photoelectron spectroscopy (XPS), cryogenic transmission electron microscopy (cryo-TEM), and *operando* electrochemical quartz-crystal microbalance (EQCM) have revealed that battery SEIs are typically 10–100 nm thick, composed of inorganic salts (*e.g.*, LiF, Li_2CO_3, Li_2O) in the inner region and polymeric organic species (*e.g.*, polycarbonates, alkoxides) toward the outer surface.[21–23] These layers evolve slowly over thousands of cycles and must endure significant mechanical stress due to volumetric changes in active materials during lithiation/delithiation.[24]

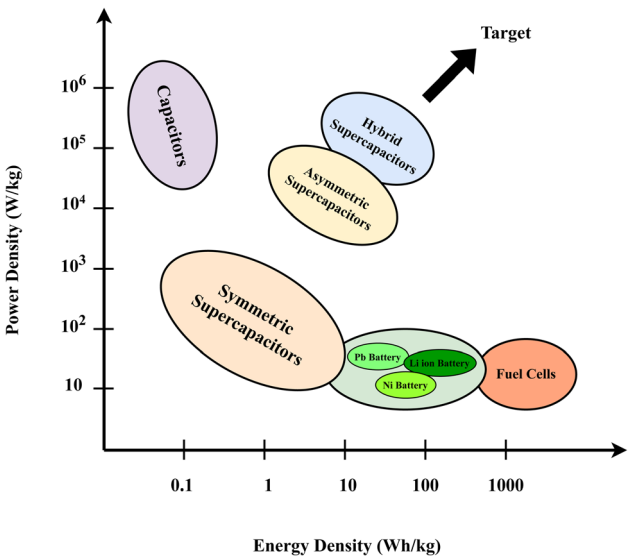

Fig. 2 The electrochemical energy–power landscape.

In contrast, the interfacial chemistry of supercapacitors has long been assumed to be purely non-faradaic, dominated by electrostatic ion adsorption at the electric double layer (EDL) without chemical bond formation or electrolyte decomposition.[25,26] However, recent high-resolution spectroscopic and microscopic investigations have challenged this assumption, revealing the presence of ultrathin (1–10 nm), dynamic SEI-like films on activated-carbon, graphene, and MXene electrodes cycled at potentials above 2.5–3.0 V in organic, ionic-liquid, and even aqueous "water-in-salt" electrolytes.[27–30] These films share compositional similarities with battery SEIs (including inorganic fluorides, carbonates, and polymeric species) but exhibit greater structural reversibility, elasticity, and continuous reconstruction under rapid charge–discharge cycling.[31–34]

Despite mounting experimental evidence for SEI formation in supercapacitors, the phenomenon remains poorly understood and lacks a unified theoretical framework. Several critical questions remain unanswered: (i) What are the thermodynamic and kinetic conditions that trigger SEI nucleation in non-faradaic systems? (ii) How do the composition, thickness, and morphology of supercapacitor SEI-like interphases differ from those in batteries, and what governs these differences? (iii) Can mechanistic insights and engineering strategies developed for battery SEIs (such as electrolyte additive design, artificial interphase coatings, and controlled formation protocols) be systematically translated to supercapacitors? (iv) How does the dynamic, self-healing nature of supercapacitor SEI-like interphases influence long-term cycling stability, self-discharge, and power performance? (Fig. 3).

To keep the Introduction focused on the unified framework developed in this review, we summarize the historical context of SEI briefly. Since early observations of passivation on alkali-

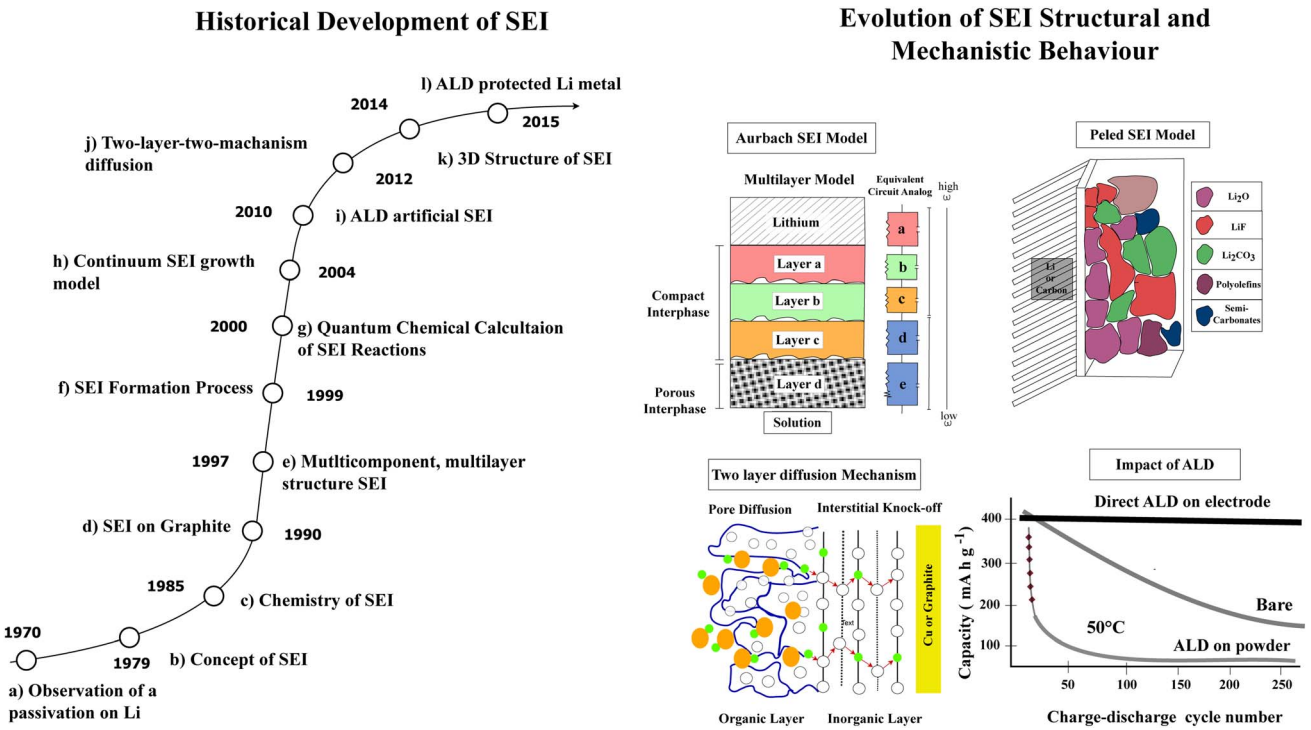

Fig. 3 Historical development and evolving structural/mechanistic understanding of the solid electrolyte interphase (SEI) on negative electrodes in lithium-based batteries. The left panel presents a timeline of key milestones in SEI research: (a) the early observation of a passivation layer on lithium by Dey in the 1970s,[35] (b) the formal introduction of the SEI concept by Peled in 1979,[13] (c) identification of SEI chemistry, including Li_2CO_3, by Nazri and Muller and Aurbach *et al.*,[36] (d) confirmation of SEI formation on graphite in 1990,[37] (e) development of the multicomponent, multilayer SEI concept and equivalent-circuit interpretation by Peled,[38] (f) mechanistic description of SEI formation initiated by electrolyte reduction from Aurbach *et al.*,[39] (g) quantum-chemical calculations of SEI-forming reactions,[40] (h) continuum modeling of SEI growth by Christensen *et al.*,[41] (i) artificial SEI design by atomic layer deposition (ALD) on graphite, demonstrated by Jung *et al.*,[42] (j) the two-layer/two-mechanism diffusion model proposed by Shi *et al.*,[43] (k) direct visualization of the 3D/multilayer SEI by *in situ* electrochemical AFM from Cresce *et al.*,[44] and (l) ALD-protected lithium metal reported by Kozen *et al.*[45] The right panel summarizes representative models and consequences of this evolution, including the Aurbach multilayer SEI model (Reproduced from ref. 36 with permission from Elsevier, copyright 2014), the Peled mosaic model (Reproduced from ref. 38 with permission from IOP Publishing, Copyright 1997), the two-layer diffusion mechanism across organic and inorganic domains (Reproduced from ref. 43 with persmission from American Chemical Society, Copyright 2012), and the beneficial effect of ALD-derived artificial SEI layers on electrochemical durability (Reproduced from ref. 45 with persmission from American Chemical Society, Copyright 2015).

metal electrodes and Peled's formal SEI concept,[13] decades of battery research have established how electrolyte decomposition produces ionically conductive yet electronically insulating interphases,[46] and how such layers govern efficiency, impedance growth, and lifetime.[46,47] Here we leverage that mature battery baseline primarily to motivate and interpret supercapacitor-relevant interphase evidence, rather than re-review battery history in detail.

Current literature on supercapacitor interphases is fragmented across materials science, electrochemistry, and device engineering, with limited cross-referencing to the extensive body of battery SEI research.[48–50] Moreover, the terminology is inconsistent: some authors refer to "interfacial films," "surface layers," or "electrolyte decomposition products" without explicitly invoking the SEI concept.[51,52] This conceptual disconnect has hindered the development of predictive models, unified characterization protocols, and transferable design principles that could accelerate supercapacitor performance optimization.[53]

This review advances a cross-platform interphase framework in which electrolyte-driven passivation is treated as a shared interfacial response, while explicitly accounting for the device-specific boundary conditions that differentiate batteries from supercapacitors (*e.g.*, pore-scale fields, rapid cycling, and defect-localized reactions).[54–56] Rather than re-stating battery SEI fundamentals, we focus on translating battery-derived concepts into supercapacitor-specific evidence, metrics, and actionable design rules across EDLC, pseudocapacitor, and hybrid systems. The distinctions between battery SEIs and supercapacitor SEI-like interphases (thickness, composition, dynamics, and mechanical properties) reflect differences in operating conditions (potential range, cycling frequency, ion flux) rather than fundamental differences in formation mechanisms.[16,20]

Throughout this review, we use interphase as the umbrella term for electrode–electrolyte films and near-surface regions. We reserve SEI for the classical solid–electrolyte interphase in batteries. For supercapacitors, where films are often ultrathin,

dynamic, and condition-dependent, we use SEI-like interphase (or SEI-like film) to denote decomposition-derived passivation layers. When discussing cross-platform similarities, we write interphase or SEI/SEI-like interphase explicitly to avoid ambiguity. Concretely, this framework is operationalized through: (i) a descriptor-to-metric mapping linking interphase signatures to leakage/self-discharge, ESR evolution, and capacitance retention; (ii) actionable design rules identifying when interphase formation is beneficial *versus* detrimental under realistic voltage windows and protocols; and (iii) an integrative summary table/decision map harmonizing evidence across EDLC, pseudocapacitor, and hybrid architectures for direct cross-study comparison.

To avoid ambiguity, we define what we mean by descriptor unification and quantitative analysis. Here, the unified descriptor set spans (i) driving-force descriptors (electrolyte stability window, electrode energetics/Fermi-level alignment, and local EDL/pore field), (ii) solvation/transport descriptors (ΔG_{solv}/desolvation propensity and effective ionic/electronic resistivity of the interphase), and (iii) interphase state variables (thickness/coverage, porosity, and inorganic/organic fraction) that map onto supercapacitor metrics (leakage/self-discharge, ESR evolution, and capacitance retention). The quantitative analysis in this review refers to synthesizing reported cross-study correlations among these descriptors and metrics, rather than proposing a single universal predictive equation.

The scope of applicability is the EDLC/pseudocapacitor/hybrid systems surveyed here in aqueous (including water-in-salt), organic, and ionic-liquid electrolytes operated within practical voltage windows. Outside these regimes (*e.g.*, severe gas evolution, conversion-dominated reactions, strongly redox-active electrolytes, or extreme conditions), descriptor-to-metric relationships may change; we therefore treat such cases as boundary conditions rather than claiming full universality.

This review synthesizes fundamental principles, experimental characterization, computational modeling, and engineering strategies for SEI control across batteries and supercapacitors, progressing systematically from atomic-scale mechanisms to device-level performance optimization.

This review synthesizes knowledge from multiple research communities (electrochemistry, materials science, battery engineering, and supercapacitor technology) to construct a unified understanding of SEI phenomena. Our literature search encompassed peer-reviewed journal articles, conference proceedings, and authoritative reviews published between 1979 (Peled's seminal SEI discovery) and 2025. Primary databases included Web of Science, Scopus, PubMed, Google Scholar, and specialized electrochemical databases. Search terms combined "solid electrolyte interphase," "SEI," "supercapacitor," "electrochemical capacitor," "EDLC," "pseudocapacitor," "interfacial film," "passivation layer," and "electrolyte decomposition" with Boolean operators to capture both battery-focused and capacitor-focused literature.

Inclusion criteria prioritized: (i) experimental studies employing advanced characterization techniques (XPS, cryo-TEM, *operando* spectroscopy) to probe interfacial chemistry; (ii) computational investigations using *ab initio* methods, molecular dynamics, or machine learning to elucidate SEI mechanisms; (iii) engineering studies demonstrating electrolyte additive effects, surface modifications, or artificial interphase strategies; and (iv) review articles synthesizing battery SEI knowledge with potential applicability to supercapacitors. We excluded purely device-performance studies lacking mechanistic insight into interfacial processes and preliminary conference abstracts without peer-reviewed follow-up.

Cross-referencing was performed to identify seminal works cited across both battery and supercapacitor communities, revealing key conceptual bridges (*e.g.*, water-in-salt electrolytes, film-forming additives, *operando* EQCM) that enable knowledge transfer between domains. Over 400 references are integrated into this review, organized thematically to guide readers from fundamental principles through cutting-edge applications.

Establishing SEI formation as a common phenomenon has profound implications for next-generation energy-storage device design. First, it enables predictive engineering: understanding how electrolyte composition, electrode surface chemistry, and operating conditions determine interphase properties allows rational design of SEIs with tailored thickness, ionic conductivity, and mechanical resilience.[57,58] Second, it facilitates cross-platform innovation: strategies proven successful in batteries (such as FEC or VC additives that form uniform fluorinated SEIs[59,60]) can be systematically adapted to stabilize high-voltage supercapacitors. Conversely, the highly dynamic, self-healing SEIs observed in ionic-liquid capacitors offer insights for designing adaptive interfaces in next-generation battery chemistries.[61,62]

Third, unified SEI frameworks accelerate multiscale modeling integration. Atomistic simulations (DFT, reactive MD) capture early-stage nucleation and chemical composition; continuum transport models describe long-term growth and impedance evolution; and machine-learning surrogates bridge these scales to predict device-level performance from molecular descriptors.[63–65] Such hierarchical workflows, validated against *operando* experimental data, will enable *in silico* optimization of electrolyte formulations and electrode architectures before costly laboratory synthesis.[66,67]

Fourth, recognizing the dynamic nature of supercapacitor SEI-like interphases (thinner, more elastic, continuously reconstructing) informs durability and reliability engineering. Unlike thick, quasi-static battery SEIs that crack under mechanical stress, supercapacitor interphases must tolerate millions of rapid charge–discharge cycles without catastrophic failure.[24,31] Designing cross-linked binder networks, self-healing polymer matrices, and resilient artificial coatings becomes paramount for achieving ultralong cycle life.[68,69]

Finally, this unified perspective supports sustainability and circular-economy goals. By understanding which SEI components are environmentally benign, biodegradable, or recyclable, researchers can design electrolytes and electrode surface treatments that minimize environmental footprint while maintaining performance.[70,71] Moreover, predictive SEI models reduce trial-and-error experimentation, lowering resource consumption and accelerating time-to-market for next-generation

supercapacitors powering electric vehicles, grid storage, and portable electronics.[53]

2 Fundamentals of the solid-electrolyte interphase (SEI) in batteries and supercapacitors

The concept of the solid-electrolyte interphase (SEI) originated in battery science, where electrolyte reduction produces a self-passivating layer that stabilizes electrode–electrolyte contact during cycling. Recent evidence suggests that analogous, albeit thinner and more dynamic, SEI-like films can also arise in supercapacitors under extreme potentials, high surface reactivity, or defect-rich conditions. Understanding these parallels allows cross-fertilization of ideas: mechanistic principles from batteries clarify interphase chemistry in capacitors, while the reversible, elastic behavior of capacitor interfaces offers new insight into SEI adaptability in batteries.

2.1 Capacitive charge storage fundamentals

Supercapacitors (also known as electrochemical capacitors) store energy through fast and reversible interfacial processes that bridge the gap between conventional capacitors and batteries. Depending on the dominant charge-storage mechanism, they are broadly classified as electric double-layer capacitors (EDLCs) and pseudocapacitors. In EDLCs, charge storage is non-faradaic and arises from electrostatic ion adsorption at the electrode–electrolyte interface. When an external potential is applied, oppositely charged ions accumulate near the electrode surface, forming an electric double layer (EDL) that acts as a nanoscale capacitor. The total stored charge depends on the accessible surface area of the electrode, the dielectric constant of the electrolyte, and the effective thickness of the EDL.[72,73] This mechanism provides excellent power density and long cycle life, as it does not involve structural changes or phase transformations in the electrode material.

Pseudocapacitors, by contrast, store charge through fast surface or near-surface faradaic reactions that involve electron transfer between the electrode and electrolyte species. Transition-metal oxides (*e.g.*, MnO_2, RuO_2) and conducting polymers (*e.g.*, polyaniline, polypyrrole) are typical pseudocapacitive materials.[74,75] The capacitance arises from reversible redox, intercalation, or adsorption processes that occur over a continuum of potentials rather than discrete battery-like plateaus. Because these reactions are surface-confined, pseudocapacitors combine the high energy densities of batteries with the power performance of EDLCs.[9,76,77] Hybrid or asymmetric supercapacitors integrate both mechanisms by pairing an EDLC-type electrode with a pseudocapacitive one, thereby expanding the voltage window and enhancing overall energy storage.[78] The interfacial charge distribution that governs these processes also defines the potential gradients that initiate electrolyte decomposition and SEI nucleation in both batteries and capacitors. To avoid ambiguity throughout this review, we distinguish three interfacial regimes in supercapacitors: (i) EDL adsorption (non-faradaic, electrostatic ion accumulation; typically rectangular (cyclic voltammograms) CVs and minimal persistent resistance drift),[79] (ii) reversible pseudocapacitive surface redox (fast faradaic but reversible surface/near-surface electron transfer; broad redox features that remain stable under cycling within a safe window),[80] and (iii) irreversible SEI-like films (electrolyte decomposition or side reactions producing new surface species and progressive performance drift).[81,82] Importantly, (ii) and (iii) can coexist on pseudocapacitive electrodes;[83] therefore, assignments should be supported by coupled electrochemical metrics (leakage/self-discharge, ESR evolution, retention) and chemistry-resolved diagnostics (*e.g.*, XPS/ToF-SIMS/FTIR) rather than by CV shape alone.[79,81]

2.2 Interfacial electric field distribution and ion dynamics

The electric double layer governs the microscopic origin of capacitance in supercapacitors. At the electrode–electrolyte interface, ions rearrange in response to the surface potential, producing a space-charge region characterized by the Stern–Gouy–Chapman model.[84–86] The inner Helmholtz plane (IHP) consists of specifically adsorbed, partially desolvated ions in direct contact with the electrode surface, while the outer Helmholtz plane (OHP) contains solvated ions whose centers are separated by one solvent-molecule thickness.[72,87] Beyond these layers lies the diffuse region, where ion distribution follows a Boltzmann potential profile. The differential capacitance depends on the local dielectric constant, ion concentration, and potential-dependent surface charge density.[72] In nanoporous electrodes, confinement effects alter ion packing and solvation structure, giving rise to non-classical phenomena such as ion desolvation, crowding, and overscreening.[88] These effects strongly influence voltage-dependent capacitance and energy density.

Spectroscopic, scattering, and molecular-dynamics studies reveal that the EDL is not a simple continuum but a dynamically fluctuating interfacial region with heterogeneous ion orientations and time-dependent correlations.[89] The interplay of ion–ion and ion–solvent interactions determines the local permittivity and thus the capacitance. In pseudocapacitive materials, surface redox reactions further modify the interfacial electric field. These same electrostatic gradients set the stage for SEI formation once the local potential exceeds the electrolyte stability limit, linking double-layer physics with interphase chemistry across both energy-storage platforms.

2.3 Origin and function of the solid-electrolyte interphase

The electrode–electrolyte interface is a chemically complex region where ion adsorption, charge transfer, and molecular decomposition occur simultaneously. While EDL formation governs the fast and reversible electrostatic storage that defines supercapacitors, parasitic reactions at the same interface can lead to the emergence of a thin, passivating SEI. Much of the mechanistic framework for interpreting such interphases derives from battery research, where SEI formation is intrinsic and indispensable. In supercapacitors, similar reactions occur

Table 1 Phenomenological comparison of interphase behavior in batteries and supercapacitors (device level perspective). Thermodynamic and kinetic formation details are given separately in Table 2

Feature	Battery SEI	Supercapacitor SEI-like film
Temporal behavior	Quasi-static after initial formation	Dynamic, continuously reconstructed under cycling
Primary function	Prevent further decomposition, enable ion intercalation	Modulate leakage current, stabilize double layer
Mechanical response	Rigid, stress-sensitive (must accommodate volume change)	Quasi-elastic, self-healing (minimal dimensional change)
Failure mode	Cracking from expansion/contraction	Resistive thickening from cumulative voltage stress

only under overstress or at defect-rich sites, producing a more transient and reversible film.

SEI-like films emerge when local interfacial conditions drive electrolyte reactions beyond the stability window, producing a thin electronically blocking but ion-permeable interphase.[13] For batteries this interphase is intentionally formed and comparatively persistent,[46] whereas in supercapacitors it is typically ultrathin and condition-dependent (*e.g.*, high-voltage operation, defects, and rapid cycling),[82] so its impact is better discussed using supercapacitor-specific observables such as leakage current, ESR evolution, and capacitance retention.

2.4 Compositional and structural distinctions across energy storage platforms

Bridging SEI behavior across these two systems clarifies how shared electrochemical principles yield different interphase dynamics. In rechargeable batteries, the SEI is essential for long-term operation: it passivates the anode against continuous electrolyte decomposition while permitting Li^+ or Na^+ transport. Battery SEIs are typically tens of nanometers thick, composed of inorganic salts (LiF, Li_2O, Li_2CO_3) in the inner region and polymeric organic components (polycarbonates, alkoxides) toward the outer surface.[15,90] Once formed, these layers remain largely static and evolve slowly over many cycles, occasionally thickening due to secondary reactions.

In contrast, supercapacitor SEI-like interphases are thinner (often below 5–10 nm) and more dynamic because charge storage occurs primarily through non-faradaic or surface-confined pseudocapacitive processes.[91] Interfacial potential fluctuations during rapid charging and discharging continually perturb the equilibrium structure, leading to reversible rearrangements or partial dissolution. Consequently, the SEI-like interphase in supercapacitors behaves as a quasi–elastic interface that expands and contracts without catastrophic failure.[92] Furthermore, since the operating voltage of supercapacitors (1–3 V) is lower than typical battery cutoff voltages, electrolyte decomposition is limited, and SEI formation depends strongly on surface defects, residual moisture, and specific ion–surface interactions.[15]

From a compositional standpoint, organic-electrolyte supercapacitors often yield SEIs containing solvent fragments (acetonitrile or propylene carbonate) mixed with anion-derived fluorinated or borate species (BF_4^-, PF_6^-).[19,93] In aqueous systems, decomposition of water forms hydroxide or oxide layers that are less stable and reconstruct during cycling, whereas ionic-liquid-based supercapacitors generate fluoride- or sulfur-enriched SEIs from anion cleavage.[93] These dynamic interphases, although thinner, exhibit higher heterogeneity, influencing self-discharge and capacitance retention.

The mechanical demands placed upon the SEI diverge considerably between the two device classes. Battery interphases must accommodate substantial volumetric expansion inherent to high-capacity anodes such as lithium metal and silicon, whereas carbonaceous and oxide electrodes characteristic of supercapacitors undergo negligible dimensional change during operation. This mechanical quiescence reduces interfacial stress yet simultaneously heightens sensitivity to potential-induced polarization and adsorption heterogeneity.[94] Collectively, these observations underscore that SEI chemistry is governed by generalizable electrochemical principles, namely electrolyte breakdown, ion-migration-limited growth, and self-passivation, while device-specific boundary conditions encompassing potential range, ion identity, and surface reactivity ultimately dictate interphase thickness, elasticity, and reversibility (Table 1).

2.5 Governing parameters in interphase evolution

The formation, composition, and stability of SEI layers depend on electrolyte formulation, operating voltage, temperature, and electrode surface characteristics.

2.5.1 Electrolyte chemistry. Solvent reduction potential, salt composition, and additives dictate SEI precursors. Low-viscosity solvents with wide electrochemical windows, such as acetonitrile, minimize decomposition but can yield thin SEIs of nitrile oligomers and anion fragments.[95] Propylene carbonate-based electrolytes polymerize upon reduction, forming thicker elastic films. The choice of salt ($TEABF_4$, $LiPF_6$, NaTFSI) determines anion-derived inorganic species.[19] Additives first optimized for Li-ion SEI stabilization, such as fluoroethylene carbonate (FEC) or vinylene carbonate (VC), are now used to regulate SEI growth in capacitors, underscoring transferable interfacial design principles.[19,58]

2.5.2 Voltage window. The applied potential defines the driving force for electrolyte decomposition. In batteries, operation intentionally exceeds the stability limit to form SEI; in capacitors, such excursions occur only locally. Below the limit,

Table 2 Comparative features of SEI formation in batteries and supercapacitors

Aspect	Batteries	Supercapacitors
Driving potential	Electrolyte reduction at anode potentials (<1 V *vs.* Li/Li^+)	Localized overpotential or defect-site fields (1–3 V window)
Film thickness	10–100 nm, diffusion-limited growth	1–10 nm, field-driven reconstruction
Dominant species	LiF, Li_2CO_3, Li_2O	Carbonates, nitriles, fluorides
Growth mode	Self-limiting, inorganic barrier	Dynamic, elastic dielectric

only EDL formation occurs; beyond it, SEI nucleation begins.[96,97] Overpotential exposure thickens the SEI and increases resistance. Optimizing voltage range balances energy density and durability, while surface heterogeneity modulates local reaction rates.[98–100]

2.5.3 Temperature. Thermal effects influence both kinetics and stability. Elevated temperatures accelerate reactions but destabilize metastable organics, whereas low temperatures yield porous, resistive films.[101] Long-term thermal cycling promotes compositional segregation where inorganic domains densify and polymeric regions soften.[102,103] Similar temperature-induced reconstructions occur in high-rate batteries, reinforcing the generality of interphase dynamics.

2.5.4 Electrode surface states. Surface chemistry and defect density determine initiation sites and adhesion strength. Graphitic carbons with basal planes form thin uniform SEIs; defective or functionalized carbons catalyze solvent reduction, yielding thicker, chemically diverse films.[19] Transition-metal oxides and MXenes with variable terminations (–O, –F, –OH) actively participate in redox reactions that reshape SEI chemistry.[104] Engineering surface functionality through doping or coatings thus provides a cross-platform strategy for controlling interphase morphology and stability.[19,103,105]

Overall, the physicochemical environment determines whether the SEI acts as a beneficial stabilizing layer or a resistive barrier. Integrating these parameters into unified electrochemical models will enable predictive interphase engineering across both batteries and supercapacitors. The following section (Section 3) examines the microscopic mechanisms that drive SEI nucleation, growth, and reconstruction, establishing the molecular basis for the interphase behaviors described above.

3 Microscopic mechanisms of SEI formation and evolution

SEI formation is a universal widely observed electrochemical phenomenon arising whenever the applied potential drives an electrolyte beyond its thermodynamic stability window.[15,106,107] In both batteries and supercapacitors, the interphase originates from coupled electron-transfer, ion-migration, and molecular-reorganization events that spontaneously self-assemble at the electrode–electrolyte boundary.[108] The distinction lies in scale rather than mechanism: battery SEIs are thick and quasi-static, whereas capacitor SEIs are ultrathin, dynamic, and continuously reconstructed under cycling.[16,20] Understanding their shared microscopic origins is essential for cross-platform interphase engineering.

3.1 Electron transfer and electrolyte reduction criteria

SEI nucleation begins when the electrode Fermi level intersects the lowest unoccupied molecular orbital (LUMO) of the electrolyte, enabling electron tunneling into solvated molecules and initiating bond cleavage.[109,110] The same criterion governs electrolyte reduction in both Li-ion batteries and carbon-based supercapacitors, although the effective overpotential and reaction timescales differ.[98] Table 2 summarizes the principal thermodynamic parallels.

Electron injection into solvent or anion orbitals initiates decomposition of carbonate (EC, PC) or nitrile (ACN) molecules.[111] Regardless of electrolyte type, the resulting fragments (carbonates, alkoxides, and nitrile oligomers) polymerize or condense on the surface, establishing the initial interphase.[109,112] Anion reduction (BF_4^-, PF_6^-, $TFSI^-$) produces inorganic fluorides and borates in both systems, yielding the dense, electronically insulating inner region that terminates further electron leakage.[113] Thus, SEI nucleation follows the same thermodynamic sequence in batteries and capacitors, differing only in potential range and material identity.

3.2 Atomistic decomposition and fragment condensation

At the atomic scale, SEI formation proceeds through multiple, overlapping routes: solvent reduction, salt decomposition, and radical polymerization.[114] In supercapacitors, decomposition pathways must be discussed in the context of electrolyte class and voltage window,[115] because the dominant fragments differ strongly between (i) organic salts (*e.g.*, $TEABF_4$ in ACN/PC),[82] (ii) ionic liquids (*e.g.*, $TFSI^-$-based RTILs), and[116](iii) highly concentrated aqueous electrolytes (water-in-salt).[117–119] In organic EDLCs, anion-derived fragments (BF_xO_y/C–F) and solvent-derived oligomers can form ultrathin films that suppress charge leakage; in RTILs, F/S-containing fragments frequently dominate; in water-in-salt, anion-derived inorganic-rich layers emerge as the key passivation motif. Therefore, supercapacitor SEI-like interphase chemistry should be summarized as electrolyte-specific evidence rather than as a battery analogy.

In ionic-liquid and water-in-salt electrolytes, coordinated water or cation fragments yield inorganic fluorides or hydroxides that emulate the protective SEIs of batteries.[120] Hence, solvent and anion decomposition chemistry is fundamentally transferable between the two device classes.

3.3 Heterogeneous interphase structure and charge selectivity

Once decomposition products accumulate, they organize into a bilayered morphology: a dense, inorganic inner layer and

a porous, polymeric outer matrix.[121] In batteries, LiF/Li_2CO_3 layers dominate the inner region.[122] On the other hand, in capacitors, $C–F/BF_xO_y$ and M–O–F domains play the same mechanical and electronic role.[123] The outer polymeric zone, composed of polycarbonate, nitrile, or ether species, acts as an ion-permeable, elastically compliant dielectric. This architecture self-regulates *via* potential-dependent current tunneling: when the film reaches a critical thickness d, the tunneling current density

$$J \propto \exp(-\beta d)$$

drops below the decomposition threshold, halting further growth. Such self-passivation, long established for battery SEIs, equally governs the stabilization of capacitor interphases.

3.4 Desolvation and ion migration through passivating films

Ion solvation governs both the onset of electrolyte reduction and the transport properties of the resulting SEI. At the interface, strong electric fields induce partial desolvation, exposing bare ions that readily accept or donate electrons.[124] In batteries, Li^+ desolvation triggers EC reduction. In supercapacitors, desolvation must be framed through pore confinement and rate:[125] ion desolvation and re-solvation occur repetitively at high frequency,[126] and the interphase must remain thin enough to avoid blocking micropores that govern capacitance.[125] Accordingly, evidence should be interpreted using measurable outputs (specifically, capacitance retention, ESR evolution, and self-discharge) rather than only molecular descriptors.[127] When a film becomes too resistive or blocks pore entrances, capacitance decreases and ESR rises; when it is thin and electronically insulating, leakage decreases without sacrificing rate capability.[127,128]

The degree of solvation controls the SEI composition: tightly bound solvates produce dense, inorganic-rich layers, while weakly solvated ions form thinner, more permeable films.[124,129–131] This relationship can be expressed by the correlation between solvation energy (ΔG_{solv}) and effective ionic conductivity (σ_{ion}):

$$\sigma_{ion} \propto \exp\left(-\frac{|\Delta G_{solv}|}{kT}\right),$$

demonstrating that interfacial transport follows widely observed relationships across devices. Molecular-dynamics studies confirm similar desolvation barriers and coordination rearrangements at Li, Na, and carbon surfaces, reinforcing the mechanistic continuity.

3.5 Dynamic reconstruction under electrochemical stress

The SEI continually evolves under electrochemical and thermal stimuli. Elevated temperature accelerates decomposition and diffusion, densifying the film in both systems;[135] low temperature slows polymerization, yielding porous, resistive layers. During potential cycling, elastic compression/relaxation and ongoing side-reaction turnover can drive reversible interphase restructuring, as observed by *operando* EQCM and cryo-TEM in both batteries and capacitors.[23] In supercapacitors, the relevant SEI-like interphase is typically ultrathin (often ~1–10 nm) and can exhibit two superimposed behaviors: (i) a baseline thickness/mass drift during early conditioning or prolonged voltage holds, and (ii) cycle-resolved fluctuations that track the charge–discharge period. Practically, the reconstruction timescale spans seconds to minutes under dynamic cycling (set by the cycling period), whereas net growth/compaction is most evident during minutes-to-hours voltage holds, consistent with diffusion-reaction control.

These oscillations follow diffusion-reaction kinetics similar to logarithmic growth laws:[136]

$$d(t) = kt^{1/2},$$

where k encapsulates ionic mobility and reaction rate constants. Such self-healing and reconstruction phenomena demonstrate that the interphase is not a static coating but a dynamic, viscoelastic interface whose measurable thickness/mass response depends on protocol (cycling frequency *vs.* hold) and local field/transport conditions.

3.6 SEI-mediated modulation of capacitance and impedance

The SEI critically influences electrochemical response by mediating ion accessibility and dielectric behavior. In both devices, its thickness and ionic conductivity determine the distance between ionic and electronic charge centers, thereby affecting differential capacitance and internal resistance.[137,138] Nyquist plots of porous electrodes often display a mid-frequency arc or depressed semicircle, but this feature is non-unique.[139,140] It may reflect interphase film response, contact/constriction effects, and/or distributed pore transport and charging (transmission-line behavior).[141–143] For this reason, we interpret mid-frequency impedance features in supercapacitors using a porous-electrode-aware framework (Section 8.2) and reserve the term "interphase resistance" for cases where the fitted film element co-varies with independent interphase diagnostics (chemistry/thickness from XPS/ToF-SIMS/cryo-TEM, or mass uptake from EQCM)[142,144] and shows consistent trends with voltage window and cycling protocol.[119]

A thin, ion-permeable SEI minimizes leakage and stabilizes coulombic efficiency, whereas a thick, resistive one increases relaxation times and lowers power density.[145,146]

Spatial heterogeneity of the SEI also modifies local permittivity: inorganic-rich domains ($\varepsilon_r \approx 5$–10) focus electric fields and promote ion layering, while polymeric regions ($\varepsilon_r \approx 20$–40) smooth potential gradients. This heterogeneity generates two characteristic time constants in impedance spectra: a fast component from electric-double-layer charging and a slower one from ion migration through the SEI.[147,148] In both batteries and capacitors, these coupled processes define the dynamic bottleneck for high-rate performance.

Furthermore, reversible redox rearrangements within the organic fraction of the SEI can contribute to pseudocapacitive charge storage. Such behavior, once noted in polymer-rich battery SEIs, equally appears in stabilized capacitor interfaces,

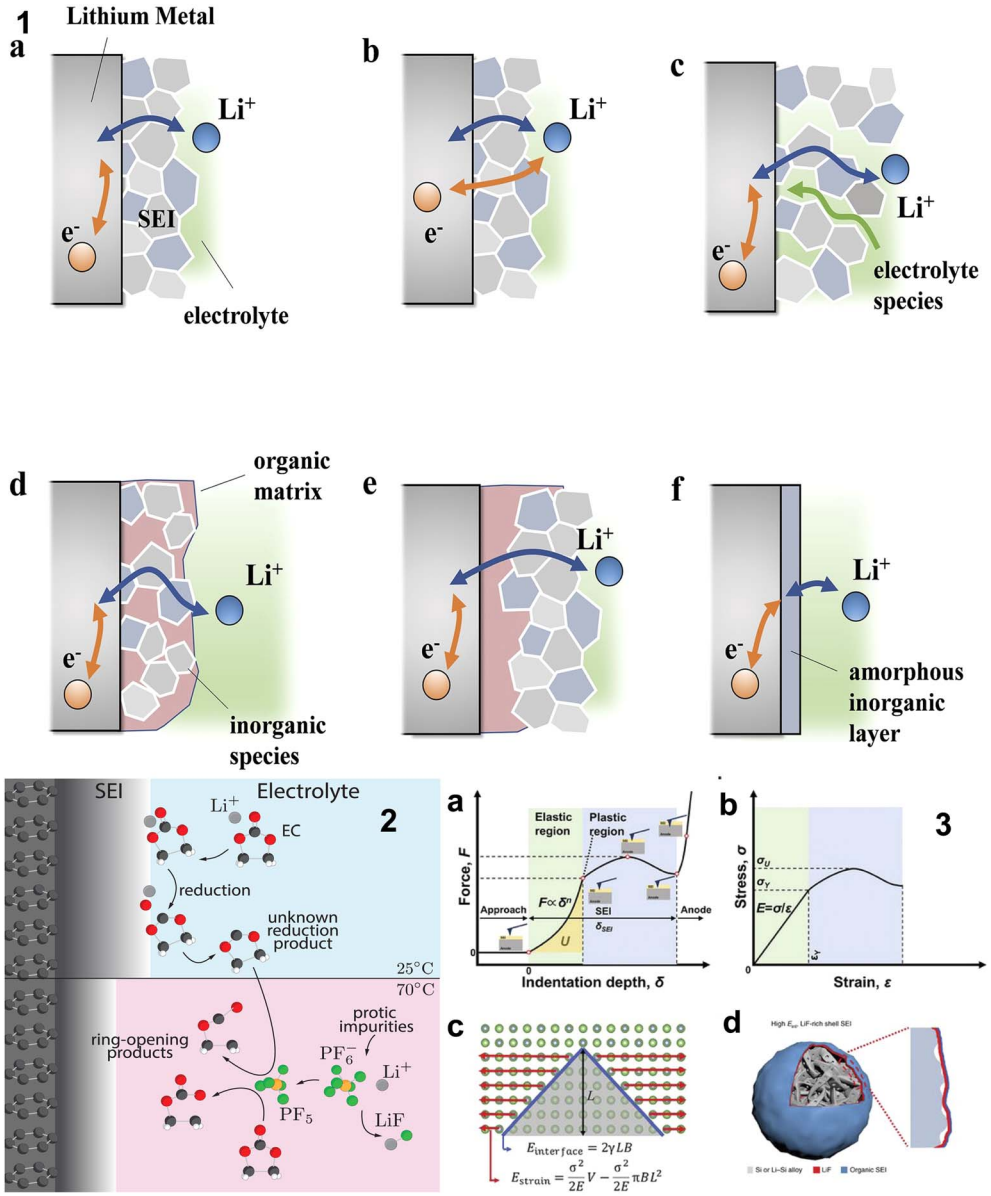

Fig. 4 Schematic overview of SEI formation across energy-storage systems, showing three common stages: (1) electron injection and inorganic nucleation. Reproduced from ref. 132 with permission from WILEY, Copyright 2021 (2) solvent/anion decomposition. Reproduced from ref. 133 with permission from IOP Publishing, Copyright 2018. and (3) mechanical relaxation. Reproduced from ref. 134 with permission from WILEY, Copyright 2025.

where the SEI-like interphase acts as an active, charge-mediating dielectric rather than a passive barrier.[149,150]

3.7 Device-class evidence and metrics for SEI-like interphases in supercapacitors (EDLC, pseudocapacitive, and hybrid)

To meet the supercapacitor community's needs, SEI-like interphases should be summarized by device class and verified by both interfacial signatures and device-level metrics.[151,152] In contrast to batteries, where SEI formation is intrinsic, supercapacitor interphases are typically triggered near the electrolyte stability boundary at defect-rich surfaces, or under aggressive voltage holds.[153,154] Therefore, evidence must be reported with explicit operating details (electrolyte, voltage window, electrode type) and quantified outcomes (leakage current, self-discharge, ESR, capacitance retention).[153,155]

In EDLCs (activated carbon, graphene, porous carbons), SEI-like films are most consistently reported in high-voltage organic and ionic-liquid electrolytes, particularly under voltage holds or extended cycling near the upper cut-off.[155] Key evidence includes: (i) emergence of F-containing and carbonate/nitrile-derived surface species (XPS/ToF-SIMS),[153] (ii) nm-scale coverage detectable by cryo-TEM/AFM in selected systems,[156] and (iii) correlated suppression of leakage current and slower self-discharge when stable films form.[157] However, excessive film growth or pore-mouth blockage causes measurable capacitance loss and ESR increase, indicating that thin and dynamic

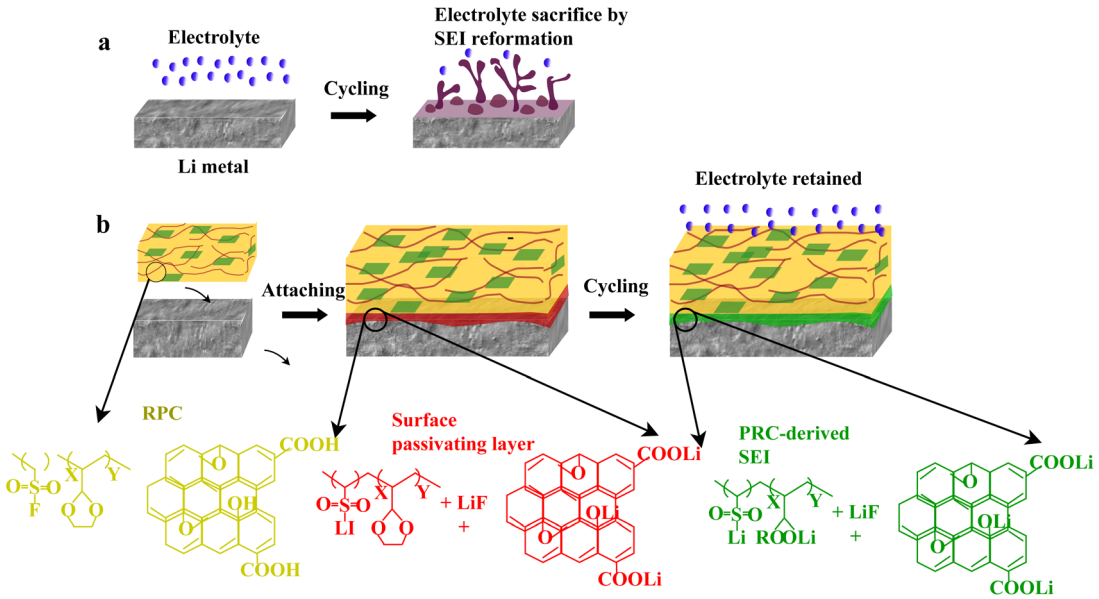

Fig. 5 Schematic illustration of polymer-condensation-driven interphase growth as part of the broader interphase-formation framework across energy-storage systems. (a) Formation of SEI *via* electrolyte decomposition. (b) Design of a polymer–inorganic SEI using the RPC precursor. Reproduced from ref. 134 with permission from Nature Publishing Group, Copyright 2019.

interphases are beneficial whereas thick and blocking interphases are detrimental.[158,159]

For pseudocapacitive electrodes (metal oxides, MXenes, conducting polymers), the interphase must be interpreted together with surface redox: some surface reactions are reversible and contribute to capacitance, while others produce irreversible films that progressively increase resistance.[160] Evidence should therefore separate: (i) reversible surface chemistry (stable redox-active states) from (ii) irreversible electrolyte decomposition products (passivating layers).[161] *Operando* EIS/EQCM combined with post-mortem XPS is particularly valuable here, because it can distinguish mass changes from adsorption *versus* irreversible film accumulation.[162] In aqueous systems, local pH shifts and proton-coupled processes can dominate, whereas in organic/IL electrolytes, fluorinated fragments and polymeric residues may accumulate at oxide/carbon interfaces.[163]

Hybrid capacitors (asymmetric devices, lithium-ion capacitors, battery-capacitor hybrids) operate in regimes where one electrode experiences more battery-like polarization.[164] As a result, interphase formation in hybrid (EDLC + faradaic) cells can be strongly electrode-selective, governed by each electrode's individual stability limits, and can dominate aging even when the full device response remains largely capacitive; therefore, evidence should name the electrode that forms the dominant interphase and correlate it to ESR/impedance rise, Coulombic-efficiency/residual-current drift, and any electrode-to-electrode charge-balance (capacitance) mismatch that develops over cycling.[31]

3.8 Unified framework for interphase formation

Fig. 4 and 5 schematically summarizes SEI formation across energy-storage systems, outlining five common stages: (1) electron injection, (2) solvent/anion decomposition, (3) inorganic nucleation, (4) polymeric condensation, and (5) mechanical relaxation.[165,166] Differences between batteries and capacitors arise primarily from potential magnitude and cycling frequency, not from reaction identity.

Across all electrochemical devices, the SEI embodies the same self-organization of matter under electric fields and chemical stress.[16,167] Recognizing this universality generality transforms the SEI from a device-specific artifact into a general design principle linking molecular chemistry to macroscopic performance. Having established the fundamental mechanisms of SEI formation, we now turn to the experimental methodologies that enable direct observation and characterization of these interphases in Section 4, followed by computational modeling frameworks in Sections 6 and 7 that predict and simulate SEI evolution across multiple scales.

4 Experimental characterization of the SEI

Understanding the chemistry, morphology, and dynamics of the solid-electrolyte interphase (SEI) requires a combination of *ex situ* structural analysis and *in situ* or *operando* spectroscopy.[168] Most techniques now used to probe SEI evolution were first developed in battery research, where stable interphases are intrinsic to operation, and have since been adapted to investigate the thinner, more dynamic SEI-like films in supercapacitors.[22,169,170] Recognizing this shared experimental heritage enables a unified interpretation of interfacial chemistry across both systems and provides critical validation for atomistic simulations and continuum models discussed in Section 6.[23,171]

4.1 *Ex Situ* techniques for interphase characterization

4.1.1 X-ray photoelectron spectroscopy (XPS). Originally established as the principal diagnostic for SEI analysis in Li-ion

batteries, XPS remains the most widely used technique for probing elemental composition and oxidation states within interphases. Depth profiling by successive argon-ion sputtering reveals characteristic compositional gradients, notably LiF- or Li_2CO_3-rich inner layers in batteries and inorganic fluorides or carbonates in capacitors.[172,173] In carbon-based supercapacitors, XPS detects C–O, C═O, and O–C═O functionalities arising from solvent oxidation, while F 1s and B 1s peaks confirm BF_4^- or PF_6^- decomposition.[174] Quantitative peak-shift analysis further provides information on local potential drops and the electronic insulation conferred by the SEI layer. Thus, XPS offers a common compositional framework for comparing SEI chemistry across batteries and capacitors.

4.1.2 Fourier-transform infrared spectroscopy (FTIR). FTIR identifies vibrational fingerprints of organic components. Bands at ~1700 cm^{-1} (C═O), ~1100 cm^{-1} (C–O–C), and carbonate stretches signal solvent decomposition and polymerization.[172] In battery studies, these signatures verified polymeric carbonates and alkoxides; analogous features in supercapacitors indicate nitrile- or carbonate-based oligomers formed from acetonitrile or propylene carbonate breakdown. Mapping FTIR intensity across electrodes reveals heterogeneity linked to potential gradients and pore accessibility.[175,176]

4.1.3 Raman spectroscopy. Raman scattering simultaneously probes electrode disorder and interphase evolution. The D/G-band ratio (I_D/I_G) reflects graphitic defect density, while new bands between 1200–1500 cm^{-1} correspond to polymeric species within the SEI.[16] Techniques such as surface-enhanced Raman spectroscopy (SERS) and tip-enhanced Raman (TERS), originally applied to map SEI growth on

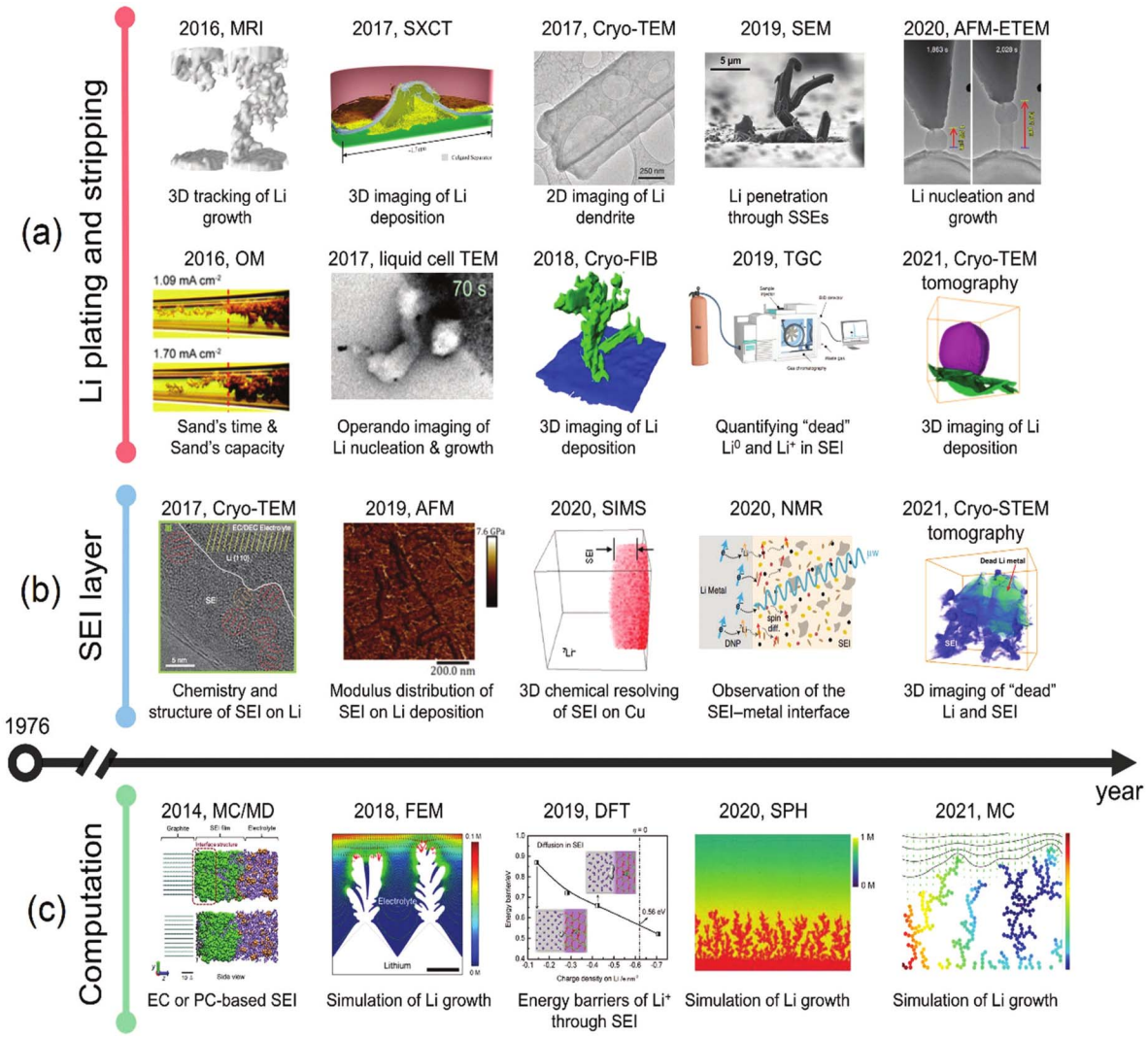

Fig. 6 Recent advances in the mechanistic understanding of Li deposition and SEI evolution using advanced characterization and theoretical modeling methods. (a) Characterization techniques for probing Li plating and stripping behavior include magnetic resonance imaging (MRI), synchrotron X-ray computed tomography (SXCT), cryo-TEM, SEM, AFM-ETEM, optical microscopy (OM), liquid-cell TEM, cryo-FIB, and thermogravimetric analysis/GC-based methods where applicable. (b) Analytical methods for SEI characterization include cryo-TEM, AFM, SIMS, NMR, and cryo-STEM tomography. (c) Theoretical and computational approaches include Monte Carlo (MC), molecular dynamics (MD), finite-element modeling (FEM), density functional theory (DFT), and smoothed-particle hydrodynamics (SPH) for investigating diffusion barriers, Li-deposition behavior, and SEI structure. Reproduced from ref. 185 with permission from Wiley, copyright 2022.

graphite anodes, now resolve nm-scale chemistry of dynamic SEI films in capacitors.[177,178]

4.1.4 Nuclear magnetic resonance (NMR). Solid-state ^{13}C, ^{19}F, and ^{1}H NMR spectroscopy provides direct insight into molecular bonding and dynamics. Broad peaks from immobilized polymeric fragments contrast with sharp resonances from free electrolyte molecules, allowing estimation of cross-linking and segmental mobility.[111] Approaches such as dynamic nuclear polarization (DNP), initially implemented to enhance SEI sensitivity in Li-ion batteries, have begun to uncover weak interfacial polymer-electrolyte coupling in supercapacitors.

4.1.5 Time-of-flight secondary ion mass spectrometry (ToF-SIMS). ToF-SIMS delivers nm-scale surface sensitivity and isotopic resolution, detecting fragment ions that pinpoint SEI precursors.[16] In both systems, cryogenic operation mitigates beam damage and preserves fragile species.[179] Depth-resolved mapping visualizes heterogeneity, ranging from LiF mosaics in batteries to mixed organic-fluoride domains in capacitors, thereby providing critical benchmarks for validating reactive-MD predictions of interphase composition.

4.2 *In situ* monitoring of SEI formation and evolution

4.2.1 Electrochemical quartz crystal microbalance (EQCM). EQCM, developed to track mass changes during battery SEI growth, now measures real-time ion adsorption and SEI formation in capacitors with nanogram sensitivity.[180] Monotonic mass increases indicate film deposition, while oscillatory trends correspond to reversible ion intercalation. Combining EQCM with electrochemical impedance spectroscopy (EIS) distinguishes elastic mass loading from viscoelastic film formation, unifying the interpretation of interphase kinetics.

Electrochemical impedance spectroscopy (EIS) provides a frequency-resolved fingerprint of interfacial and porous–electrode processes, but in porous supercapacitor electrodes the mid-frequency semicircle is not uniquely attributable to an SEI.[181] Similar semicircles (or depressed arcs) can arise from a convolution of (i) interphase film response ($R_f \| \mathrm{CPE}_f$), (ii) contact/constriction resistance within the current collector-electrode network, and (iii) distributed pore transport and surface charging captured by transmission-line behavior.[181] Accordingly, interphase resistance should be assigned only when (a) a film-like time constant is consistently observed across conditions and (b) complementary evidence (*e.g.*, XPS/ToF-SIMS thickness/chemistry trends, EQCM mass uptake) covaries with the fitted film element.[151] In this review we therefore treat EIS-derived "R_{SEI}" as an operational metric that requires a porous-electrode-aware fitting framework rather than a one-to-one identifier of SEI formation.[181]

4.2.2 *In situ* Raman and infrared spectroscopy. *Operando* Raman and attenuated-total-reflectance (ATR) infrared spectroscopy capture real-time bond formation and cleavage under bias. Frequency shifts in C≡N or S═O stretching modes trace reversible ion solvation or irreversible decomposition leading to SEI formation.[182] These techniques, originally applied to monitor electrolyte degradation in Li-ion cells, now enable spatially resolved mapping of interfacial heterogeneity in capacitors.

4.2.3 Cryogenic transmission electron microscopy (cryo-TEM). Cryo-TEM, which revolutionized SEI imaging in batteries, preserves native interfacial structures by rapid freezing.[183] Its adaptation to supercapacitors has revealed ultrathin, self-healing SEIs in ionic-liquid systems, providing direct evidence that reversible reconstruction is a common property of electrochemical interphases.

4.2.4 Atomic force microscopy (AFM) and electrochemical AFM (EC-AFM). AFM quantifies topography and mechanical stiffness of SEIs with nanometer precision. Force–distance curves and current-sensing AFM (CS-AFM) map film elasticity and local conductivity.[19,184] EC-AFM, conducted under potential control, dynamically visualizes SEI evolution in liquid environments, linking morphology, adhesion, and charge-transfer resistance across both device types (Fig. 6).

4.3 Cross-technique validation and data synthesis

Correlating chemical and electrochemical data is crucial for understanding SEI function in any electrochemical system. In both batteries and capacitors, combining XPS-derived composition with EIS-extracted R_{SEI} values links specific motifs (fluorides, carbonates, phosphates) to fitted interphase resistivity/impedance (*e.g.*, R_{SEI} or R_{int}) with explicitly traceable quantitative sources.[19] FTIR and Raman features associated with polymeric carbonates often coincide with higher leakage currents or reduced capacitance, indicating partial electronic conductivity through conjugated species. EQCM mass–change profiles synchronized with cyclic-voltammetry (CV) peaks directly reveal the competition between capacitive ion adsorption and interphase growth.[186] These cross-correlations provide quantitative descriptors, such as "interphase efficiency" or "ionic utilization ratio," that unify SEI analysis across technologies.

Multimodal platforms now integrate spectroscopy, microscopy, and electrochemistry in real time. *Operando* Raman/EIS coupling simultaneously tracks vibrational and impedance signatures, while synchrotron-based soft X-ray absorption spectroscopy (sXAS) resolves element-specific oxidation states.[187] These hybrid systems establish feedback loops between experiment and simulation, enabling parameter calibration for molecular-dynamics and DFT models and strengthening the link between mechanistic insight and performance metrics.

4.4 Comparative studies across electrode and electrolyte systems

A major barrier to unifying supercapacitor interphase literature is that many studies report surface chemistry without connecting it to device-level consequences, or report performance without identifying interphase chemistry.[188] To enable actionable comparison across EDLC, pseudocapacitor, and hybrid systems, supercapacitor interphase evidence should be summarized in a standardized, metrics-linked format.[188,189]

4.4.1 Recommended evidence axes. Interphase signature (composition/thickness/morphology) + operating condition (electrolyte + voltage window + protocol) + device metrics (leakage, self-discharge, ESR, retention). This review therefore recommends that supercapacitor interphase claims be

Table 3 Representative techniques for SEI characterization and their cross-system adaptation

Technique	Battery application	Supercapacitor adaptation	Insight bridged
XPS	Depth profiling of LiF/Li_2CO_3 SEI	Detection of fluorinated/nitrile films	Composition and oxidation states
FTIR/Raman	Organic carbonate identification	Nitrile/carbonate vibrations	Functional-group evolution
Cryo-TEM	SEI morphology on Li metal	Dynamic reconstruction in IL-based capacitors	Structural reversibility
EQCM/EIS	Mass and impedance evolution	Film growth *vs.* ion adsorption	Kinetic coupling
AFM/EC-AFM	Nanomechanical mapping	Interphase elasticity and adhesion	Mechanical response

accompanied by at least one direct metric from each category: (i) leakage current or self-discharge rate; (ii) ESR evolution from EIS; and (iii) capacitance retention over cycling. When possible, coupling these metrics with *operando* EQCM/EIS and post-mortem XPS/ToF-SIMS establishes a causal link between film growth and performance drift.[88] On carbonaceous electrodes, XPS and EQCM studies in both battery and capacitor contexts reveal oxygen- and fluorine-containing SEIs forming above 2.5 V in organic electrolytes such as $TEABF_4$/ACN.[190] The interphase suppresses solvent oxidation but raises series resistance. In aqueous KOH or Na_2SO_4, Raman and AFM detect transient hydroxide layers that dissolve upon potential reversal, demonstrating the reversible nature of aqueous SEIs.[191]

For transition-metal-oxide electrodes (*e.g.*, MnO_2, NiO, V_2O_5), XPS and FTIR reveal hybrid SEIs combining metal–oxygen species and organic fragments.[192] Such interphases facilitate proton or cation insertion in both batteries and capacitors, though excessive growth hinders diffusion and causes capacitance fading.

Ionic-liquid-based systems exhibit inorganic-rich SEIs dominated by F- and S-containing fragments ($TFSI^-$ or PF_6^- derivatives).[61] Cryo-TEM and ToF-SIMS confirm dense coverage that stabilizes both Li–metal and carbon interfaces. In solid or gel polymer electrolytes, FTIR and NMR reveal polymer-electrode cross-linking and hydrogen-bond networks controlling interfacial ion mobility.[169,193] These case studies underscore that SEI chemistry reflects shared electrochemical principles, modified by electrode material, electrolyte chemistry, and potential range, rather than device category.

4.5 Sources of uncertainty and inter-laboratory variability

Despite progress, SEI characterization faces common limitations in both research domains. Ultrathin, reactive films challenge sample preparation and air-free transfer.[194] *Ex situ* methods capture static snapshots, whereas *in situ* techniques often trade spatial resolution for time resolution.[195] Discrepancies among laboratories arise from differences in cell geometry, electrolyte purity, and reference calibration.[196] The adoption of glovebox-integrated, cryogenic, and statistically replicated protocols now improves reproducibility. Moreover, coupling experimental outputs with simulation benchmarks, including radial distribution functions and predicted binding energies, provides cross-validation and minimizes interpretational ambiguity (Table 3).

4.6 Summary

The migration of SEI-characterization methods from batteries to supercapacitors has unified interphase science across energy-storage technologies. Techniques once reserved for thick, inorganic-rich films now resolve nanometer-thin, reversible SEIs in capacitors. Establishing standardized cross-system protocols, including consistent potential referencing, cryogenic handling, and quantitative multimodal analysis, will enable reproducible comparison and accelerate the integration of experimental data with computational modeling.

The experimental insights presented in this section provide the empirical foundation for the materials and interface engineering strategies discussed in Section 5, the multiscale modeling frameworks in Section 6, and the machine-learning approaches in Section 7 that translate observed interphase properties into predictive design tools.

5 Materials and interface engineering strategies

Performance and durability in both batteries and supercapacitors are governed by the interplay among electrodes, electrolytes, separators, and fabrication protocols. Although their energy-storage mechanisms differ, the fundamental challenge is the same: controlling interfacial reactions to form a stable, ion-conductive, and electronically insulating solid-electrolyte interphase (SEI).[197,198] This section consolidates materials selection, electrolyte design, surface modification, artificial interphase strategies, and mechanical stabilization approaches that have traditionally evolved in battery science but are now being systematically translated to supercapacitors, establishing a coherent framework for cross-platform SEI engineering.

The organization follows a logical progression: electrode materials and their surface engineering (Section 5.1), electrolyte chemistry and additive design (Section 5.2), architectural design principles (Section 5.3), manufacturing and structure–property relationships (Section 5.4), and actionable design rules (Section 5.5). Each subsection highlights how insights from batteries inform capacitor design, and *vice versa*.

5.1 Active material and interface modification approaches

The electrode acts as both the electronic conductor and the reactive template on which electrolyte decomposition initiates. In batteries, electrode surfaces catalyze reduction of solvent molecules and salts, forming SEI layers that regulate ion transport. A similar, though thinner and more dynamic, interphase develops in supercapacitors under high potentials.[199,200] Understanding this shared interfacial chemistry requires analyzing structure, composition, and surface functionality of the electrode, as well as deliberate surface modification strategies.

Table 4 Comparative summary of SEI-like/interphase behavior across major supercapacitor electrode families (carbons, metal oxides, MXenes)[a]

Electrode family	Primary stability limitation	Practical stabilization levers	Ref.
Porous carbons (AC, CNT, graphene, CDC)	Voltage-hold aging and local hot spots → pore blocking and ESR drift; oxidative decomposition at the positive electrode near V_{max}	Limit time at high V (avoid long holds); control defect density/ functional groups; heteroatom doping to suppress parasitic reactions; conformal ultrathin coatings to homogenize fields	31, 216 and 217
Transition-metal oxides (*e.g.*, MnO_2, NiO, V_2O_5)	Dissolution/surface reconstruction and irreversible film thickening → loss of active sites, rising resistance, fading capacitance	Electrolyte/pH control (in aqueous); surface coatings (carbon/ALD oxides) to suppress dissolution; protocol control near onset potentials; engineered porosity to reduce local flux hot spots	218–223
MXenes (*e.g.*, $Ti_3C_2T_x$)	Termination evolution/oxidation and resistive film growth under aggressive potentials; electrolyte-specific decomposition products accumulate with time/holds	Control termination chemistry and processing; select electrolyte to minimize oxidation; apply protective ultrathin coatings if ESR drift dominates; avoid sustained overpotential during holds	224–229

[a] Windows are representative ranges commonly used in the supercapacitor literature and should be interpreted as practical operating windows rather than universal limits; the stable window depends on electrolyte chemistry, electrode microstructure/defects, and testing protocol (rate *vs.* hold).

5.1.1 Carbon-based electrodes. Carbon materials remain the foundation of both Li-ion battery anodes and electric double-layer capacitors (EDLCs). Activated carbon, carbon nanotubes (CNTs), graphene, and carbide-derived carbons provide large surface areas and excellent conductivity.[201,202] In batteries, defects and oxygenated groups nucleate SEI formation; in capacitors, analogous surface terminations guide adsorption and mild solvent decomposition, yielding ultrathin SEI films.[203] Thus, tuning defect density and heteroatom doping (N, S, P) emerges as a universal handle for modulating SEI chemistry, balancing capacitance retention with interfacial stability.[204,205]

5.1.2 Metal oxide and conducting polymer systems. Transition-metal oxides such as MnO_2, NiO, and V_2O_5, along with their analogs in battery cathodes, share redox-active surfaces that catalyze both beneficial charge transfer and parasitic electrolyte decomposition.[206,207] The resulting hybrid SEIs contain inorganic (M–O, M–F) and polymeric components that regulate ion transport.[208,209] Stabilization strategies pioneered in batteries, including surface coating with carbon or ALD oxides and defect moderation, are now applied to pseudocapacitive electrodes to achieve similar durability and SEI uniformity.[19,57]

5.1.3 Nanostructured composites. Composite electrodes such as graphene/MnO_2 and CNT/PPy integrate conductivity and redox activity.[210,211] Their multiphase interfaces resemble those in composite battery electrodes, where heterogeneous electronic environments induce spatially varying SEI composition.[212,213] Managing these local variations through interface functionalization or graded heterostructures has become a cross-cutting strategy for both technologies.

5.1.4 Emerging electrode families. MXenes, metal–organic frameworks (MOFs), and covalent-organic frameworks (COFs) are bridging materials that blur the line between capacitor and battery electrodes.[214] MXenes exhibit metallic conductivity and surface terminations (–O, –OH, –F) that facilitate controlled SEI formation in both Li-ion and solid-state supercapacitors.[215] MOF- and COF-derived carbons offer tunable porosity and heteroatom content, improving charge storage and interfacial uniformity.[204] Their adaptability highlights a common principle: surface chemistry, not device classification, governs SEI behavior.

To improve cross-material comparison, Table 4 summarizes how carbon electrodes, redox-active metal oxides, and MXenes differ in their dominant interphase/SEI-like behavior, practical stability limits, and the typical voltage windows used in supercapacitor operation.

5.1.5 Surface chemistry engineering. Functional-group engineering provides an atomistic handle on interphase chemistry. Oxygenated carbons (C–O, C=O) improve wettability and ion accessibility but can catalyze side reactions if uncontrolled; nitrogen or fluorine doping, by contrast, lowers surface free energy, anchors inorganic fragments, and suppresses solvent decomposition.[230,231] In both batteries and capacitors, heteroatom doping modifies the electronic density of states near the Fermi level, shifting the onset potential for electrolyte reduction and enabling more benign, self-passivating SEI evolution.

Conformal coatings, including atomic layer deposited (ALD) oxides, molecular-layer-deposited (MLD) polymers, polydopamine (PDA), and graphene-oxide (GO) films, pre-form artificial buffer layers that moderate the first contact between electrode and electrolyte.[19,232] Thin (<5 nm) alumina or titania ALD coatings, proven to stabilize Li metal and Si anodes, have direct analogues in supercapacitors where they homogenize the interfacial field, prevent localized ion crowding, and mechanically reinforce porous structures.[233] Recent advances in

nanoscale electrode architecture, such as hierarchical porosity, vertically aligned nanotubes, and core–shell heterostructures, enable simultaneous control of ion transport and SEI uniformity.

Surface topology and curvature also influence SEI homogeneity. Hierarchically porous or scaffolded electrodes distribute ionic flux uniformly, reducing hot spots that trigger uncontrolled film growth.[232] For flexible or solid-state configurations, the combination of engineered surface morphology and compliant gel electrolytes produces solid–solid interfaces with enhanced mechanical tolerance.[198]

5.1.6 Structure–interphase relationships. Across both systems, the electrode's microstructure and surface modification dictate the morphology and chemistry of the SEI. Planar graphitic surfaces favor uniform organic SEIs; rough or catalytically active oxides promote thicker, inorganic-rich films that raise resistance.[19] Pore curvature, confinement, and doping tune local electric fields and electron density, leading to more homogeneous passivation layers. A mechanically stable and chemically uniform SEI ensures efficient ion transport and long-term cycling, whereas heterogeneity accelerates degradation. Thus, interfacial design principles, namely defect control, doping, surface functionalization, and conformal coatings, transcend device categories and form a transferable toolkit for SEI engineering.

5.2 Electrolyte formulation for controlled interphase formation

Electrolyte formulation is the second axis of SEI control. The electrolyte acts as both reactant and architect of the SEI, supplying the molecular precursors from which the interphase self-assembles.[98,234] Regardless of whether the system stores charge through ion adsorption or faradaic reactions, electrolyte decomposition initiates interphase formation. Concepts first proven in battery electrolytes are now being systematically adapted to capacitors, revealing consistent mechanisms governing SEI chemistry.

5.2.1 Role of electrolytes in interphase formation. The electrolyte conducts ions while insulating electrons between electrodes. Its dielectric constant, ion-solvation strength, and electrochemical stability window (ESW) define both energy density and SEI composition.[235,236] In both devices, wide-ESW electrolytes (organic or ionic-liquid) permit higher voltages but trigger reductive or oxidative decomposition that yields passivating films.[237] Therefore, electrolyte chemistry simultaneously enables performance and dictates interphase evolution.

5.2.2 Solvent and salt selection criteria. Aqueous electrolytes (Na_2SO_4, KOH) offer high conductivity but narrow voltage windows, forming transient hydroxide SEIs.[49,238] "Water-in-salt" formulations extend this window and generate inorganic-rich SEIs analogous to those in aqueous batteries.[239] Organic solvents such as acetonitrile (ACN) or propylene carbonate (PC) paired with $TEABF_4$ yield higher voltages but undergo anion-driven decomposition forming fluorinated SEIs similar to $LiPF_6$-based systems.[240] Room-temperature ionic liquids (RTILs) further stabilize interfaces through intrinsic ion pairing and preorganized solvation shells.[241] These parallels indicate that solvent chemistry is a primary driver of SEI structure, independent of device label.

5.2.3 Film-forming additives. Additives such as vinylene carbonate (VC) and fluoroethylene carbonate (FEC), long established in Li-ion batteries, are increasingly explored as interphase stabilizers in high-voltage supercapacitors.[59] In this context, additive success must be judged primarily by supercapacitor-relevant metrics, namely reduced leakage current and self-discharge without sustained ESR growth or loss of high-rate capacitance, rather than by battery-style SEI descriptors alone.

When effective, film-forming additives promote early formation of thin, electronically blocking yet ion-permeable interphases that suppress continuous electrolyte degradation; when ineffective, they can accelerate resistive thickening and pore blocking, increasing ESR and degrading power performance. Similarly, corrosion inhibitors or pH regulators in aqueous systems can stabilize surface chemistry and mitigate parasitic reactions, analogous to redox-mediated additives in batteries.[242] Machine-learning-guided screening of additive/solvent/electrode combinations is emerging as a shared optimization tool across both research domains,[243] but candidate additives should be down-selected using the actionable criteria summarized in Section 5.5 (design rules for leakage/ESR/retention trade-offs).

5.2.4 Electrolyte structure and SEI morphology relationships. Highly solvated ions favor polymeric, organic-rich SEIs; desolvated ions yield dense, inorganic layers.[28] This solvation-desolvation balance, previously quantified for Li^+ and Na^+ systems, equally determines the film composition on carbon electrodes in capacitors. Such cross-platform correlations between ion solvation energy and SEI density provides a bridge for modeling interphase formation across energy-storage technologies.

5.2.5 Electrolyte and separator coupling. Electrolyte and separator engineering collectively define ionic pathways and interfacial stability. Polyolefin (PP/PE) and PVDF separators ensure mechanical strength, while oxide-ceramic coatings (Al_2O_3, TiO_2) or cellulose membranes enhance wettability and dielectric robustness.[244,245] These design rules, originally optimized for lithium batteries, are now applied to supercapacitors to mitigate leakage and enable safe high-voltage operation.

5.3 Architectural design principles

Device architecture transforms material-level control into macroscopic performance. Symmetric cells with identical electrodes mirror the balanced configurations of dual-ion batteries, whereas asymmetric and hybrid designs emulate full cells by coupling capacitive and faradaic electrodes.[246] The same interfacial concerns, including contact resistance, electrolyte wetting, and mechanical adhesion, govern both technologies. Optimization therefore relies on common engineering metrics: minimized IR drop, uniform current distribution, and stable SEI adhesion.

5.4 Manufacturing and structure–property relationships

Electrode fabrication directly impacts SEI nucleation and evolution. Active materials (carbon, oxide, or polymer) are

typically mixed with conductive additives (carbon black, CNTs) and binders such as PVDF or PTFE.[25,247] The slurry is cast onto metallic current collectors (Al, Ni, stainless steel) and processed by doctor-blade or drop-casting, then dried and compressed for uniform thickness. Binder-free architectures such as graphene foams, carbon cloths, and vertically aligned CNT arrays minimize inactive mass and enhance conductivity.[248] These structural motifs, analogous to 3D current collectors in batteries, promote homogeneous SEI formation and mechanical stability.

5.4.1 Characterization and cross-system correlation. Structural and chemical analyses connect fabrication parameters with interfacial properties. Microscopy (SEM/TEM) visualizes pore architecture and SEI coverage; BET quantifies accessible area; XRD and Raman assess crystallinity and defect density; XPS and FTIR identify chemical species.[249,250] These same diagnostics, standard in both battery and capacitor research, provide a unified dataset for correlating morphology with electrochemical behavior. Integrating such multimodal data through statistical or machine-learning models establishes transferable descriptors (*e.g.*, SEI thickness, roughness, and impedance) that enable predictive interphase design.

5.5 Actionable design rules for supercapacitor interphases (EDLC/pseudocapacitor/hybrid)

The supercapacitor literature increasingly confirms that SEI-like interphases can be either beneficial (suppressing leakage/self-discharge) or detrimental (raising ESR and driving capacitance fade), depending on voltage stress, electrolyte chemistry, and electrode surface functionality.[169] To translate mechanistic understanding into practice, this section summarizes actionable design rules that connect (i) operating conditions, (ii) interphase signatures, and (iii) device-level metrics. These rules are intended to be applied together with the evidence-to-metric mapping framework introduced in Section 4 (metrics-linked reporting of interphase claims).

5.5.1 Boundary definitions (EDL *vs.* reversible pseudocapacitance *vs.* irreversible SEI-like films). To avoid conflating distinct interfacial processes in supercapacitors, we use the following practical boundaries. (i) EDL adsorption is *non-faradaic* charge storage dominated by electrostatic ion adsorption/desorption; its signatures are nearly rectangular CVs, minimal peak hysteresis, and largely reversible response with little new surface chemistry.[251] (ii) Reversible pseudocapacitive surface redox is *fast faradaic but reversible* electron-transfer (often surface/near-surface), typically producing broad redox features with limited polarization and stable peak position/shape over cycling; it should not cause persistent resistance growth when operated within a safe window.[252] (iii) Irreversible SEI-like films arise from *electrolyte decomposition* (or side reactions such as dissolution/deposition and surface reconstruction) and are identified by progressive accumulation of new species (*e.g.*, by XPS/ToF-SIMS/FTIR), together with monotonic drift in performance metrics (especially increasing ESR and/or accelerating capacitance loss).[169] Importantly, reversible redox and irreversible film formation can coexist on pseudocapacitive electrodes,[160] and therefore must be diagnosed using coupled electrochemical metrics and chemistry probes (consistent with Rule 6).

5.5.2 Practical "good *vs.* bad interphase" decision map (when interphase formation helps *vs.* hurts). In supercapacitors, an interphase is considered beneficial only when it reduces parasitic reactions without creating a dominant transport barrier.[253] A minimal decision workflow is: (1) Check leakage/self-discharge trend: if leakage current (or self-discharge rate) decreases or stabilizes with cycling/holds, interphase passivation is plausible. (2) Check ESR evolution (EIS): if ESR remains stable (no persistent mid-/low-frequency resistance growth), the interphase is not acting as a blocking layer. (3) Check capacitance retention: stable retention under cycling and modest voltage-hold protocols indicates the interface remains accessible (no major pore blocking/loss of redox sites). (4) Confirm chemistry-to-metric consistency: new surface species should correlate with beneficial metric shifts (lower leakage with stable ESR), not merely with degradation (ESR rise and capacitance fade).

Thus, good interphase ⇒ leakage/self-discharge ↓ (or stable) and ESR stable and retention stable; whereas bad interphase ⇒ ESR ↑ persistently and/or retention ↓ (often with pore blocking or loss of accessible redox sites), even if surface films are detected (Fig. 7).

5.5.3 Rule 1: treat a practical voltage threshold as a design constraint, not a performance target. For a given electrolyte and electrode, define an empirical onset potential V_{crit} above which irreversible interphase growth becomes measurable. In device optimization, the usable operating window should be selected such that (i) leakage current does not increase monotonically with cycling, and (ii) ESR does not drift upward persistently.[254] Practically, V_{crit} should be extracted from a combination of (a) leakage/self-discharge trends, (b) EIS-derived ESR evolution, and (c) corroborating surface chemistry (*e.g.*, XPS/ToF-SIMS).[255]

5.5.4 Rule 2: a thin, dynamic interphase is beneficial only if it lowers leakage without penalizing ESR. An ultrathin, partially reversible film can be performance-positive when it suppresses parasitic electrolyte decomposition and reduces self-discharge while maintaining fast ion exchange.[255] The operational signature of a beneficial dynamic interphase is: (i) decreased (or stabilized) leakage current with cycling; (ii) stable ESR (no sustained increase); and (iii) capacitance retention that remains insensitive to modest voltage-hold protocols.[256] If ESR rises systematically while leakage remains unchanged, the interphase is acting primarily as a resistive barrier rather than a passivating stabilizer.[257]

5.5.5 Rule 3: use protocol control (formation and conditioning) to steer interphase chemistry. Interphase chemistry in supercapacitors is highly protocol-dependent. When operating near V_{crit}, apply controlled conditioning steps rather than allowing uncontrolled early-cycle decomposition.[255] Practical strategies include: (i) stepwise voltage ramping; (ii) limited-duration voltage holds at subcritical potentials; and (iii) avoiding aggressive initial current densities that promote local hot spots.[258] Protocol control should be reported explicitly (current, hold time, temperature), because it can dominate film composition and thickness.[259]

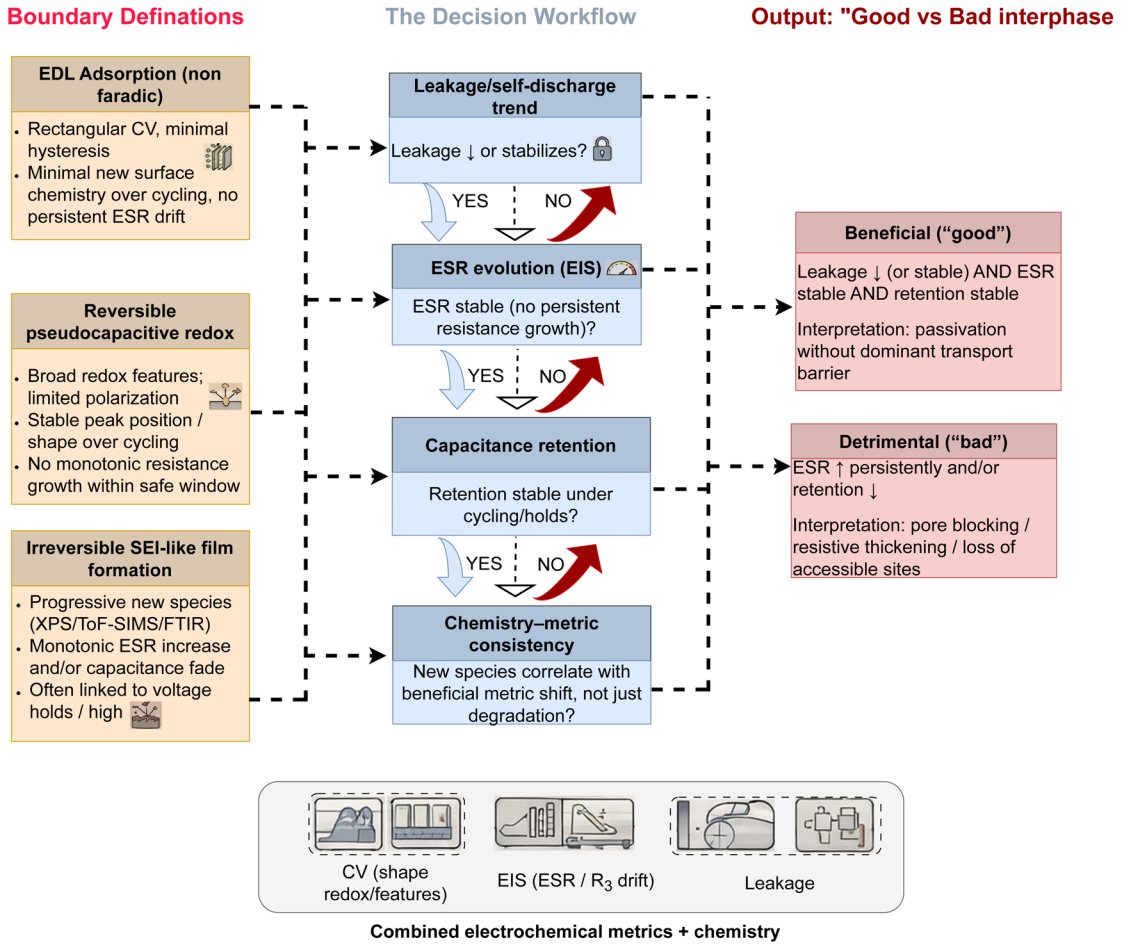

Fig. 7 Boundary definitions and decision workflow for distinguishing interfacial regimes in supercapacitor electrodes. The schematic separates (i) EDL adsorption (non-faradaic), identified by rectangular CV behavior, minimal hysteresis, and little persistent surface-chemistry or ESR evolution; (ii) reversible pseudocapacitive redox, characterized by broad redox features, limited polarization, stable peak shape/position, and no monotonic resistance growth within the safe operating window; and (iii) irreversible SEI-like film formation, indicated by progressive new interfacial species, monotonic ESR increase and/or capacitance fade, and frequent association with voltage holds or high-voltage operation. A decision workflow based on leakage/self-discharge trends, ESR evolution, capacitance retention, and chemistry–metric consistency is then used to classify the interphase as beneficial ("good") or detrimental ("bad").

5.5.6 Rule 4: transfer battery additive logic cautiously; target the metric outcome, not the chemistry slogan. Film-forming additives and salt/solvent choices that produce stable passivation in batteries can be useful in supercapacitors only when they demonstrably improve capacitor-relevant metrics (leakage/self-discharge, ESR drift, capacitance retention).[260] Additive screening in supercapacitors should therefore follow a metric-first workflow: (i) identify the limiting failure mode (leakage-dominated *vs.* ESR-dominated *vs.* gas-evolution/instability); (ii) test a small additive set designed to address that mode; (iii) accept an additive only if it improves at least two metrics simultaneously (*e.g.*, lower leakage and stable ESR).[259,260] This prevents "battery-style SEI improvement" claims that do not translate to capacitor performance.

5.5.7 Rule 5: engineer surface chemistry to suppress localized over-stress and defect-driven nucleation. Defect-rich sites, heterogeneities in wettability, and sharp curvature regions concentrate electric field and ionic flux, promoting nonuniform film growth.[261,262] Surface chemistry tuning can therefore be used as a stability lever (i) optimize heteroatom doping/functional groups to reduce reactive defect density; (ii) apply ultrathin conformal coatings (*e.g.*, oxide or carbon-based) to homogenize interfacial fields; and (iii) favor hierarchical porosity that distributes ionic flux and mitigates hot spots.[54,262,263] A successful surface strategy is indicated by more uniform interphase coverage together with reduced ESR drift.[263]

5.5.8 Rule 6: in pseudocapacitors, separate reversible surface redox from irreversible film formation. For pseudocapacitive materials, reversible surface redox can coexist with irreversible electrolyte decomposition.[264] To avoid conflating these processes, pseudocapacitor studies should (i) track redox-feature stability over cycling (*e.g.*, persistence/position of faradaic signatures); (ii) quantify irreversible resistance growth *via* EIS; and (iii) confirm whether new surface species correlate with loss of accessible redox sites.[265–267] Design

Table 5 Comparative interphase characteristics and actionable design rules for batteries and supercapacitors (EDLC/pseudocapacitor/hybrid)

System	Typical voltage window	Interphase nature	Dominant mechanism	Beneficial *vs.* detrimental outcomes	Actionable design rule	Key ref.
Battery (Li-ion/Li-metal)	~2.5–4.5 V (cell), anode at low potential	Thicker, relatively persistent (10–100 nm), slowly evolving	Electrolyte reduction at negative electrode; self-limiting passivation (inner inorganic/outer organic)	Beneficial: passivation, high CE, safety; detrimental: Impedance rise, Li loss, cracking under strain	Form SEI *via* controlled formation; use additives/coatings to minimize resistive growth and mechanical failure	14, 20, 273 and 274
EDLC (organic; AC/graphene)	~2.5–3.0 V (typ.)	Ultrathin, dynamic/patchy; pore- and defect-localized	High-field decomposition near V_{max}, especially at defects/micropores; partial reconstruction	Beneficial: leakage/self-discharge suppression; detrimental: pore blocking, ESR rise, capacitance loss	Operate below practical V_{crit}; if high V is required, use brief conditioning + additives only if leakage drops without ESR drift	28, 29 and 190
EDLC (ionic liquid/high-voltage)	~3.0–3.5 V (typ.)	Thin but more inorganic-rich; dynamic under rapid cycling	Anion/salt-driven decomposition (F/S-containing fragments); film formation under holds	Beneficial: stabilizes high V; detrimental: resistive thickening under long holds	Avoid long potentiostatic holds; choose salts/additives that form ion-permeable films; validate by leakage + ESR + rate-capacitance	27, 61, 275–278
Pseudocapacitor (metal oxides; aqueous)	~0–1 V (electrode-dependent; device ~1–2 V)	Highly condition-dependent; coupled to surface redox and local pH	Reversible surface redox *vs.* irreversible side reactions (dissolution/deposition/film)	Beneficial: stable redox capacitance; detrimental: active-site blocking, dissolution, ESR growth	Separate reversible redox from irreversible film growth (*operando* EIS/EQCM); tune pH regulators/coatings to preserve redox while suppressing parasitics	191, 192 and 218
Pseudocapacitor (MXene/polymers)	~0–1.2 V (electrode-dependent)	Interphase tied to terminations/solvation; can be reversible or aging-driven	Termination chemistry + solvent/salt reactions; polymer over-oxidation (for CPs)	Beneficial: stable pseudocapacitance; detrimental: resistive film/termination loss/over-oxidation	Control surface terminations; limit V to avoid irreversible chemistry; use ultrathin ion-permeable coatings if ESR drift dominates	26, 33, 279 and 280
Hybrid (LIC/battery-capacitor)	Device ~3.8 V (typ), electrode-selective polarization	Asymmetric: battery-like SEI on one electrode + capacitor film on the other	One electrode experiences battery-like overpotential; imbalance drives aging	Beneficial: stabilized anode; detrimental: ESR drift, capacity imbalance, rapid fade if overpolarized	Mass-balance to avoid sustained overpolarization; monitor electrode potentials (3-electrode) where possible; accept additives only if both leakage and ESR improve	11, 12, 281 and 282

choices (electrolyte, voltage window, coatings) should prioritize preserving reversible redox while suppressing irreversible film thickening.[266]

5.5.9 Rule 7: in hybrid (battery-capacitor) systems, mass-balance and electrode polarization control are mandatory. Hybrid devices often fail when one electrode is unintentionally driven into a battery-like overpotential regime that accelerates irreversible interphase growth.[268] Therefore: (i) electrode mass balancing should be chosen to prevent sustained over-polarization under the intended power profile; (ii) the negative electrode must be protected against reductive decomposition during high-rate charging; and (iii) development testing should include monitoring of polarization (ideally using three-electrode or reference-assisted diagnostics).[269–271] A hybrid design is acceptable only when both electrodes exhibit stable ESR evolution and high retention under realistic duty cycling.[272]

5.5.10 Minimum reporting checklist (to make design rules actionable). For each supercapacitor interphase claim, report at least: electrolyte composition; voltage window and protocol; electrode type and surface state; leakage/self-discharge; ESR evolution; capacitance retention; and at least one chemistry-resolved interphase probe (*e.g.*, XPS/ToF-SIMS) linked to the observed metric trends (Table 5).

5.6 Summary

Material and interface engineering strategies that stabilize SEIs in batteries, including controlled surface reactivity, electrolyte additive tuning, nanostructured architecture, artificial coatings, and mechanical stabilization, are directly translatable to supercapacitors. The convergence of electrode and electrolyte design principles across these technologies demonstrates that SEI formation follows universal shared chemical and mechanical rules rather than device-specific phenomena. By integrating experimental workflows (Section 4) and computational models (Sections 6 and 7), researchers can derive cross-platform descriptors linking composition, morphology, and transport. These descriptors provide the foundation for connecting SEI microstructure to macroscopic device performance, as discussed in Section 8.

6 Multiscale modeling and simulation of SEI formation

Understanding the solid-electrolyte interphase (SEI) requires bridging phenomena that span more than ten orders of magnitude in time and length. Bond cleavage and charge transfer occur at the quantum level, while film growth and mechanical evolution unfold across nanometers to micrometers and over thousands of cycles. Modeling frameworks must therefore integrate electronic-structure theory, molecular dynamics (MD), continuum transport, and device-scale formalisms within a coherent hierarchy.[212,283] Although the materials differ (Li metal anodes in batteries *versus* carbon electrodes in supercapacitors), the governing processes of electron tunneling, ion migration, and interphase reconstruction follow remarkably similar multiscale couplings.[284,285] This section reviews computational approaches that link the

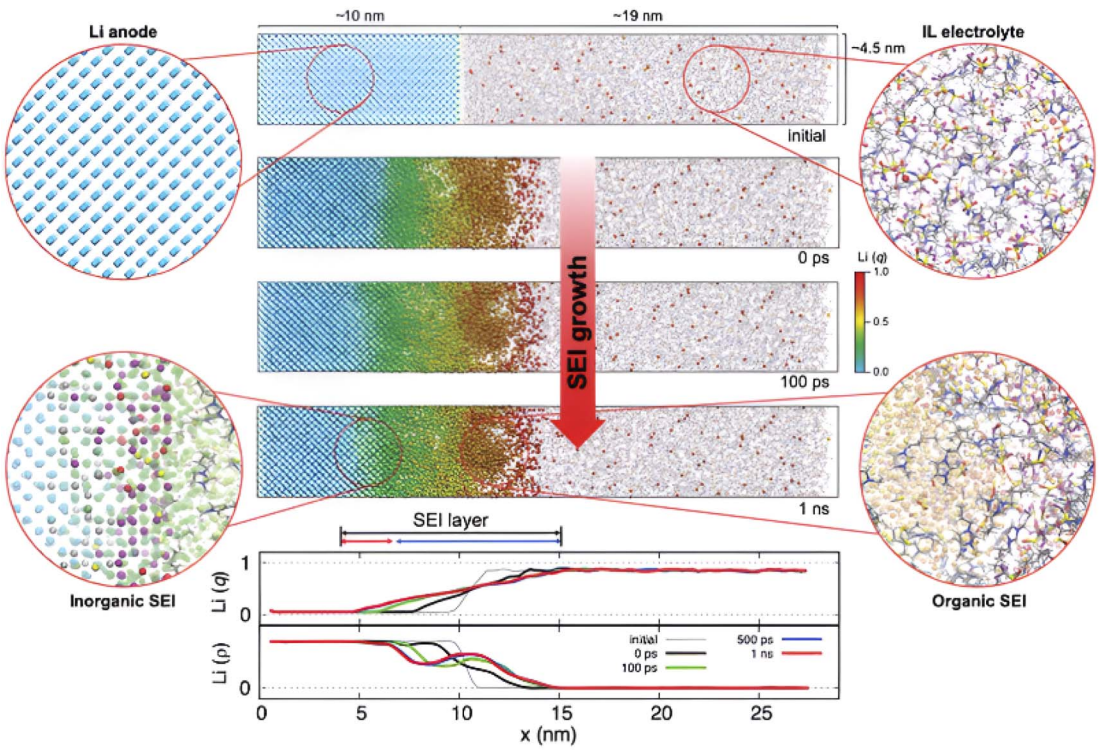

Fig. 8 Schematic overview of SEI-layer formation obtained from ReaxFF molecular-dynamics simulation at 300 K, showing the initial system configuration and the evolution of interphase species during early-stage electrolyte decomposition at the electrode interface. Reproduced from ref. 62 with permission from WILEY, Copyright 2023.

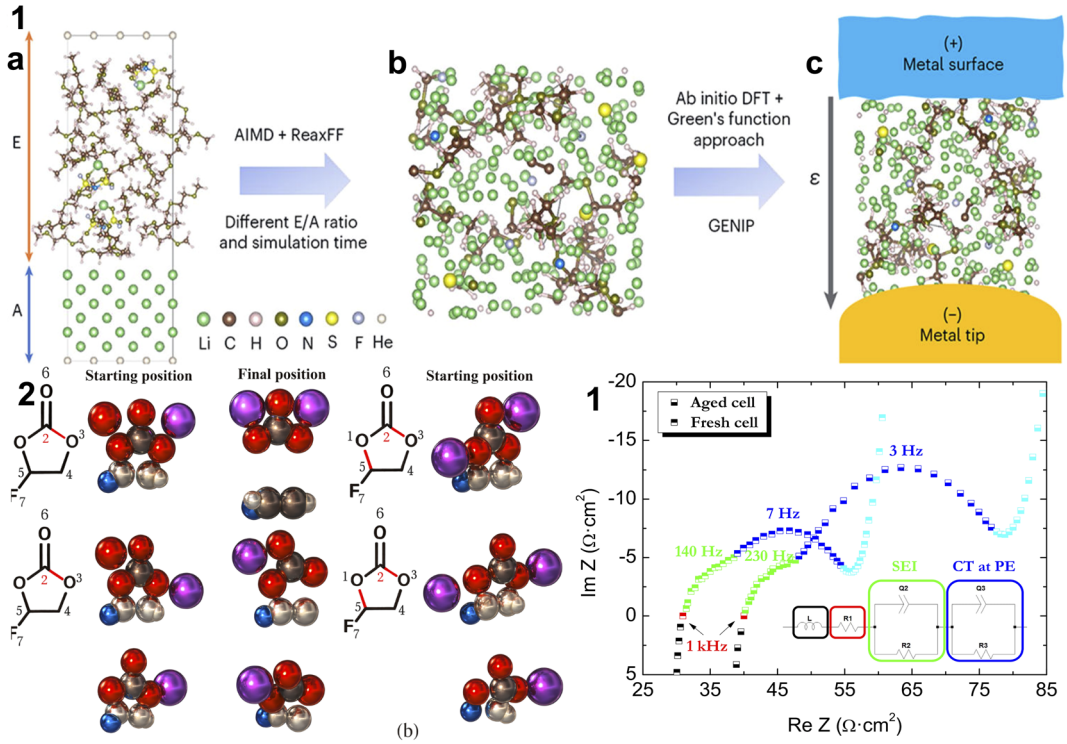

Fig. 9 (1) Atomistic modeling workflow: (a) AIMD/ReaxFF simulations capturing electrolyte decomposition under varying electron-to-atom (E/A) ratios; (b) structural evolution of SEI precursor species; and (c) GENIP-based *ab initio* DFT + Green's-function framework used to evaluate interfacial electronic properties between the SEI and metal surface. Reproduced from ref. 303 with permission from Nature Publishing Group, Copyright 2023. (2) The first type of initial bond breaking mechanism of FEC leading to the formation of SEI. Reproduced from ref. 304 with permission from IOP Publishing, copyright 2020. (1) Electrochemical impedance spectra (EIS) of fresh *vs.* aged cells, highlighting characteristic frequency regimes associated with SEI resistance and charge transfer processes at the porous electrode (CT at PE). Reproduced from ref. 305 with permission from MDPI, Copyright 2018 under CC BY 4.0 (http://creativecommons.org/licenses/by/4.0/).

microscopic mechanisms described in Section 3 with the experimental observables from Section 4, establishing predictive frameworks for SEI design.

6.1 Atomistic simulation methods

MD provides the fundamental atomistic perspective on SEI structure and dynamics. Atoms are treated as classical particles whose trajectories obey Newton's equations, evaluated through empirical or reactive interatomic potentials.[286–288] In both batteries and supercapacitors, MD captures ion adsorption, desolvation, and transport near polarized surfaces, thereby resolving the molecular origins of electric-double-layer formation and early electrolyte decomposition.[289–291] Analyses of velocity-autocorrelation and residence-time functions yield diffusion coefficients and relaxation constants that can be directly compared with electrochemical impedance or cyclic-voltammetry measurements. These correlations position MD as the molecular bridge linking interfacial structure with experimentally measurable capacitance and resistance.[292] The integrated atomistic-electronic workflow connecting AIMD/ReaxFF decomposition pathways to experimental impedance signatures is summarized in Fig. 9.

6.2 Electrostatic treatment of polarized interfaces

Capturing realistic electrode polarization is central to simulating SEI nucleation. Constant-charge (CCM) and constant-potential (CPM) models remain the two canonical approaches. CCM assigns fixed atomic charges and thus reproduces qualitative ion layering but underestimates capacitance under strong electric fields. CPM dynamically adjusts atomic charges to maintain an imposed electrode potential, reproducing metallic screening and local charge redistribution.[293,294] Recent extensions, including generalized (GCPM), heteroatomic (HCPM), and moment-tensor (mCPM) formulations, incorporate DFT-derived electronegativity and hardness, enabling accurate simulation of doped carbons, MXenes, and Li metal.[295,296] Such self-consistent polarization models now delineate the spatial onset of electron tunneling and electrolyte reduction, providing mechanistic routes to SEI nucleation in both capacitors and batteries.[296]

6.3 Chemical reactivity in force-field frameworks

The reliability of any MD study ultimately rests on its interatomic potential. Fixed-charge force fields such as OPLS, AMBER, and COMPASS are computationally efficient but nonreactive. Polarizable models, including induced-dipole and Drude-oscillator schemes, introduce electronic response, while charge-equilibration (QEq) and fluctuating-charge (FQ) approaches extend this to metallic polarization.[297,298] Reactive potentials such as ReaxFF explicitly describe bond formation and scission, thereby allowing simulation of electrolyte decomposition and SEI film growth.[299] In Li-ion systems,

ReaxFF has clarified ethylene carbonate reduction to Li_2CO_3, whereas in supercapacitors it reproduces acetonitrile and ionic-liquid fragmentation that yields CN- or F-containing interphases.[111,300] These studies consistently reveal heterogeneous nucleation, characterized by initial anchoring of inorganic fragments on the electrode followed by polymeric condensation. A representative ReaxFF simulation of SEI nucleation and early film formation is illustrated in Fig. 8, showing the molecular evolution captured during electrolyte decomposition.

Machine-learning (ML) potentials such as DeepMD, NequIP, and SpookyNet offer near-*ab initio* accuracy with classical scalability.[301] Trained on DFT trajectories for representative battery ($LiPF_6$/EC) and capacitor ($TEABF_4$/ACN) chemistries, these models reproduce many-body polarization, reactive events, and charge redistribution across diverse interfaces. Integration with active-learning and coarse-graining protocols has extended the accessible time window from nanoseconds to milliseconds, allowing direct simulation of interphase evolution under operational conditions.[302]

6.4 Mesoscale and macroscopic film evolution models

At larger scales, continuum and kinetic models treat the SEI as an effective mixed ionic-electronic conductor. Classical battery formulations by Peled and Newman describe diffusion-limited thickening with $d \propto t^{1/2}$,[306] while supercapacitor adaptations incorporate the rapid charge–discharge cycles and mechanical elasticity of thin interphases. The temporal evolution of film thickness can be expressed as

$$\frac{\partial d}{\partial t} = \frac{J_e M}{nF\rho} - k_{diss} d,$$

where J_e is electron flux, M and ρ are the molar mass and density of the SEI, and k_{diss} captures dissolution or reconstruction. This formalism unifies the diffusion-limited growth observed in batteries with the dynamic breathing and partial reconstruction characteristic of supercapacitor interphases.[307] Parameterization from MD or experimental data, such as ionic conductivity, reaction rate constants, and porosity, enables direct prediction of macroscopic ESR and capacitance decay.

6.5 Cross-scale coupling strategies

Multiscale coupling integrates information across five hierarchical tiers: (1) *ab initio* MD or DFT to resolve bond breaking and electronic structure; (2) reactive or ML-enhanced MD to describe nanometer-scale nucleation; (3) phase-field or coarse-grained dynamics for mesoscale morphology; (4) continuum transport for effective conductivity and mechanical response; and (5) device-level porous-electrode or equivalent-circuit models for performance metrics. Cross-scale demonstrations have revealed consistent scaling trends laws linking SEI thickness, ionic resistance, and energy efficiency in both Li-ion cells and ionic-liquid supercapacitors. Remaining challenges include rigorous parameter transfer, uncertainty propagation, and maintaining consistent boundary conditions for potential, solvation, and geometry across scales.[212,308,309]

6.6 Model benchmarking and future directions

Reliable SEI modeling requires consistent methodologies and quantitative validation. While battery modeling benefits from established community benchmarks, comparable datasets for capacitors are scarce.[310,311] Developing shared protocols encompassing standard boundary conditions, force-field benchmarks, and open reaction databases would enable direct cross-comparison and accelerate transferability of results. *Operando* XPS, Raman, and cryo-TEM provide indispensable validation for both technologies, while ML surrogates trained on combined battery-capacitor datasets may expose common descriptors such as local electric-field intensity, surface work function, and solvation number.[312] Outstanding challenges include bridging the temporal gap between nanosecond simulations and hour-scale degradation, expanding reaction libraries beyond carbonates to nitriles and ionic liquids, and quantifying mechanical coupling between SEI formation and electrode deformation.[313,314] Progress in these directions, anchored by interoperable datasets and open-source workflows, will transform SEI modeling from qualitative visualization to quantitative prediction, ultimately enabling rational interphase design that combines the energy density of batteries with the power capability of supercapacitors.

The multiscale simulation frameworks established in this section provide the theoretical foundation for the machine-learning approaches discussed in Section 7, where data-driven methods accelerate prediction, enable inverse design, and bridge the gap between atomistic accuracy and device-scale applicability.

7 Machine learning and data-driven SEI design

Machine learning (ML) has become a transformative tool for understanding and designing solid-electrolyte interphases (SEIs) across all electrochemical energy-storage systems. Whether in lithium-ion batteries or high-power supercapacitors, the SEI emerges from coupled electrochemical and chemical processes that span multiple scales—from bond breaking and radical formation to film growth, ion transport, and mechanical reconstruction. Because these processes are complex and interdependent, traditional modeling alone cannot capture their full hierarchy. Data-driven approaches, trained on both simulation and experimental results, now provide an adaptive framework that connects quantum accuracy with device-scale predictability. This section highlights how machine-learning interatomic potentials, spectroscopic analytics, and hybrid multiscale workflows jointly accelerate SEI discovery and design in both batteries and supercapacitors.

7.1 Machine learning-enhanced potentials for atomistic simulation

Machine-learning interatomic potentials (MLIPs) bridge the gap between first-principles fidelity and large-scale molecular dynamics (MD) simulation applicable to complex interfacial chemistry.[315,316] Traditional classical force fields, while efficient, cannot capture bond formation, charge polarization, or reactive

dynamics essential for SEI evolution. MLIPs trained on density-functional theory (DFT) data incorporate these phenomena at near-ab initio accuracy but at orders-of-magnitude lower computational cost.[315–317] This paradigm has already proven valuable in both $LiPF_6$/EC battery electrolytes and $TEABF_4$/ACN capacitor electrolytes, indicating that the same ML frameworks can learn transferable interfacial chemistry across different devices.[318]

A typical MLIP workflow begins with the generation of a representative dataset encompassing bulk electrolyte configurations, electrode surfaces (including doped carbons, Li metal, MXenes, and defects), solvation shells, and early decomposition products.[319,320] Neural-network or graph-neural-network architectures—such as Deep Potential (DeepMD-kit),[321] NequIP,[322] Allegro,[323] and SpookyNet—predict energies and forces from atomic configurations while enforcing rotational and translational equivariance (E(3) symmetry).[324] Such architectures capture the diverse bonding motifs present in SEIs: inorganic fluorides, organic carbonates, nitrile polymers, and metal–oxygen–fluorine species. Their data efficiency enables accurate modeling even when trained on relatively small, chemically diverse DFT datasets.[66,325]

When applied to SEI formation, MLIPs reproduce both the reductive decomposition of solvents and the nucleation of inorganic fragments. For example, the same potential can learn EC → Li_2CO_3 reduction pathways relevant to batteries and ACN → poly(CN) polymerization seen in capacitors.[67,320] Because MLIPs combine reactivity with scalability, they capture film nucleation, cross-linking, and mechanical densification—phenomena inaccessible to fixed-charge MD. They also allow microsecond-scale trajectories and nanometer-scale system sizes, bridging the gap between *ab initio* MD and continuum models.[67]

Nevertheless, successful deployment demands broad and physically balanced training sets. Datasets must cover the full configuration space—bulk, interface, radical intermediates, and decomposed fragments—to avoid extrapolation artifacts. In both batteries and capacitors, charge transfer and polarization are key; MLIPs must include charge-equilibration schemes or explicit electrostatics.[326] Transferability across potential windows and electrode chemistries remains a challenge: models trained solely on bulk or low-bias conditions can fail under extreme potentials unless continually retrained. Active learning, uncertainty quantification, and on-the-fly data generation mitigate these issues by automatically sampling configurations where prediction confidence is low.[327,328]

Thus, MLIPs offer a unified platform: they translate electronic-structure fidelity to mesoscale simulations, enabling predictive studies of SEI formation, growth, and failure across all electrochemical systems.

7.2 Data-driven interpretation of experimental characterization

As the SEI increasingly defines the performance envelope of both batteries and supercapacitors, the ability to predict its chemistry from experimental observations becomes critical.[15] ML-based analysis of spectroscopic and imaging data now provides this capability, transforming large, heterogeneous datasets into quantitative chemical maps.[329]

High-dimensional data acquired from X-ray photoelectron spectroscopy (XPS), time-of-flight secondary-ion mass spectrometry (ToF-SIMS), Raman and infrared spectroscopy, or hyperspectral electron microscopy contain the full chemical fingerprint of interphases but are notoriously difficult to deconvolute.[330] Traditional chemometric techniques—principal-component analysis, multivariate curve resolution—offer limited linear separation and cannot capture nonlinear correlations between spectral features and local chemistry.[331] In contrast, modern ML methods such as convolutional neural networks (CNNs), autoencoders, and graph-based architectures excel at uncovering hidden relationships among peaks, textures, and morphologies.[332]

In SEI analysis, supervised networks are trained on curated datasets linking spectra or images to ground-truth composition obtained *via* XPS deconvolution or *ex situ* chemical analysis. For example, CNNs applied to ToF-SIMS maps can distinguish inorganic-rich from polymer-rich domains; recurrent networks analyzing *operando* Raman time-series can detect transition points from stable to degrading interphases. Cross-domain learning between battery and capacitor datasets—where both share core chemical species (C–O, C–F, LiF, BF_xO_y)—improves generalization and reduces data requirements.

The benefits are multifold. First, ML accelerates screening of electrode/electrolyte combinations by predicting probable SEI compositions from rapid spectral snapshots.[67] Second, data-derived composition vectors can serve as direct inputs for continuum or transport models, eliminating assumptions about generic SEI chemistry.[333] Third, inverse modeling enables performance-to-chemistry inference: given capacitance fade or impedance growth, ML can estimate likely compositional shifts and identify underlying degradation pathways.[334]

To ensure reliability, datasets must include diverse electrode materials (graphite, doped carbons, MXenes, Li metal), electrolyte families (carbonates, nitriles, ionic liquids), and cycling histories.[335–337] Label accuracy and balance are critical; semi-supervised learning, transfer learning, and data augmentation help address data scarcity and imbalance. Interpretability tools—such as attention maps and SHAP analyses—link spectral features to specific bonds or chemical groups, ensuring that models retain physical meaning.[338] Uncertainty quantification should accompany all predictions, particularly when models guide design decisions or automated optimization.

As large, labelled spectral and imaging repositories become available, ML-based SEI composition prediction will evolve from a diagnostic tool to a predictive engine guiding electrolyte and electrode design in both battery and capacitor technologies (Fig. 10).[339]

7.3 Computational design of optimized interphases

Machine learning now acts as the connective tissue linking atomistic simulations, materials discovery, and device-level performance modeling. In both Li-ion batteries and

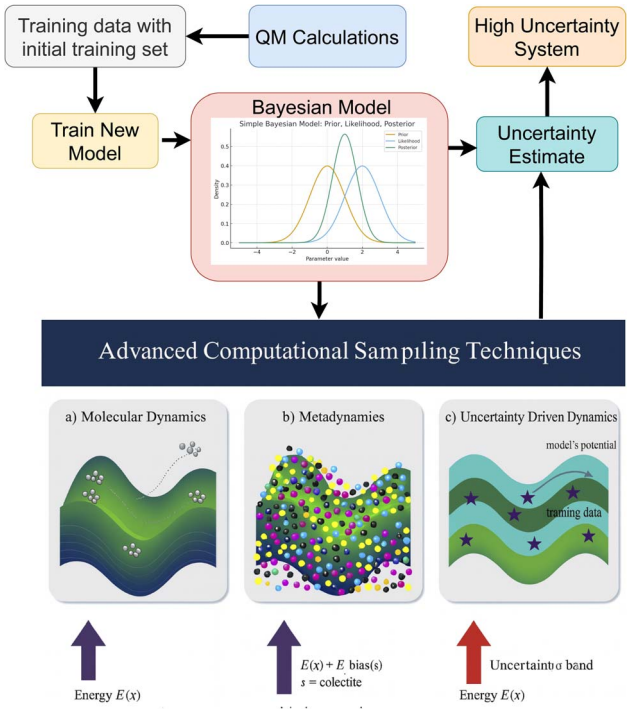

Fig. 10 Overview of an iterative workflow for developing interatomic potentials. A Bayesian model trained on QM data provides uncertainty estimates that guide additional sampling. Advanced techniques—including molecular dynamics, metadynamics, and uncertainty-driven dynamics—are used to explore the energy landscape and refine the potential.

supercapacitors, the SEI evolves through reaction-diffusion-mechanical processes spanning orders of magnitude in time and space.[340] ML frameworks integrate information from these scales to predict, optimize, and ultimately design interphases with tailored functionality. To make this mapping explicit, we provide one illustrative, end-to-end example (inputs → model targets → interphase properties → device metrics) using a supercapacitor-relevant configuration.Illustrative ML mapping example (supercapacitor EDLC case). Consider an activated carbon EDLC operated near the upper stability limit in an organic electrolyte (*e.g.*, $TEABF_4$/acetonitrile) where ultrathin SEI-like films may form and alter leakage and impedance.[341] An ML pipeline that links chemistry to performance can be defined with a transparent input–output structure:

• Inputs (descriptors) provided to the model. (i) Electrolyte descriptors: solvent reduction/oxidation tendency (*e.g.*, computed/estimated redox potentials), donor number/polarity, viscosity, dielectric constant; salt identity and anion chemistry; additive identity and concentration.[342,343] (ii) Electrode descriptors: surface functional groups/heteroatom content (XPS-derived O/C, N/C), defect density proxy (Raman I_D/I_G), and pore-size regime (micro/mesopore fraction).[344] (iii) Operating protocol: V_{max} (or cell window), presence/absence of voltage holds, temperature, and current density (or scan rate).[344]

• Training labels/targets (what the model learns to predict). Two linked target layers are used: (i) interphase properties (chemistry/structure): film thickness (EQCM mass-to-thickness proxy or microscopy), inorganic/organic fraction (*e.g.*, F-containing species, carbonates, nitrile-derived oligomers from XPS/ToF-SIMS), and an effective ionic/electronic resistivity proxy (from impedance fitting under a stated circuit hypothesis).[345] (ii) Device metrics: leakage current or self-discharge rate, ESR evolution from EIS, and capacitance retention over cycling/holds (as recommended in the evidence-to-metric reporting framework (Fig. 11)).[346]

• Model output and interpretation. Given candidate electrolyte/additive choices and a protocol near V_{max}, the trained model outputs: (i) a predicted interphase state vector $\{d, f_{inorg}, \rho_{ion/elec}\}$ and (ii) predicted metric trends $\{\Delta$leakage, ΔESR, $\Delta C\}$ under the specified protocol.[347] A beneficial prediction corresponds to leakage/self-discharge reduction without persistent ESR growth and with stable retention; a detrimental prediction corresponds to ESR drift and/or retention loss consistent with pore blocking or resistive thickening.[254]

• Decision/use case (actionable). The pipeline is then used to rank candidate electrolyte/additive/protocol combinations by a stability objective, *e.g.*, minimize leakage and ESR drift subject to a retention constraint. Importantly, this example is illustrative: the review does not claim a single universal model, but clarifies how reported descriptors (electrolyte/electrode/protocol) can be mapped to measurable interphase properties and supercapacitor-relevant metrics in a reproducible ML workflow.

7.3.1 Accelerating prediction. Surrogate ML models trained on high-fidelity DFT or MD datasets can instantly estimate SEI descriptors—film thickness, ionic conductivity, dielectric constant, or diffusivity—as functions of electrolyte formulation, potential, and temperature.[320] By learning complex nonlinear dependencies, these models bypass direct integration of differential equations, reducing computation while retaining interpretability.[348] In batteries, such surrogates predict LiF/Li_2CO_3 layer thickness under cycling; in capacitors, they forecast leakage-current evolution or impedance rise due to polymeric residue accumulation.[131] When coupled with continuum aging models, ML surrogates convert atomistic insights into lifetime and stability maps, providing a direct link between nanoscale chemistry and macroscopic performance.[284]

7.3.2 Data-guided inverse design. Beyond prediction, ML enables targeted electrolyte and additive discovery. Supervised and Bayesian-optimization frameworks learn mappings between molecular descriptors (reduction potential, donor number, viscosity) and SEI metrics (composition, resistance, ionic transport).[349,350] Once trained, these models can propose new solvent/salt/additive combinations that maximize interphase stability while minimizing electronic leakage. Battery-oriented efforts have already demonstrated automated electrolyte screening; extending these pipelines to capacitors requires inclusion of parameters relevant to EDL structure, dielectric constant, and surface wettability.[351] Feature-importance analyses reveal mechanistic trends—such as the dominant role of anion reduction potential or solvent polarity—that hold across both technologies.[349]

7.3.3 Hybrid multiscale workflows. The ultimate goal is a closed AI + physics loop where quantum calculations,

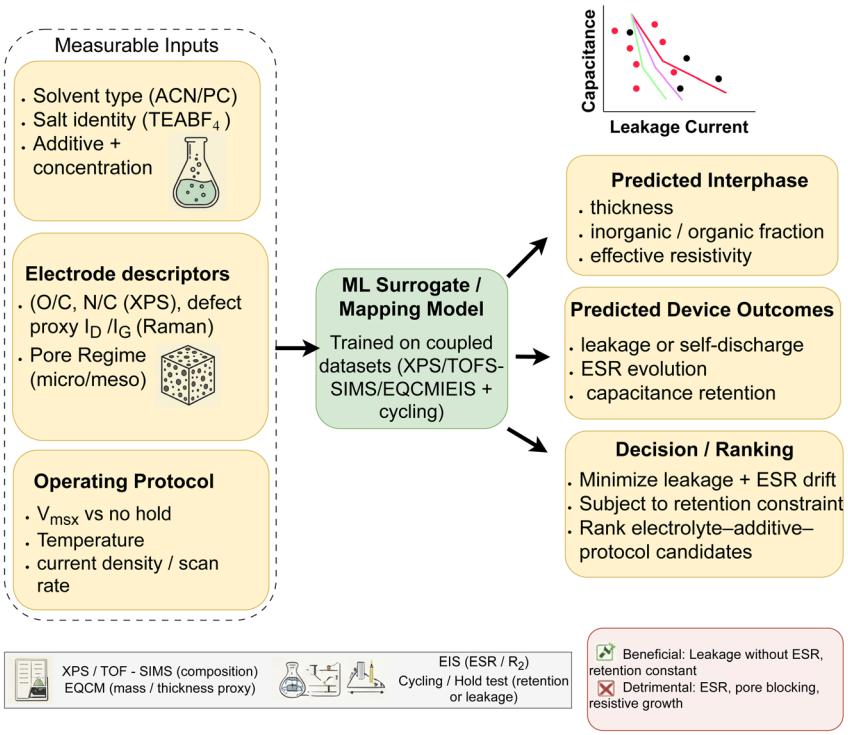

Fig. 11 Illustrative machine-learning workflow for interphase-aware screening in supercapacitor systems. Measurable inputs include electrode descriptors (*e.g.*, O/C and N/C from XPS, defect proxy I_D/I_G from Raman, and pore regime), electrolyte variables (solvent type, salt identity, additive chemistry and concentration), and operating-protocol descriptors (maximum voltage, presence or absence of voltage hold, temperature, and current density/scan rate). These inputs feed an ML surrogate or mapping model trained on coupled experimental datasets (XPS/ToF-SIMS/EQCM/EIS/cycling), which predicts interphase attributes such as thickness, inorganic/organic fraction, and effective resistivity, together with device-level outcomes including leakage/self-discharge, ESR evolution, and capacitance retention. The resulting predictions enable decision-making and ranking of electrolyte–additive–protocol combinations by minimizing leakage and ESR drift subject to retention constraints, while distinguishing beneficial interphases from detrimental resistive or pore-blocking growth.

atomistic MD, continuum models, and experiments continuously inform one another. A representative pipeline begins with DFT screening of reduction barriers for solvent and anion fragments; ML-enhanced MD simulates interphase nucleation and structural evolution; surrogate models extrapolate long-time growth; and continuum or equivalent-circuit models predict capacitance fade, ESR increase, or coulombic inefficiency. Experimental feedback—spectroscopic composition or impedance evolution—updates ML models through active learning, ensuring fidelity and uncertainty calibration. Such hybrid workflows automate interphase discovery and enable rapid prototyping of stable chemistries for both high-energy and high-power devices.

Together, these approaches constitute an ML-driven multiscale paradigm where data, physics, and experiment converge. By linking microscopic descriptors of SEI chemistry (bond energies, solvation motifs) to macroscopic metrics (resistance, capacitance retention), ML transforms SEI research from descriptive observation to predictive and generative design, unifying battery and capacitor interphase engineering.

7.4 Infrastructure for reproducible SEI research

The foundation of machine-learning progress is high-quality, interoperable data. While the battery community has begun establishing open datasets for electrolyte decomposition and SEI characterization, comparable resources for supercapacitors remain scarce. A unified benchmark repository—spanning both technologies—would dramatically accelerate cross-fertilization of modeling approaches.[352,353]

An ideal dataset would record electrolyte composition (solvent, salt, additive, concentration), electrode characteristics (surface area, functionalization, defect density), cycling conditions (voltage range, current density, cycle number), measured SEI properties (thickness, composition from XPS/ToF-SIMS, ionic/electronic resistance), and device-level performance (capacitance retention, self-discharge, ESR). Consistent metadata—temperature, humidity, geometry—must accompany every entry. Such structured datasets would allow ML models trained on one class of devices to transfer learning to another, enabling joint benchmarking and discovery of shared interphase descriptors.[19]

Recent community initiatives[314,354] advocate standardized protocols and open-source repositories for interphase modeling. Adapting these practices to the supercapacitor domain—and linking them with battery databases—will create the first truly interoperable SEI dataset ecosystem. This infrastructure will enable reproducibility, quantitative benchmarking, and generative design workflows where algorithms autonomously propose optimal electrolyte/electrode combinations for specific stability, conductivity, or mechanical targets.

7.5 Emerging paradigms in interphase discovery

Machine learning and data-driven modeling now stand at the frontier of SEI research.[186] Their integration with physical theory (Section 6) and experimental validation (Section 4) promises a future in which interphase chemistry is not merely characterized but computationally designed. By unifying datasets, algorithms, and modeling protocols across batteries and supercapacitors, the community can establish a shared predictive foundation—accelerating discovery of robust, adaptive SEIs that deliver both the high energy of batteries and the high power of capacitors.[355,356]

The modeling and machine-learning frameworks established in Sections 6 and 7 provide the theoretical and computational tools for SEI prediction and optimization. The materials and interface engineering strategies consolidated in Section 5 show how deliberate control of electrode surfaces, electrolyte chemistry, artificial coatings, and mechanical stabilization enables targeted SEI design in real devices.

8 Connecting SEI microstructure to device performance

The architecture and performance of supercapacitors are governed not only by the individual components (electrodes, electrolyte, and separator) but by the interplay of their interfaces, most notably the electrode–electrolyte interphase. In batteries this corresponds to the classical SEI, whereas in supercapacitors it is often an SEI-like interphase. This section explores how the microscopic features of these interphases, encompassing composition, thickness, ionic resistance, uniformity, and morphology, translate into macroscopic device parameters such as capacitance, leakage current, equivalent series resistance (ESR), self-discharge, and cycle life.[21,357,358] We then examine how these interfacial attributes may be incorporated into device-level models (equivalent circuits, porous-electrode frameworks) to enable predictive links between materials design and performance.[359,360]

8.1 Microstructural determinants of electrochemical metrics

The solid-electrolyte interphase (SEI) exerts a decisive influence on the electrochemical performance of supercapacitors by bridging nanoscale interfacial chemistry with macroscopic device behavior. Because the SEI occupies the immediate region between the electrode surface and the electrolyte, its thickness, composition, and uniformity directly regulate ion accessibility, charge–transfer pathways, and parasitic reactions.[357,361] A thin, ion-permeable SEI enables rapid ion adsorption and desorption, preserving high specific capacitance and low internal resistance. In contrast, a thick or defective SEI impedes ion migration, reduces accessible surface area, and induces localized ionic starvation, manifesting as lower capacitance and higher equivalent-series resistance (ESR). Experimental aging studies consistently link capacitance fading and ESR growth to electrolyte decomposition, pore blockage, and interfacial degradation.[21,357,358]

Beyond capacitance, the SEI critically modulates leakage current and self-discharge. Leakage current in a charged supercapacitor partly arises from unintended faradaic reactions at the electrode–electrolyte boundary. A stable SEI that is electronically insulating yet ionically conductive suppresses these parasitic currents and minimizes self-discharge, whereas a heterogeneous or discontinuous interphase promotes ongoing electrolyte breakdown and charge loss.[16,362] From an electrical standpoint, both ionic and electronic resistances contribute to ESR: ion transport through the SEI film and continuity of the conductive network across the electrode/SEI–electrolyte junction determine overall device impedance. As the SEI thickens or becomes more tortuous, ESR rises, diminishing rate capability and power output.[146,359]

These mechanistic correlations translate directly into measurable device-level outcomes, but meaningful comparison across studies requires that each claim be reported together with (i) electrolyte identity, (ii) cell configuration, and (iii) voltage window/protocol. For example, CNT-based electrodes protected by an ultrathin ALD-derived Al_2O_3 interlayer show reduced leakage current and improved capacitance retention relative to uncoated controls (cell: symmetric two-electrode; electrolyte: 1 M $TEABF_4$/ACN; window: 0–4 V; protocol: galvanostatic cycling + voltage-hold aging).[159,363,364] Likewise, fluoroethylene carbonate (FEC) as an electrolyte additive promotes a thinner, LiF-enriched interphase that suppresses parasitic reactions and improves capacitance retention (cell: symmetric two-electrode; electrolyte: 1 M $LiPF_6$/EC:DMC + 5 wt% FEC; window: 0–2.7 V; protocol: galvanostatic cycling).[365,366] In pseudocapacitive hybrid electrodes (*e.g.*, MnO_2/graphene), controlled voltage protocols and electrolyte selection can suppress ESR growth and dissolution (cell: two-electrode asymmetric; electrolyte: 0.5 M Na_2SO_4 (aq); window: 0–1.8 V; rate: 1 A g^{-1}).[189,216] In these cases, post-cycling surface analysis (XPS/ToF-SIMS/FTIR) is most informative when explicitly tied to the above operating conditions and to quantitative metric drift (leakage/self-discharge, ESR evolution, retention).[367,368] Accordingly, throughout this review we report supercapacitor interphase evidence in a minimally comparable format: electrolyte + voltage window/protocol + cell configuration + at least one metric (leakage/self-discharge, ESR drift, retention).

Collectively, these observations establish a coherent interphase-to-performance link: optimized SEI formation through artificial coatings, electrolyte or additive design, and mechanical stabilization enhances ion accessibility, suppresses leakage and ESR growth, and extends cycle life. Treating the SEI as a designed component rather than a passive by-product thus enables supercapacitors that combine high energy and power densities with exceptional long-term reliability (Fig. 12).[369,370]

8.2 Embedding interphase physics in device models

To translate interphase-level understanding into device-level predictive capability, modeling frameworks must embed SEI properties explicitly. Two modelling paradigms dominate: equivalent circuit modelling and porous-electrode (continuum) modelling.

Equivalent circuit models represent the supercapacitor as an ideal capacitor in series and parallel with resistive and reactive

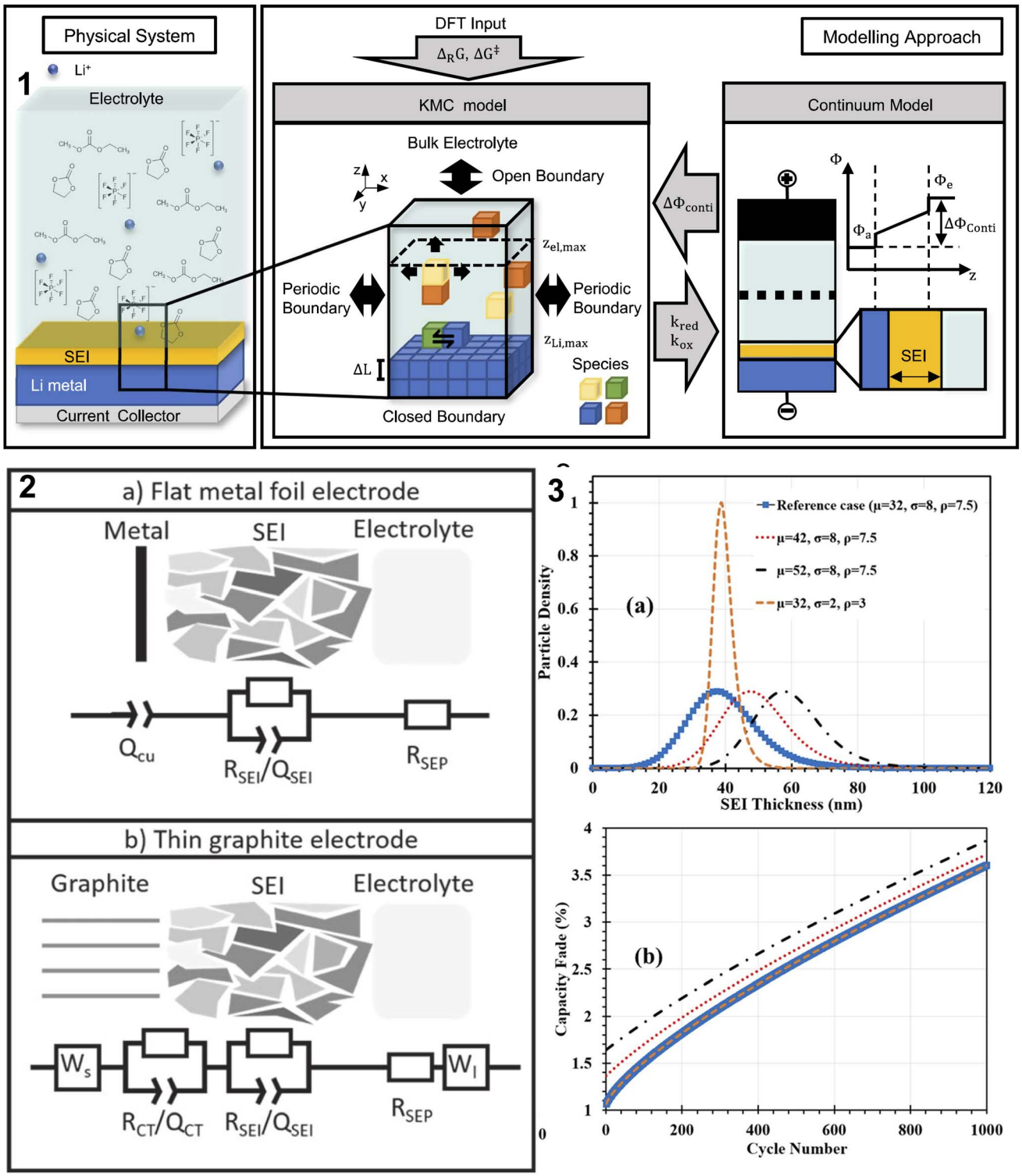

Fig. 12 (1) Schematic overview linking the physical Li/electrolyte system with KMC-based SEI growth modeling and continuum-scale electrochemical transport. Reproduced from ref. 371 with permission from Nature Publishing Group, Copyright 2013. (2) Equivalent circuit models for the SEI analysis a metal foil equivalent circuit. Reproduced from ref. 145 with permission from IOP Publishing, copyright 2024. (3) SEI-thickness-distribution (a) and corresponding capacity fade including the cycle number (b) Reproduced from ref. 372 with permission from IOP Publishing, copyright 2017.

elements: typically capacitance (C), equivalent series resistance (ESR), leakage resistance (R_{leak}), and sometimes a distributed transmission-line component to represent pore impedance.[359] Within this simplified framework, the SEI may be represented as an additional resistive and capacitive layer: a series resistance and a parallel leakage path reflecting ion transport and

parasitic reactions respectively. As the interphase evolves (thickness increases, transport resistance grows, composition changes), the corresponding circuit parameters change.[359,373] For example, ESR rises, leakage resistance lowers, and effective capacitance is reduced. Careful calibration of equivalent-circuit elements to EIS data can link impedance evolution to interfacial degradation, but for porous electrodes the mapping is not one-to-one.[374,375] Mid-frequency arcs can originate from interphase films (R_f||CPE_f), electronic/contact limitations, or pore transport/surface charging that is better represented by a transmission-line model (TLM).[376] Therefore, we recommend reporting EIS-derived interphase metrics only within an explicit interpretation framework: (i) fit at least one porous-electrode-aware circuit (TLM-based) in addition to a lumped circuit; (ii) demonstrate parameter robustness across state-of-charge/voltage window and electrode thickness; and (iii) corroborate the assigned interphase element using independent interphase evidence (XPS/ToF-SIMS/cryo-TEM thickness/chemistry or EQCM mass evolution). Under these constraints, trends in fitted film resistance/capacitance can be used as quantitative indicators of interphase growth, pore blockage, or contact degradation rather than as a unique SEI "signature."

8.2.1 Practical interpretation framework (porous electrodes). To distinguish interphase resistance from pore-transport/contact effects, a minimal workflow is: (1) verify the high-frequency intercept (R_Ω) using electrolyte conductivity and cell geometry; (2) test thickness dependence: contact/constriction and electronic limitations often scale differently with electrode mass loading than a true film element; (3) compare symmetric *vs.* full cells (electrode/electrode *vs.* electrode/counterelectrode) to isolate interfacial contributions; (4) fit using a porous-electrode transmission-line representation and report confidence intervals/covariances to highlight non-uniqueness.

8.2.2 Representative circuits recommended for this review. (i) Lumped (non-porous/diagnostic baseline): R_Ω–(R_{ct}|| CPE_{dl})–W.[377] (ii) Porous EDLC (distributed charging): R_Ω–TLM_{pore} (distributed ionic resistance + distributed double-layer CPE).[378] (iii) Porous electrode with interphase film: R_Ω–(R_f|| CPE_f)–TLM_{pore}, optionally plus $R_{contact}$ when validated by thickness/current-

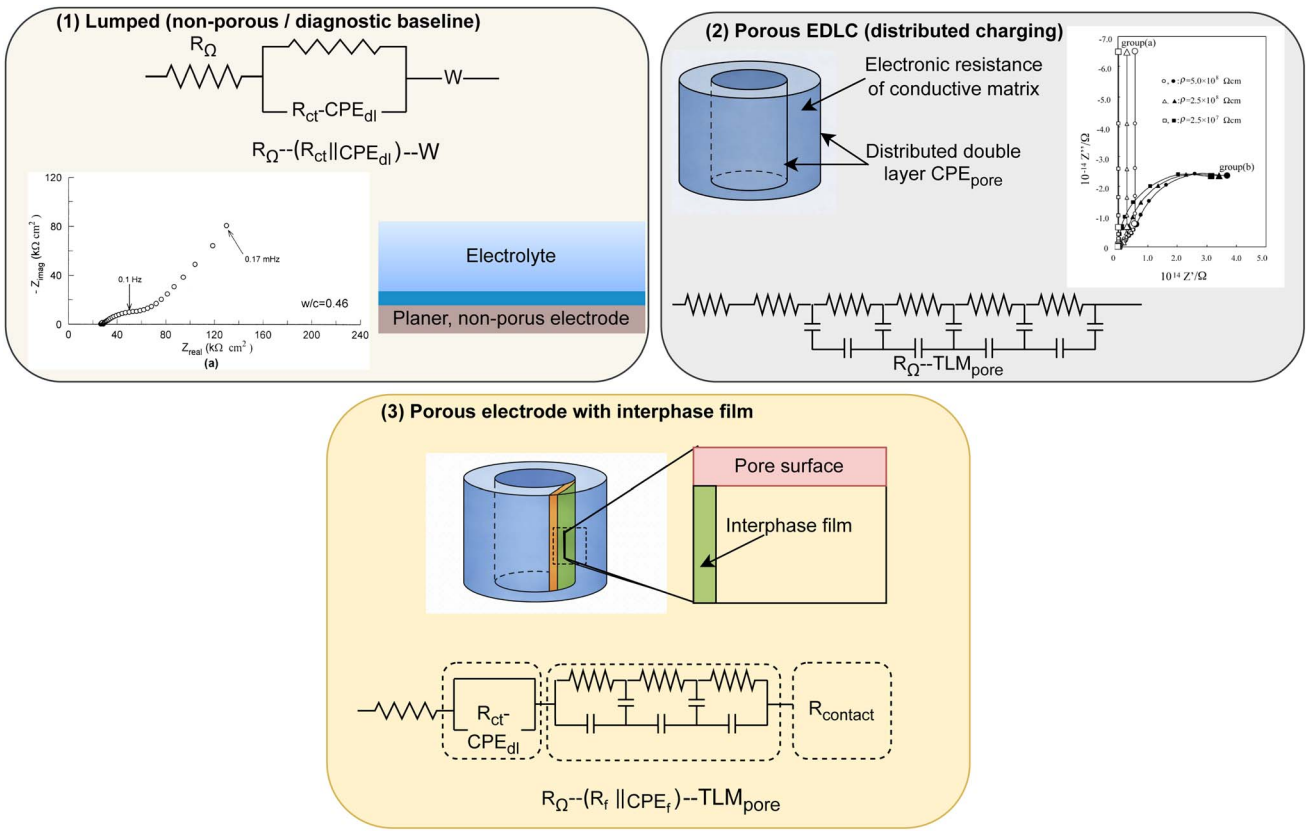

Fig. 13 Representative equivalent-circuit frameworks recommended for interpreting interphase-related impedance in porous electrochemical systems. Panel (1) shows a lumped, non-porous diagnostic baseline, R_Ω–(R_{ct}|| CPE_{dl})–W, appropriate for compact electrodes where charge-transfer and diffusion contributions can be approximated without distributed pore effects. Panel (2) shows a porous EDLC transmission-line representation, R_Ω–TLM_{pore}, in which distributed ionic resistance and double-layer charging within the pore network generate the characteristic impedance response of porous carbon electrodes. Panel (3) shows a porous electrode with an interphase-film contribution, R_Ω–(R_f|| CPE_f)–TLM_{pore}, optionally including $R_{contact}$ when supported by thickness- or current-collector-dependent tests. Together, these schematics emphasize that mid-frequency arcs in porous systems may arise from overlapping pore-transport, contact, and film-related processes, so assignment of R_f as an SEI/interphase term should be made only when corroborated by independent interphase diagnostics and protocol-dependent trends.

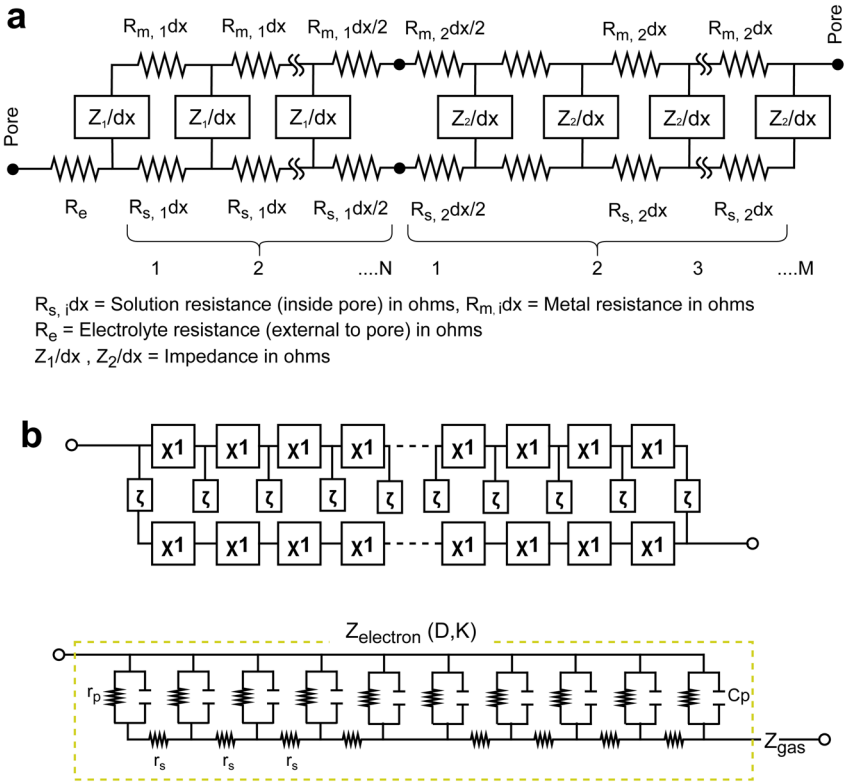

Fig. 14 Representative porous-electrode transmission-line schematics used to describe distributed impedance in porous systems: (a) a detailed pore model including electrolyte resistance external to the pore (R_e), solution resistance inside the pore ($R_{s,i}dx$), metal resistance ($R_{m,i}dx$), and distributed local impedance elements (Z_1/dx, Z_2/dx). Reproduced from ref. 381 with permission from IOP Publishing, copyright 2009; and (b) a simplified ladder-network representation highlighting distributed ionic/electronic pathways and interfacial contributions, including pore resistance (r_p), series resistance (r_s), pore capacitance (C_p), and terminal impedance terms $Z_{electron}(D, K)$ and Z_{gas}. Reproduced from ref. 382 with permission from the Korean Ceramic Society, copyright 2016, under CC BY-NC 4.0 (http://creativecommons.org/licenses/by-nc/4.0/). These schematics illustrate how porous-electrode architectures naturally generate distributed impedance responses, motivating porous-electrode-aware interpretation of Nyquist features.

collector tests.[379] We emphasize that (ii) and (iii) can produce similar mid-frequency arcs; assignment of R_f as an interphase/SEI term should be made only when supported by independent interphase diagnostics and consistent protocol-dependent trends.

Porous-electrode models build on more physically realistic descriptions of ionic and electronic transport within electrode architectures. They couple mass transport in electrolyte, ion adsorption at electrode surfaces (double-layer or pseudocapacitive behaviour), electron conduction in the solid phase, and interfacial kinetics.[359] In such frameworks, the SEI can be modelled as an interfacial film with defined thickness, ionic conductivity, porosity, and reaction kinetics.[360] For example, ionic diffusion through pore networks is slowed by an SEI film that reduces pore diameter or increases tortuosity; thereby, the effective ionic diffusivity and active surface area are reduced.[359] Recent reviews of transport in charged porous media highlight how film layers and pore constrictions modulate ion accessibility and charge dynamics. By embedding SEI parameters into porous electrode models (for instance, adding an ionic resistance layer, reducing pore cross-section, or adjusting double-layer capacitance per unit area), one obtains predictive time-dependent performance simulations: charge–discharge curves, rate capability envelopes, EIS Nyquist spectra evolution, and cycle life prediction. These models enable bridging between atomic-scale SEI properties (thickness, composition, ionic transport) and system metrics (capacitance retention, ESR drift, self-discharge). Moreover, multi-physics modelling (coupling electrochemical, thermal and mechanical submodels) can incorporate temperature effects on SEI conductivity, mechanical cracking of the film, and consequent performance degradation (Fig. 13–15).[212,380]

8.3 Synergistic experimental-computational platforms

In modern supercapacitor research, the interphase between electrode and electrolyte no longer remains a mere passive layer but has evolved into a controllable interface through the convergence of *in situ*/*operando* measurement techniques, molecular dynamics (MD) modelling, and machine learning (ML)-based data interpretation.[384] This closed-loop approach begins with high-temporal-resolution experimental measurements such as electrochemical impedance spectroscopy (EIS), electrochemical quartz-crystal microbalance (EQCM), *operando* Raman or X-ray reflectivity, and cryo-TEM imaging, all of which provide real-time signatures of the solid-electrolyte interphase

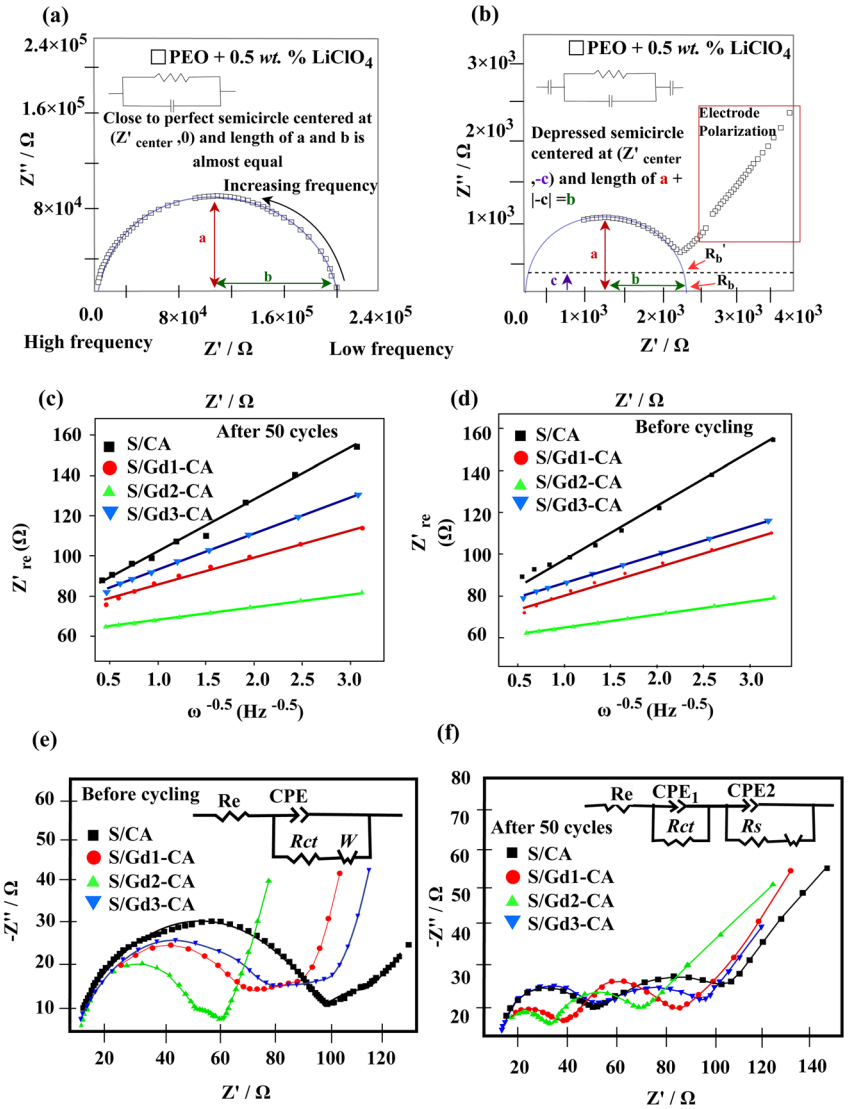

Fig. 15 Representative impedance analyses showing that Nyquist features in porous electrochemical systems arise from multiple overlapping processes rather than from a unique SEI resistance. Panels (a) and (b) illustrate ideal and depressed semicircles, highlighting the influence of electrode polarization and interfacial heterogeneity on arc shape. Reproduced from ref. 383 with permission from De Gruyter, copyright 2021, under CC BY 4.0 (https://creativecommons.org/licenses/by/4.0/). Panels (c) and (d) show the linear relationship between Z'_{re} and $\omega^{-0.5}$ before and after cycling, indicating diffusion-related impedance evolution. Panels (e) and (f) present Nyquist plots before cycling and after 50 cycles with corresponding equivalent-circuit fits, showing that cycling alters the combined contributions of bulk transport, charge transfer, interfacial response, and diffusion. Reproduced from ref. 382 with permission from the Korean Ceramic Society, copyright 2016, under CC BY-NC 4.0 (http://creativecommons.org/licenses/by-nc/4.0/). Together, these panels emphasize that impedance changes must be interpreted with physically justified circuit models and supporting interphase evidence.

(SEI) formation, ion transport changes and morphological evolution under cycling.[171,385] These experimental datasets feed into ML algorithms that rapidly interpret spectral, imaging and impedance features, infer SEI metrics (*e.g.*, thickness, ionic resistance, porosity, heterogeneity) and compare them to predictive models derived from MD. The ML output then informs MD (or ML-surrogate) simulations under the updated interphase state, applied voltage protocols and electrolyte conditions.[62,386] Simultaneously, device-level performance metrics, including capacitance drift, leakage current increase, and equivalent series resistance (ESR) growth, are monitored to validate or recalibrate the model, thereby creating a feedback loop: experiment → ML insight → simulation → updated experiment.

For supercapacitors, where high rate cycling, thin films and rapid interphase evolution are typical, this feedback loop enables real-time interphase management. For example, when impedance growth accelerates unexpectedly, the ML model can signal that the SEI ionic resistance has reached a threshold, prompting an adjusted cycling protocol (*e.g.*, reduced voltage hold, rest period) or trigger an additive injection. The MD component provides mechanistic insight—how desolvation barriers, pore blockage or ion-film interaction evolve with film composition—thus strengthening the predictive fidelity of the

workflow.[387] This proactive framework transforms the SEI from a passive, post-mortem phenomenon into an actively managed interface.

The power of this integrated loop extends to accelerated lifetime prediction: early-cycle fingerprints of SEI growth (*e.g.*, rapid increase in ionic resistance or specific Raman shifts) are correlated by ML with long-term cycle performance, enabling the simulation of interphase evolution under projected usage conditions. This anticipatory capability is especially valuable in high-power supercapacitors, where ensuring interphase stability over thousands of fast cycles is a prerequisite. By tying simulation parameters to actual device conditions (ion concentration, pore wetting state, morphological change) rather than idealised models, the feedback approach significantly reduces the gap between laboratory insight and real-world device behaviour.[388]

Nevertheless, successful deployment of such *in situ*/ML/MD feedback loops demands rigorous data synchronisation (experiment *vs.* simulation time scales), transparency of ML decision-making (avoiding black-box predictions), and sufficiently large and diverse training datasets linking SEI signatures to performance across cycling regimes and chemistries. In spite of these challenges, the closed-loop paradigm stands as a transformative route toward predictive, real-time SEI control and device-level interphase optimisation in next-generation supercapacitors.[389]

8.4 Interphase engineering for advanced device configurations

Hybrid supercapacitors, which combine characteristics of both batteries (high energy) and capacitors (high power), alongside solid-state supercapacitor architectures impose distinctive demands on the solid-electrolyte interphase (SEI).[390] In battery-capacitor hybrids (such as Li-ion or K-ion insertion anode paired with a capacitive cathode), the SEI must tolerate high current density, large ion flux, and broad voltage swings while enabling rapid ion exchange typical of capacitors. In such systems, the negative electrode often undergoes faradaic insertion and SEI formation similar to battery anodes.[391,392] Studies on non-aqueous potassium-ion hybrid supercapacitors reveal that formation protocols influence SEI composition (*e.g.*, KF content) and cycling stability, demonstrating the critical role of the interphase in hybrid performance.[393,394] Meanwhile, in solid-state supercapacitors (polymer or ceramic electrolytes), the interphase becomes a "solid–solid" boundary layer that must maintain mechanical and ionic continuity under compression, bending or thermal cycling. Here, the SEI must be ionically conductive, electronically insulating, and mechanically robust, often serving simultaneously as the electrolyte interface and protective interphase.[284]

From a modelling and engineering perspective, these hybrid and solid-state systems demand tailored SEI strategies. For hybrids, simulation must incorporate ion insertion kinetics, interphase growth under dynamic flux, and coupling between faradaic and capacitive processes.[395] For solid-state systems, interphase modelling must include mechanical deformation, adhesion, stress propagation, and film continuity under mechanical load.[284] The engineering implications are significant: electrodes must be designed to tolerate mechanical strain and rapid flux, while electrolytes must be formulated to produce interphases that resist delamination, preserve ion pathways and mitigate interface degradation.[396] Accordingly, SEI design in hybrid supercapacitors demands a holistic view integrating insertion chemistry, interphase transport, mechanical resilience and high-rate operation, enabling devices that deliver both high energy and high power with durability.[390]

8.5 Design for sustainability and end-of-life recovery

Beyond immediate performance improvements, the engineering of the SEI must address long-term sustainability and recyclability of supercapacitor technologies.[70] The interphase layer, frequently composed of decomposition products, polymer fragments or engineered coatings, influences device lifecycle, end-of-life behaviour and material recovery. From a materials-circularity standpoint, SEI design must consider environmentally benign solvents, salts and additives, low-toxicity coatings, and film formulations that facilitate safe disposal or regeneration. For instance, avoiding high-toxicity fluorinated additives or unstable polymer residues may reduce environmental footprint and simplify recycling workflows.[397]

Recycling supercapacitors often requires predictable interphase chemistry: electrodes coated with stable but removable or convertible layers allow more efficient separation of electrode, current collector and electrolyte during end-of-life processing. Engineered SEIs that deposit uniform inorganic salt layers (rather than uncontrolled polymeric debris) enable more consistent recycling behaviour and material recovery. Moreover, the reduction of self-discharge and leakage current through optimized SEI design extends device lifetime and thereby reduces waste associated with early replacement.

From a manufacturing and lifecycle perspective, SEI engineering also influences formation times (with energy savings), cell safety (reduced leakage), and module durability (fewer replacements).[71] By integrating sustainability considerations into interphase design—selecting benign chemistries, designing films that facilitate separation or recovery, and minimising long-term degradation—researchers align high performance with environmental and economic viability.[186,398] Ultimately, treating the SEI not only as a performance filter but as a sustainability fulcrum ensures that next-generation supercapacitors deliver high energy, high power and high longevity while embodying circular-economy principles.

8.6 Summary

This section has demonstrated how SEI microstructure—composition, thickness, ionic resistance, and morphology—directly determines macroscopic device metrics including capacitance, leakage current, ESR, and cycle life. By embedding interphase parameters into equivalent-circuit and porous-electrode models, and by establishing *in situ* feedback loops that couple MD, ML, and experiment, researchers can now predict and control device performance from first principles.

The insights from Sections 2 through 8—spanning fundamental electrochemistry, microscopic mechanisms, experimental characterization, multiscale modeling, machine learning, materials engineering, and device integration—collectively establish a comprehensive framework for SEI science in supercapacitors. Section 9 builds on this foundation to identify strategic future directions that will transform SEI engineering from an empirical art to a predictive science.

9 Future directions and opportunities

As the field of solid-electrolyte interphase (SEI) engineering for supercapacitors matures, several overarching opportunities emerge that promise to elevate interphase design from empirical trial-and-error to predictive, data-driven, and sustainable engineering. We highlight five strategic frontiers: unification of interphase theory across batteries and capacitors; artificial-intelligence (AI)-accelerated multiscale simulation for real-time interface evolution; open databases for SEI chemistries and degradation pathways; coupling quantum-electronic transport simulations with interfacial models; and design of sustainable electrolytes and eco-friendly SEI layers for next-generation energy storage.

9.1 Unified theory across energy-storage modalities

Historically, SEI research has primarily focused on rechargeable batteries, especially lithium-ion systems, where the SEI at the anode plays a critical role in capacity retention and safety.[134,399] In contrast, SEI phenomena in supercapacitors have received only limited attention, despite the fact that electrode–electrolyte interphases in high-power capacitive devices face analogous challenges (*e.g.*, electrolyte decomposition, ion-transport impediment, interphase mechanical fatigue). A unifying theoretical framework that spans both battery and supercapacitor interphases would facilitate cross-pollination of mechanistic insights—such as electron tunnelling, ion–solvent reorganisation, interphase growth kinetics and mechanical failure modes.[19,28]

Such convergence requires systematic comparison of interphase chemistries, growth pathways, transport resistances and mechanical behaviours under the distinct operating regimes of batteries (slow charge, deep insertion, large volumetric changes) and capacitors (fast charge/discharge, high ion flux, minimal diffusion depth). By leveraging common descriptors (*e.g.*, electron tunnelling barrier, ion-film diffusivity, film fracture toughness), researchers can develop shared modelling tools, standardised measurement protocols and unified degradation metrics.

9.2 Machine-learning-enhanced multiscale modeling

A second frontier lies in the deployment of artificial intelligence (AI) to accelerate multiscale simulations that capture SEI formation and evolution in real time. Recent advances in physics-informed machine-learning workflows have shown that neural-network potentials and surrogate models can bridge atomic resolution to device timescales by several orders of magnitude.[400,401] For SEI in supercapacitors, a coherent pipeline might begin with density-functional theory (DFT) calculations of solvent/salt reduction barriers, feed into molecular dynamics (MD) or reactive-force-field simulations of early film nucleation, and then leverage ML surrogates to predict film growth, ionic transport and impedance evolution over thousands of rapid charge/discharge cycles.

Incorporating AI into this loop enables adaptive simulations: based on evolving interphase properties (thickness, porosity, composition) the ML model adjusts boundary conditions or cycling protocols and predicts future behaviour before experimental validation.[402] Such "closed-loop modelling" is particularly powerful in supercapacitors, where fast kinetics and high-rate protocols dominate and where limited time exists for long-term ageing experiments.

9.3 Community data repositories and standards

The third strategic opportunity is the creation of shared, open databases linking electrolyte formulation, electrode surface chemistry, SEI composition and performance degradation metrics.[354] Currently, data in interphase research are fragmented—individual studies report specific electrode/electrolyte pairs and SEI analyses, but lack standard formats, metadata or cross-system comparability. Establishing a comprehensive database would enable machine-learning models to learn from a broader chemical space, quantify trends, identify outliers and propose new interphase chemistries.

A meaningful SEI database could include parameters such as solvent identity, salt species and concentration, additive content, electrode material and surface functionalisation, SEI thickness/composition (XPS, ToF-SIMS), ionic resistance and capacitance fade across cycling.[354] This repository would support benchmarking of simulation models, facilitate transfer learning across systems, and catalyse inverse design of interphases.

9.4 First-principles treatment of interfacial charge transfer

While much of SEI modelling emphasises ion transport, film growth kinetics and mass-transport limitations, a crucial—but less explored—axis is electron transport through the interphase.[403] Recent quantum-transport studies reveal that heterogeneous interfaces (*e.g.*, LiF/Li_2CO_3 combinations) severely influence electron tunnelling barriers and defect-mediated leakage paths.[404] For supercapacitors operating at high voltages and fast charge/discharge rates, even minor electron conduction through the interphase may trigger continuous electrolyte breakdown, self-discharge or power loss.

Thus, coupling quantum-mechanical simulations (NEGF, DFT) of interphase materials with MD and continuum models offers a holistic picture where electron tunnelling, ion migration, solvent breakdown and film evolution all interplay.[404] Integrating these quantum calculations into multiscale modelling enables designers to propose SEIs that are not only ionically conductive but also electronically insulating—minimising parasitic reactions and enhancing cycle life.

9.5 Green chemistry and eco-friendly electrolytes

Finally, the longevity, recyclability and environmental footprint of energy storage systems depend heavily on the interphase. While performance has often dominated research priorities, future supercapacitors must align with circular-economy principles. This means deploying electrolytes that are non-toxic, flame-retardant and low-cost, and engineering interphases (including SEI-like films where relevant) that are stable but amenable to safe end-of-life processing.[68,405]

Sustainable SEI design involves selecting solvents and salts whose decomposition products are benign, coatings and additives that avoid critical raw-material scarcity, and interphases that enable recycling of electrode materials without extensive chemical breakdown. For instance, replacing fluorine-rich additives with alternative film-formers or employing bio-derived polymer interphases could reduce environmental burden while maintaining performance.[68] Formation protocols that minimise energy consumption, reduce gas evolution and limit parasitic side-products will further improve life-cycle impact.

By embracing these five strategic directions—unified theory, AI-driven simulation, open data, quantum-informed modelling and sustainability—SEI engineering for supercapacitors can transition from incremental improvements to a generative, predictive design paradigm. This transformation will underpin the development of high-energy, high-power, durable and environmentally compatible supercapacitor technologies.

10 Concluding remarks and outlook

The scientific understanding of SEIs has advanced substantially over the past decade, driven by parallel progress in interface-sensitive experimental techniques and increasingly sophisticated computational methods. While traditional electrochemical measurements and *ex situ* surface analyses laid the foundation of SEI research, they are now complemented by *operando* spectroscopy, cryogenic microscopy, and multiscale simulation frameworks capable of resolving interfacial dynamics with atomic precision. Together, these developments have transformed interphase science from a phenomenological concept into a quantifiable, chemically heterogeneous interphase governing performance in both battery SEIs and supercapacitor SEI-like interphases.

In this review, we have focused on the microscopic to mesoscopic mechanisms underlying SEI formation, evolution, and transport, emphasizing the roles of electronic-structure theory, reactive and machine-learning molecular dynamics, continuum models, and device-scale formulations. These approaches, adapted over the years to capture electron transfer, solvation breakdown, and polarization at complex electrode–electrolyte interfaces, now provide access to structural, chemical, and transport properties that were previously inaccessible through experiments alone.

Comparison with experiments provides a critical benchmark for validating multiscale SEI models. In most cases, simulations reproduce the qualitative trends observed in *operando* XPS, impedance spectroscopy, and cryo-TEM, lending confidence to the underlying assumptions regarding reduction pathways, ion transport, and interphase morphology. Quantitative agreement is increasingly attainable, particularly when simulation parameters are calibrated against *ab initio* energetics and experimentally measured reaction barriers, though such accuracy often comes at the cost of extensive sampling and high computational demand. The primary benefit of these computational approaches lies in their ability to resolve nanoscale structure, electron redistribution, and decomposition kinetics that remain invisible to most experimental probes. In batteries and supercapacitors alike, these insights have clarified the origins of inorganic–organic layering, elucidated the polarization-controlled onset of electrolyte reduction, and revealed how local electric fields guide SEI nucleation. Moreover, simulations have begun to suggest rational strategies for interface engineering, such as tuning solvent composition, optimizing surface terminations, and exploiting heterogeneous polarization, to stabilize thin, ionically conductive interphases. Although many of these design principles remain challenging to implement experimentally, they provide mechanistic routes for future improvements in interphase stability and device lifetime.

Despite these successes, significant challenges remain for achieving a fully predictive description of SEI formation and evolution across electrochemical technologies. In both battery and supercapacitor systems, the accessible time and length scales of atomistic simulations remain far smaller than those associated with long-term interphase growth, mechanical reconstruction, or electrolyte aging. Bridging these gaps will require tighter coupling between reactive MD, ML-augmented potentials, and continuum models capable of capturing ion transport, stress generation, and dissolution/redeposition dynamics. Methodologically, two major obstacles must be addressed. First, current force fields and ML potentials, while increasingly accurate, still struggle to represent the full chemical diversity of real electrolytes, particularly when multiple solvents, salts, or radical intermediates participate simultaneously in reduction processes. Extending these models to incorporate more explicit electronic descriptors and rare–event pathways will be essential for capturing system-specific reactivity. Second, transferring parameters and boundary conditions across scales remains nontrivial: polarization, solvation, and porosity must be represented consistently from the quantum level to the porous–electrode scale. These issues, combined with the computational cost of reactive simulations and the memory demands of high-resolution mesoscale models, continue to limit the direct simulation of realistic electrode architectures. Overcoming these bottlenecks is therefore central to advancing SEI modeling in the coming years.

In the case of MD-based approaches, substantial progress has been made in representing electrode surfaces and interfacial chemistry, yet important limitations persist. More explicit treatment of electronic structure, particularly localized charge transfer, image-charge effects, and tunneling, would markedly improve predictions of reduction onset and interphase

composition, while incorporating bond flexibility and mechanical compliance in electrode models would enable the study of stress-driven SEI cracking and reconstruction during cycling. On the electrolyte side, models have evolved from fixed-charge representations to polarizable and reactive descriptions, yet coupling self-consistent solvent polarization with dynamically fluctuating electrode charges remains technically challenging and is not widely available in mainstream MD engines. Finally, although supercapacitor electrolytes undergo fewer faradaic reactions than battery systems, rare decomposition events can still influence long-term stability, but modeling these pathways lies beyond the reach of most classical and semiclassical methods. Ongoing efforts in battery SEI modeling — particularly multistate reaction networks, ML-accelerated rare-event sampling, and electronically informed reactive potentials—provide a valuable foundation, and adapting these advances to capacitor chemistries will be essential for capturing degradation and interphase evolution in high-voltage ionic-liquid and organic systems.

However, the most difficult challenges arise when extending SEI modeling to the broader family of emerging electrode and electrolyte chemistries used in both batteries and supercapacitors. While this review concentrated on carbonaceous systems and conventional carbonate or acetonitrile-based electrolytes, next-generation interfaces increasingly involve multicomponent materials whose reactive behavior and electronic structure differ substantially from the paradigms commonly studied. High-voltage spinel oxides, doped carbons, MXenes, and redox-active 2D materials introduce heteroatom-dependent surface states, variable metallicity, and nonuniform polarization, all of which complicate the description of electron transfer and electrolyte decomposition. Similarly, advanced electrolytes such as ionic liquids, water-in-salt solutions, fluorinated additives, and hybrid organic–inorganic systems exhibit complex solvation and reduction pathways that current empirical and reactive potentials do not always capture reliably. Properly representing these systems will require refined models capable of differentiating site-specific charge response, accommodating element-dependent hardness, and resolving situations in which only a subset of atomic species participate in metallic screening. Incorporating these chemical descriptors into constant-potential, reactive, and machine-learning based frameworks remains a demanding task, but doing so is essential for accurately predicting SEI composition and stability across the increasingly diverse set of materials used in modern electrochemical energy-storage devices.

Even greater complexity emerges when considering SEI formation on transition-metal oxides, alloying hosts, and other redox-active surfaces where proton transfer, surface reconstruction, and multielectron redox processes strongly influence interphase chemistry. In aqueous or hybrid electrolytes, these mechanisms couple tightly to solvent reorganization and acid–base equilibria, placing them outside the reliable domain of classical MD and most reactive force fields. Capturing such effects requires more advanced methods, most notably DFT-based *ab initio* molecular dynamics or finite-field electronic-structure calculations capable of resolving charge transfer, interfacial polarization, and proton-coupled electron transfer at each time step. Initial demonstrations of these approaches have successfully described early reduction events and potential-dependent solvation structure, but their applicability remains limited by system size: *ab initio* MD can typically simulate only a few hundred atoms, far smaller than the extended interfaces and nanostructured electrodes relevant for practical SEI studies. Machine-learned interatomic potentials trained on large DFT datasets offer a promising route to bridge this gap, providing near-DFT accuracy with classical scalability. However, current models remain at an early stage for complex electrolytes and multicomponent electrode surfaces, and substantial development is still required to ensure transferability across diverse chemistries and operating conditions.

Recent experimental advances have likewise expanded the landscape of SEI-relevant electrolytes. Highly concentrated formulations such as water-in-salt and solvent-in-salt systems introduce new interfacial chemistries, exhibiting nanostructured solvation environments and nonclassical reduction pathways that remain poorly understood at the molecular scale. Their complex organization near charged interfaces, together with experimentally observed coupling to pore topology and surface functionality, presents an open challenge for simulation and demands models capable of capturing collective structuring, fluctuating ion–solvent clusters, and voltage-dependent solvation breakdown. Emerging chemistries such as ionic liquids, fluorinated additives, redox-active ionic liquids, and hybrid organic-inorganic electrolytes offer routes to engineer more robust, self-limiting SEIs, yet their redox behavior requires methods that can treat reactive events and multiple electronic states with comparable accuracy. Conventional MD lacks this capability, motivating the development of electronically informed reactive potentials and nonadiabatic approaches such as surface-hopping to resolve coupled electron–ion dynamics. Taken together, these directions indicate that SEI research across batteries and supercapacitors will remain a vibrant field in the coming decade, with substantial opportunities for advancing microscopic simulation methods, expanding chemical realism, and establishing predictive models that unify interphase behavior across diverse electrochemical systems.

Key challenges and opportunities for future SEI research:

- Extending reactive and ML-certified force fields to cover the full chemical complexity of modern electrolytes and electrode surfaces (mixed solvents, ionic liquids, doped carbons, 2D materials, *etc.*).
- Building robust multiscale coupling pipelines that consistently preserve solvation, polarization, and porosity across electronic, atomistic, mesoscale, and device levels.
- Implementing constant-potential, electronically informed reactive simulations that are computationally tractable for realistic electrode architectures and long-time evolution.
- Developing open, interoperable datasets and benchmark protocols covering both battery and supercapacitor chemistries, to enable transfer learning, model validation, and community-wide comparison.

Future Roadmap: Short-, Mid-, and Long-Term Priorities for Interphase Engineering To maximize impact and accelerate

translation from mechanistic insight to device-level reliability, we outline practical research priorities across three time horizons.

Short-term priorities (0–2 years): establish comparability and causal evidence. (i) Standardize reporting of interphase claims using a minimum set of operating details (electrolyte identity, voltage window, protocol/holds, cell configuration) together with at least one metric from each category: leakage/self-discharge, ESR evolution (EIS), and capacitance retention. (ii) Cross-validate characterization by routinely pairing surface chemistry (XPS/ToF-SIMS/FTIR) with *operando* electrochemical signatures (EIS/EQCM) to distinguish reversible pseudocapacitance from irreversible film growth. (iii) *Define practical onset thresholds* (*e.g.*, V_{crit}). for common electrolyte classes and electrode families under realistic cycling and hold protocols, enabling voltage-window selection as a design constraint rather than a performance target.

Mid-term priorities (2–5 years): engineer controllable, durable SEI-like interphases. (i) Protocol-guided formation (conditioning/stepwise ramping) and additive/coating strategies should be optimized against metric-first objectives (lower leakage and stable ESR, not chemistry alone). (ii) *Porous-electrode-aware impedance interpretation* (transmission-line models, DRT analysis) should become routine so that fitted interphase parameters are physically meaningful and comparable across laboratories. (iii) *Materials-by-design interphases*: develop ultrathin, ion-permeable, mechanically resilient coatings and binder networks that suppress defect-localized decomposition while preserving fast ion access and pseudocapacitive redox sites.

Long-term priorities (5–10 years): predictive, closed-loop interphase design across platforms. (i) *Multiscale, validated digital twins* integrating atomistic chemistry, mesoscale porous transport, and device-level degradation should enable quantitative lifetime prediction under realistic duty cycles (including holds and temperature variations). (ii) *Data-driven inverse design*: closed-loop workflows combining high-throughput experiments/simulations with ML should optimize electrolyte/electrode/protocol combinations toward targeted interphase state vectors (thickness, inorganic/organic fraction, effective resistivity) linked to stability metrics. (iii) *Sustainable interphase engineering*: prioritize electrolytes/additives and coatings with improved environmental compatibility and recyclability, while maintaining passivation efficacy and long-term safety.

Collectively, these priorities convert the unified interphase perspective into a practical roadmap for achieving high-voltage, long-life supercapacitors and transferable interface-control principles across next-generation electrochemical energy-storage technologies.In summary, while the road ahead is challenging, the convergence of advanced experiments, physics-based modeling, and machine learning offers strong prospects for a predictive, technology-agnostic SEI science — one capable of steering future interface design for both high-energy and high-power electrochemical devices.

Conflicts of interest

There are no conflicts of declare.

Data availability

Data sharing is not applicable to this article as no new data were generated or analysed.

References

1 K. Detka and K. Górecki, Selected technologies of electrochemical energy storage—a review, *Energies*, 2023, **16**, 5034.
2 G. Navarro, J. Torres, M. Blanco, J. Nájera, M. Santos-Herran and M. Lafoz, Present and future of supercapacitor technology applied to powertrains, renewable generation and grid connection applications, *Energies*, 2021, **14**, 3060.
3 T. Ramachandran, R. K. Raji and M. Rezeq, From lab to market: the future of zinc–air batteries powered by MOF/MXene hybrids, *J. Mater. Chem. A*, 2025, **13**, 12855–12890.
4 M. S. Whittingham, Ultimate limits to intercalation reactions for lithium batteries, *Chem. Rev.*, 2014, **114**, 11414–11443.
5 J. B. Goodenough and K.-S. Park, The Li-ion rechargeable battery: a perspective, *J. Am. Chem. Soc.*, 2013, **135**, 1167–1176.
6 I. Beyers, A. Bensmann and R. Hanke-Rauschenbach, Ragone plots revisited: A review of methodology and application across energy storage technologies, *J. Energy Storage*, 2023, **73**, 109097.
7 A. Burke, Ultracapacitors: why, how, and where is the technology, *J. Power Sources*, 2000, **91**, 37–50.
8 J. Ahn, M. M. Doeff and G. Chen, Strategies and Perspectives on Enhancing Energy Density in Lithium-Ion Batteries, *ECS Meet. Abstr.*, 2024, **245**, 509.
9 Y. Lin, S. Zhang, L. Guan and J. Tao, Prospect of Ni-related metal oxides for high-performance supercapacitor electrodes, *J. Mater. Sci.*, 2021, **56**, 1897–1918.
10 C. Choi, D. S. Ashby, D. M. Butts, R. H. DeBlock, Q. Wei, J. Lau and B. Dunn, Achieving high energy density and high power density with pseudocapacitive materials, *Nat. Rev. Mater.*, 2020, **5**, 5–19.
11 S. Li, Z. Luo, L. Li, J. Hu, G. Zou, H. Hou and X. Ji, Recent progress on electrolyte additives for stable lithium metal anode, *Energy Storage Mater.*, 2020, **32**, 306–319.
12 Y. Wang, Y. Song and Y. Xia, Electrochemical capacitors: mechanism, materials, systems, characterization and applications, *Chem. Soc. Rev.*, 2016, **45**, 5925–5950.
13 E. Peled, The electrochemical behavior of alkali and alkaline earth metals in nonaqueous battery systems—the solid electrolyte interphase model, *J. Electrochem. Soc.*, 1979, **126**, 2047.
14 E. Peled and S. Menkin, SEI: past, present and future, *J. Electrochem. Soc.*, 2017, **164**, A1703.
15 H. Adenusi, G. A. Chass, S. Passerini, K. V. Tian and G. Chen, Lithium batteries and the solid electrolyte interphase (SEI)—progress and outlook, *Adv. Energy Mater.*, 2023, **13**, 2203307.
16 S. J. An, J. Li, C. Daniel, D. Mohanty, S. Nagpure and D. L. Wood, The state of understanding of the lithium-

ion-battery graphite solid electrolyte interphase (SEI) and its relationship to formation cycling, *Carbon*, 2016, **105**, 52–76.

17 H. Wu, H. Jia, C. Wang, J.-G. Zhang and W. Xu, Recent progress in understanding solid electrolyte interphase on lithium metal anodes, *Adv. Energy Mater.*, 2021, **11**, 2003092.

18 X.-B. Cheng, R. Zhang, C.-Z. Zhao, F. Wei, J.-G. Zhang and Q. Zhang, A review of solid electrolyte interphases on lithium metal anode, *Adv. Sci.*, 2016, **3**, 1500213.

19 J. Tan, L. Ma, Z. Li, Y. Wang, M. Ye and J. Shen, Structural insights into solid electrolyte interphase (SEI) on lithium metal anode: From design strategies to the stability evaluation, *Mater. Today*, 2023, **69**, 287–332.

20 A. Wang, S. Kadam, H. Li, S. Shi and Y. Qi, Review on modeling of the anode solid electrolyte interphase (SEI) for lithium-ion batteries, *npj Comput. Mater.*, 2018, **4**, 15.

21 J. E. Owejan, J. P. Owejan, S. C. DeCaluwe and J. A. Dura, Solid electrolyte interphase in Li-ion batteries: evolving structures measured in situ by neutron reflectometry, *Chem. Mater.*, 2012, **24**, 2133–2140.

22 W. Huang, P. M. Attia, H. Wang, S. E. Renfrew, N. Jin, S. Das, Z. Zhang, D. T. Boyle, Y. Li and M. Z. Bazant, others Evolution of the solid–electrolyte interphase on carbonaceous anodes visualized by atomic-resolution cryogenic electron microscopy, *Nano Lett.*, 2019, **19**, 5140–5148.

23 P. G. Kitz, M. J. Lacey, P. Novák and E. J. Berg, Operando EQCM-D with simultaneous in situ EIS: new insights into interphase formation in Li ion batteries, *Anal. Chem.*, 2018, **91**, 2296–2303.

24 J. D. McBrayer, C. A. Apblett, K. L. Harrison, K. R. Fenton and S. D. Minteer, Mechanical studies of the solid electrolyte interphase on anodes in lithium and lithium ion batteries, *Nanotechnology*, 2021, **32**, 502005.

25 P. Simon and Y. Gogotsi, Materials for electrochemical capacitors, *Nat. Mater.*, 2008, **7**, 845–854.

26 M. Salanne, B. Rotenberg, K. Naoi, K. Kaneko, P.-L. Taberna, C. P. Grey, B. Dunn and P. Simon, Efficient storage mechanisms for building better supercapacitors, *Nat. Energy*, 2016, **1**, 1–10.

27 E. Frackowiak, Electrode materials with pseudocapacitive properties, *Supercapacitors: Materials, Systems, and Applications*, 2013, pp. 207–237.

28 T. Quan, E. Hark, Y. Xu, I. Ahmet, C. Hohn, S. Mei and Y. Lu, Unveiling the formation of solid electrolyte interphase and its temperature dependence in "water-in-salt" supercapacitors, *ACS Appl. Mater. Interfaces*, 2021, **13**, 3979–3990.

29 M.-E. Yvenat, B. Chavillon, E. Mayousse, E. De Vito, A. Boulineau, F. Perdu and P. Azaïs, Study of the influence of the formation protocol on the SEI layer formed at the graphite electrode surface of a non-aqueous potassium-ion hybrid supercapacitor (KIC) through STEM and XPS analyses, *Sustainable Energy & Fuels*, 2023, **7**, 4150–4159.

30 T. Ramachandran, F. Hamed, Y. A. Kumar, R. K. Raji and H. Hegazy, Multifunctional covalent-organic frameworks (COFs)-2D MXenes composites for diverse applications, *J. Energy Storage*, 2023, **73**, 109299.

31 E. Pameté, L. Köps, F. A. Kreth, S. Pohlmann, A. Varzi, T. Brousse, A. Balducci and V. Presser, The many deaths of supercapacitors: degradation, aging, and performance fading, *Adv. Energy Mater.*, 2023, **13**, 2301008.

32 G. S. Hwang, Fundamental Understanding of Faradaic and Non-Faradaic Processes in Carbon-Based Supercapacitors, *ECS Meet. Abstr.*, 2019, **235**, 644.

33 C. Ding, T. Liu, X. Yan, L. Huang, S. Ryu, J. Lan, Y. Yu, W.-H. Zhong and X. Yang, An ultra-microporous carbon material boosting integrated capacitance for cellulose-based supercapacitors, *Nano-Micro Lett.*, 2020, **12**, 63.

34 A. M. Bogale, T. Ramachandran, M. E. Suk, B. B. Badassa, M. M. Solomon, J. He, A. Yusuf, R. K. Raji, B. A. Zenebe and N. K. Amare, others Boosted charge storage in symmetric supercapacitors using Zn-Co/MgCo2O4 hybrid nanosheets, *J. Phys. Chem. Solids*, 2025, 113079.

35 A. Dey, Film formation on lithium anode in propylene carbonate, *J. Electrochem. Soc.*, 1970, 117.

36 V. A. Agubra and J. W. Fergus, The formation and stability of the solid electrolyte interface on the graphite anode, *J. Power Sources*, 2014, **268**, 153–162.

37 R. Fong, U. Von Sacken and J. R. Dahn, Studies of lithium intercalation into carbons using nonaqueous electrochemical cells, *J. Electrochem. Soc.*, 1990, **137**, 2009.

38 E. Peled, D. Golodnitsky and G. Ardel, Advanced model for solid electrolyte interphase electrodes in liquid and polymer electrolytes, *J. Electrochem. Soc.*, 1997, **144**, L208.

39 D. Aurbach, B. Markovsky, M. Levi, E. Levi, A. Schechter, M. Moshkovich and Y. Cohen, New insights into the interactions between electrode materials and electrolyte solutions for advanced nonaqueous batteries, *J. Power Sources*, 1999, **81**, 95–111.

40 Y. Wang, S. Nakamura, M. Ue and P. B. Balbuena, Theoretical studies to understand surface chemistry on carbon anodes for lithium-ion batteries: reduction mechanisms of ethylene carbonate, *J. Am. Chem. Soc.*, 2001, **123**, 11708–11718.

41 J. Christensen and J. Newman, A mathematical model for the lithium-ion negative electrode solid electrolyte interphase, *J. Electrochem. Soc.*, 2004, **151**, A1977.

42 Y. S. Jung; A. S. Cavanagh; L. A. Riley; S.-H. Kang; A. C. Dillon; M. D. Groner; S. M. George; S.-H. Lee *Ultrathin Direct Atomic Layer Deposition on Composite Electrodes for Highly Durable and Safe Li-Ion Batteries*. 2010,.

43 S. Shi, P. Lu, Z. Liu, Y. Qi, L. G. Hector Jr, H. Li and S. J. Harris, Direct calculation of Li-ion transport in the solid electrolyte interphase, *J. Am. Chem. Soc.*, 2012, **134**, 15476–15487.

44 A. v. Cresce, S. M. Russell, D. R. Baker, K. J. Gaskell and K. Xu, In situ and quantitative characterization of solid electrolyte interphases, *Nano Lett.*, 2014, **14**, 1405–1412.

45 A. C. Kozen, C.-F. Lin, A. J. Pearse, M. A. Schroeder, X. Han, L. Hu, S.-B. Lee, G. W. Rubloff and M. Noked, Next-

generation lithium metal anode engineering via atomic layer deposition, *ACS Nano*, 2015, **9**, 5884–5892.
46 E. Peled and H. Yamin, Solid Electrolyte Interphase (SEI) Electrodes. Part 1. The Kinetics of Lithium in LiAlCl4-SOCl2, *Isr. J. Chem.*, 1979, **18**, 131–135.
47 E. Peled, Film forming reaction at the lithium/electrolyte interface, *J. Power Sources*, 1983, **9**, 253–266.
48 J. M. Lim, Y. S. Jang, H. V. T. Nguyen, J. S. Kim, Y. Yoon, B. J. Park, D. H. Seo, K.-K. Lee, Z. Han and K. K. Ostrikov, others Advances in high-voltage supercapacitors for energy storage systems: materials and electrolyte tailoring to implementation, *Nanoscale Adv.*, 2023, **5**, 615–626.
49 M. Pathak, D. Bhatt, R. C. Bhatt, B. S. Bohra, G. Tatrari, S. Rana, M. C. Arya and N. G. Sahoo, High energy density supercapacitors: an overview of efficient electrode materials, electrolytes, design, and fabrication, *Chem. Rec.*, 2024, **24**, e202300236.
50 A. Patel, S. K. Patel, R. Singh and R. Patel, Review on recent advancements in the role of electrolytes and electrode materials on supercapacitor performances, *Discover Nano*, 2024, **19**, 188.
51 R. Yuan, Y. Dong, R. Hou, S. Zhang and H. Song, Influencing factors and suppressing strategies of the self-discharge for carbon electrode materials in supercapacitors, *J. Electrochem. Soc.*, 2022, **169**, 030504.
52 D. Xu, X. Zhang, K. Zhang, Y. Han, X. Sun, Y. Xu, C. Li, K. Wang, X. Zhang and Y. Ma, Recent advances in high-voltage lithium-ion capacitors, *J. Solid State Electrochem.*, 2025, 1–27.
53 Y. Yao, X. Rui, R. Bai, Y. Ouyang, G. Li, Y. Zhao, Y.-H. Zhu, M. Zhao, B.-Q. Li and X. Zhang, others Roadmap for Next-Generation Electrochemical Energy Storage Technologies: Secondary Batteries and Supercapacitors, *ACS Nano*, 2025, **19**, 30568–30687.
54 X. Liu, D. Lyu, C. Merlet, M. J. Leesmith, X. Hua, Z. Xu, C. P. Grey and A. C. Forse, Structural disorder determines capacitance in nanoporous carbons, *Science*, 2024, **384**, 321–325.
55 K. Mazloomian, H. Lancaster, C. Howard, P. Shearing and T. Miller, Supercapacitor degradation: Understanding mechanisms of cycling-induced deterioration and failure of a pseudocapacitor, *Batteries Supercaps*, 2023, **6**(8), e202300214.
56 Y. Wu, G. Ge, S. Wang, L. Xiong and Z. He, Formation mechanisms of solid electrolyte interphase and its influence on lithium battery performance, *Mater. Today Energy*, 2025, 102124.
57 H. Wan, J. Xu and C. Wang, Designing electrolytes and interphases for high-energy lithium batteries, *Nat. Rev. Chem.*, 2024, **8**, 30–44.
58 X. Jiang, H. Zhang, Y. Qu, Z. Wang, Y. Xie, W. Zhang, H. Hu and Z. He, Engineering electrolyte strong-weak coupling effect toward wide-temperature supercapacitor, *Energy Storage Mater.*, 2024, **68**, 103374.
59 Y. B. Yohannes, S. D. Lin, N.-L. Wu and B.-J. Hwang, SEI grown on MCMB-electrode with fluoroethylene carbonate and vinylene carbonate additives as probed by in situ DRIFTS, *J. Electrochem. Soc.*, 2019, **166**, A2741.
60 P. G. Kitz, M. J. Lacey, P. Novák and E. J. Berg, Operando investigation of the solid electrolyte interphase mechanical and transport properties formed from vinylene carbonate and fluoroethylene carbonate, *J. Power Sources*, 2020, **477**, 228567.
61 P. Jankowski, W. Wieczorek and P. Johansson, Functional ionic liquids: cationic SEI-formers for lithium batteries, *Energy Storage Mater.*, 2019, **20**, 108–117.
62 M. Y. Yang, S. V. Zybin, T. Das, B. V. Merinov, W. A. Goddard, E. K. Mok, H. J. Hah, H. E. Han, Y. C. Choi and S. H. Kim, Characterization of the solid electrolyte interphase at the Li metal–ionic liquid interface, *Adv. Energy Mater.*, 2023, **13**, 2202949.
63 F. Du, H. Wang, J. Chen, H. Huang, T. Ye, S. Duan, R. Zhang, J. Liu and H. Hu, Atomistic Insights into Fluorinated/Chlorinated Ether-Based LHCEs on Lithium Metal: Decomposition Mechanisms via Multiscale Simulations, *J. Phys. Chem. B*, 2025, **129**, 8919–8932.
64 B. Kim, H. Shin, J. Choi and M. Cho, Multiscale modeling of load transfer characteristics in crosslinked epoxy nanocomposites, *Mech. Adv. Mater. Struct.*, 2022, **29**, 4768–4778.
65 Y. You, D. Zhang, F. Wu, X. Cao, Y. Sun, Z.-Z. Zhu and S. Wu, Principal component analysis enables the design of deep learning potential precisely capturing LLZO phase transitions, *npj Comput. Mater.*, 2024, **10**, 57.
66 J. Chen, X. Fan, Q. Li, H. Yang, M. R. Khoshi, Y. Xu, S. Hwang, L. Chen, X. Ji and C. Yang, others Electrolyte design for LiF-rich solid–electrolyte interfaces to enable high-performance microsized alloy anodes for batteries, *Nat. Energy*, 2020, **5**, 386–397.
67 X. Liu, V. Koverga, H. T. Nguyen, A. T. Ngo and T. Li, Exploring solvation structure and transport behavior for rational design of advanced electrolytes for next generation of lithium batteries, *Applied Physics Reviews*, 2024, **11**, 021307.
68 Z. Ju, X. Tao, Y. Wang, Q. Yang, T. Liu, J. Nai, W. Zhang, S. Chen, Y. Liu and H. Tian, others A self-healing Li-crosslinked elastomer promotes a highly robust and conductive solid–electrolyte interphase, *Energy Environ. Sci.*, 2024, **17**, 4703–4713.
69 Y. Liu, D. Lin, P. Y. Yuen, K. Liu, J. Xie, R. H. Dauskardt and Y. Cui, An artificial solid electrolyte interphase with high Li-ion conductivity, mechanical strength, and flexibility for stable lithium metal anodes, *Adv. Mater.*, 2016, **29**, 1605531.
70 B. Ng, P. T. Coman, W. E. Mustain and R. E. White, Non-destructive parameter extraction for a reduced order lumped electrochemical-thermal model for simulating Li-ion full-cells, *J. Power Sources*, 2020, **445**, 227296.
71 Z. Huang, J.-C. Lai, S.-L. Liao, Z. Yu, Y. Chen, W. Yu, H. Gong, X. Gao, Y. Yang and J. Qin, others A salt-philic, solvent-phobic interfacial coating design for lithium metal electrodes, *Nat. Energy*, 2023, **8**, 577–585.
72 S. Sikiru, J. O. Olutoki, S. A. Musa, L. O. Afolabi and M. M. Mahat, The projection role of surface charge

density in electric double-layer capacitance for enhanced energy storage, *J. Energy Storage*, 2025, **138**, 118728.
73 S. SHIRAISHI and Y. HATAKEYAMA, Electrode Carbon Material for Electric Double Layer Capacitors, *Vac. Surf. Sci.*, 2019, **62**, 703–708.
74 T. Ramachandran, F. Hamed, R. K. Raji, S. M. Majhi, D. Barik, Y. A. Kumar, R. M. Jauhar, M. Pachamuthu, L. Vijayalakshmi and S. Ansar, Enhancing asymmetric supercapacitor performance with NiCo2O4–NiO hybrid electrode fabrication, *J. Phys. Chem. Solids*, 2023, **180**, 111467.
75 T. Ramachandran, A.-H. I. Mourad, R. K. Raji, R. Krishnapriya, N. Cherupurakal, A. Subhan and Y. Al-Douri, KOH mediated hydrothermally synthesized hexagonal-CoMn2O4 for energy storage supercapacitor applications, *Int. J. Energy Res.*, 2022, **46**, 16823–16838.
76 B. U. Tale, K. R. Nemade and P. V. Tekade, Novel graphene based MnO2/polyaniline nanohybrid material for efficient supercapacitor application, *J. Porous Mater.*, 2024, **31**, 2053–2065.
77 R.-J. Zhu, J. Liu, C. Hua, H.-Y. Pan, Y.-J. Cao and M. Li, Preparation of vanadium-based electrode materials and their research progress in solid-state flexible supercapacitors, *Rare Met.*, 2024, **43**, 431–454.
78 T. Ramachandran, M. Pachamuthu, R. Raji and F. R. M. S. Raj, A Layered Fe–SnO2/MXene Nanohybrid with 1225.6 F/g Capacitance and Long-Term Cycle Durability, *Mater. Chem. Phys.*, 2025, 131860.
79 B. E. Conway, *Electrochemical Supercapacitors: Scientific Fundamentals and Technological Applications*, pringer Science & Business Media, 2013.
80 J. Zheng, P. Cygan and T. Jow, Hydrous ruthenium oxide as an electrode material for electrochemical capacitors, *J. Electrochem. Soc.*, 1995, **142**, 2699.
81 J. Phojaroen, P. Wuamprakhon, T. Sangsanit, K. Santiyuk, K. Homlamai, N. Anansuksawat, W. Tejangkura, R. Songthan and M. Sawangphruk, Investigation of Electrolyte Decomposition Byproducts in Gas and Liquid Phases Due to Water Impurities in Large-Scale Acetonitrile-Based Supercapacitors, *Batteries Supercaps*, 2025, **8**, e202400738.
82 R. Songthan, J. Phojaroen, T. Sangsanit, P. Wuamprakhon, W. Tejangkura and M. Sawangphruk, Correlation Between Electrolyte Degradation Products and Overcharging Voltages in Supercapacitors, *J. Electrochem. Soc.*, 2025, **172**, 040509.
83 K. Mazloomian, H. J. Lancaster, C. A. Howard, P. R. Shearing and T. S. Miller, Supercapacitor degradation: understanding mechanisms of cycling-induced deterioration and failure of a pseudocapacitor, *Rare Met.*, 2023, **6**, e202300214.
84 O. Stern, Zur theorie der elektrolytischen doppelschicht, *Z. Phys. Chem.*, 1924, **30**, 508–516.
85 M. Gouy, Sur la constitution de la charge électrique à la surface d'un électrolyte, *J. Phys. Theor. Appl.*, 1910, **9**, 457–468.
86 D. L. L. I. Chapman, A contribution to the theory of electrocapillarity, *London, Edinburgh Dublin Philos. Mag. J. Sci.*, 1913, **25**, 475–481.
87 T. Dong, T. Qin, W. Zhang, Y. Zhang, Z. Feng, Y. Gao, Z. Pan, Z. Xia, Y. Wang and C. Yang, others Nature of the electric double layer to modulate the electrochemical behaviors of Fe2O3 electrode, *Acta Mater.*, 2024, **263**, 119500.
88 K. Ge, H. Shao, Z. Lin, P.-L. Taberna and P. Simon, Advanced characterization of confined electrochemical interfaces in electrochemical capacitors, *Nat. Nanotechnol.*, 2025, **20**, 196–208.
89 J. Tan, Z. Li, M. Ye and J. Shen, Nanoconfined space: Revisiting the charge storage mechanism of electric double layer capacitors, *ACS Appl. Mater. Interfaces*, 2022, **14**, 37259–37269.
90 J. Grill and J. Popovic-Neuber, Long term porosity of solid electrolyte interphase on model silicon anodes with liquid battery electrolytes, *Commun. Chem.*, 2024, **7**, 297.
91 R. Akhter and S. S. Maktedar, MXenes: A comprehensive review of synthesis, properties, and progress in supercapacitor applications, *J. Materiomics*, 2023, **9**, 1196–1241.
92 S. Zhao, G. Li, B. Zhang, T. Li, M. Luo, B. Sun, G. Wang and S. Guo, Technological roadmap for potassium-ion hybrid capacitors, *Joule*, 2024, **8**, 922–943.
93 Z. Huang, X. Li, Z. Chen, P. Li, X. Ji and C. Zhi, Anion chemistry in energy storage devices, *Nat. Rev. Chem.*, 2023, **7**, 616–631.
94 R. He, L. Zhou, R. Tenent and M. Zhou, Basics of the scanning electrochemical microscope and its application in the characterization of lithium-ion batteries: a brief review, *Mater. Chem. Front.*, 2023, **7**, 662–678.
95 J. Chen, J. Vatamanu, L. Xing, O. Borodin, H. Chen, X. Guan, X. Liu, K. Xu and W. Li, Improving electrochemical stability and low-temperature performance with water/acetonitrile hybrid electrolytes, *Adv. Energy Mater.*, 2020, **10**, 1902654.
96 Z. T. Gossage, N. Ito, T. Hosaka, R. Tatara and S. Komaba, Understanding the Development and Properties of SEI in Concentrated Aqueous Electrolytes Via Scanning Electrochemical Microscopy, *ECS Meet. Abstr.*, 2023, **244**, 2900.
97 F. Wang and J. Cheng, Unraveling the origin of reductive stability of super-concentrated electrolytes from first principles and unsupervised machine learning, *Chem. Sci.*, 2022, **13**, 11570–11576.
98 S. Ko, T. Obukata, T. Shimada, N. Takenaka, M. Nakayama, A. Yamada and Y. Yamada, Electrode potential influences the reversibility of lithium-metal anodes, *Nat. Energy*, 2022, **7**, 1217–1224.
99 K.-H. Ko, K. Kim, Y. Kim, S. Han, J. Park, H. Park, J. Yang, B. Kim, J. Park and K. Kang, Degradation Mechanism Induced by Depth-Dependent Inhomogeneity in Thick High-Areal-Capacity Graphite Electrode, *Small*, 2025, **21**, 2410795.
100 Z. Chen, D. L. Danilov, L. H. Raijmakers, K. Chayambuka, M. Jiang, L. Zhou, J. Zhou, R.-A. Eichel and P. H. Notten,

Overpotential analysis of graphite-based Li-ion batteries seen from a porous electrode modeling perspective, *J. Power Sources*, 2021, **509**, 230345.

101 J. G. Lee, J. Kim, T. J. Lee, J. B. Lee, H.-s. Kim, J. Soon, J. H. Ryu and S. M. Oh, Damage of Solid Electrolyte Interphase (SEI) Layer By the Mechanical Stress Induced By Volume Change of Si Electrode, *ECS Meet. Abstr.*, 2016, 1140.

102 R. D. Deshpande and D. M. Bernardi, Modeling solid-electrolyte interphase (SEI) fracture: coupled mechanical/chemical degradation of the lithium ion battery, *J. Electrochem. Soc.*, 2017, **164**, A461.

103 M. Pavone, F. Fasulo and A. B. Munoz Garcia, Reactivity of VC Electrolyte at Li-Metal Electrode: New Insights on SEI Initial Formation from Density Functional Embedding Theory, *ECS Meet. Abstr.*, 2022, **242**, 486.

104 G. Zhang, X. Wei, X. Wang, S. Chen, J. Zhu and H. Dai, Evolution mechanism and non-destructive assessment of thermal safety for lithium-ion batteries during the whole lifecycle, *Nano Energy*, 2024, **126**, 109621.

105 P. Barai and V. Srinivasan, Impact of Solid Electrolyte Interphase (SEI) Stiffness on Lithium Dendrite Growth, *ECS Meet. Abstr.*, 2019, **235**, 100.

106 L. Suo, D. Oh, Y. Lin, Z. Zhuo, O. Borodin, T. Gao, F. Wang, A. Kushima, Z. Wang and H.-C. Kim, others How solid-electrolyte interphase forms in aqueous electrolytes, *J. Am. Chem. Soc.*, 2017, **139**, 18670–18680.

107 E. W. C. Spotte-Smith, R. L. Kam, D. Barter, J. Self, X. Xie, T. Hou, S. Dwaraknath, S. M. Blau and K. A. Persson, Towards a Mechanistic Explanation for Solid Electrolyte Interphase Formation in Lithium-Ion Batteries, *ECS Meet. Abstr.*, 2022, **241**, 2268.

108 J. Ding, J. Lian, X. Li, J. Huang, K. Sun, H. Yang, L. Gong and P. Tan, Quantitative understanding of coupled electron-ion transfer at the silicon-electrolyte interphase of lithium-ion batteries, *Chem. Eng. J.*, 2024, **500**, 157109.

109 B. Li, Y. Chao, M. Li, Y. Xiao, R. Li, K. Yang, X. Cui, G. Xu, L. Li and C. Yang, others A review of solid electrolyte interphase (SEI) and dendrite formation in lithium batteries, *Electrochem. Energy Rev.*, 2023, **6**, 7.

110 M. C. Madhusudhanan, S. A. Kumar, S. Nair, N. Srinivasan, M. Buragohain and S. Kunnikuruvan, Revisiting the Relation Between the Stability of the LUMO of the Electrolytes and the Kinetics of Solid Electrolyte Interface Formation in Lithium-and Post-Lithium-ion Batteries, *Rare Met.*, 2023, **6**, e202200430.

111 Y. Wang, Y. Liu, Y. Tu and Q. Wang, Reductive decomposition of solvents and additives toward solid-electrolyte interphase formation in lithium-ion battery, *J. Phys. Chem. C*, 2020, **124**, 9099–9108.

112 S. M. Russell, A. v. Cresce and K. Xu, *Electrolyte-Electrode Interactions and Interphases*, Electrochemical Society Meeting Abstracts imlb2016, 2016, pp 303.

113 E. K. Andersson, L.-T. Wu, L. Bertoli, Y.-C. Weng, D. Friesen, K. Elbouazzaoui, S. Bloch, R. Ovsyannikov, E. Giangrisostomi and D. Brandell, others Initial SEI formation in LiBOB-, LiDFOB-and LiBF 4-containing PEO electrolytes, *J. Mater. Chem. A*, 2024, **12**, 9184–9199.

114 S. Banerjee and S. S. Yamijala, Formation and evolution of the solid electrolyte interphase at calcium surfaces, *ACS Appl. Energy Mater.*, 2025, **8**, 5936–5947.

115 P. Wuamprakhon, J. Phojaroen, T. Sangsanit, K. Santiyuk, K. Homlamai, W. Tejangkura and M. Sawangphruk, Unveiling a Novel Decomposition Pathway in Propylene Carbonate-Based Supercapacitors: Insights from a Jelly Roll Configuration Study, *ChemSusChem*, 2024, **17**, e202400053.

116 B. Karamanova, L. Soserov, E. Lefterova, T. Stankulov and A. Stoyanova, Influence of Acetonitrile on the Electrochemical Behavior of Ionic Liquid-Based Supercapacitors, *Batteries*, 2024, **10**, 266.

117 M. M. Amaral, V. Y. Yukuhiro, R. Vicentini, A. C. Peterlevitz, L. M. Da Silva, P. Fernandez and H. Zanin, Direct observation of the CO2 formation and C–H consumption of carbon electrode in an aqueous neutral electrolyte supercapacitor by in-situ FTIR and Raman, *J. Energy Chem.*, 2022, **71**, 488–496.

118 Y. Yang, J. Li, J. Shi, F. Pan, S. Wu, D. Zhang, Y. Zhu and W. Zhang, Expanding the electrochemical stable window of aqueous-based electrolytes via competitive solvation induced by aprotic solvents, *J. Power Sources*, 2025, **644**, 236925.

119 R. Venancio, R. Vicentini, D. A. Corrêa, A. N. Miranda, A. C. Queiroz, F. T. Degasperi, L. J. Siqueira, L. M. Da Silva and H. Zanin, others Combining electrochemical, molecular simulation and operando techniques to investigate the stability of electrodes and organic electrolytes used in EDLCs, *Energy Storage Mater.*, 2023, **62**, 102943.

120 J. Sun, L. A. O'Dell, M. Armand, P. C. Howlett and M. Forsyth, Anion-derived solid-electrolyte interphase enables long life Na-ion batteries using superconcentrated ionic liquid electrolytes, *ACS Energy Lett.*, 2021, **6**, 2481–2490.

121 C. Yan, L.-L. Jiang, Y.-X. Yao, Y. Lu, J.-Q. Huang and Q. Zhang, Nucleation and growth mechanism of anion-derived solid electrolyte interphase in rechargeable batteries, *Angew. Chem.*, 2021, **133**, 8602–8606.

122 L. Wang, J. Guo, Q. Qi, X. Li, Y. Ge, H. Li, Y. Chao, J. Du and X. Cui, Revisiting dipole-induced fluorinated-anion decomposition reaction for promoting a LiF-rich interphase in lithium-metal batteries, *Nano-Micro Lett.*, 2025, **17**, 111.

123 H. Wu, J. Qu, X. Yan, S. Zhang, X. Wang, J. Liang, N. Zhang, B. Dai, J. Yue and T. Pang, others Revealing the Underlying Role of Li2CO3 in Enhancing Performance of Oxyhalide-Based Solid-State Batteries, *Adv. Mater.*, 2025, 2502067.

124 J.-A. Lee, C. Song, S. H. Han, B. Kim and N.-S. Choi, Designing Anode-Electrolyte Interfaces for Low-Temperature Lithium-and Sodium-Ion Batteries: Challenges and Strategies, *ACS Energy Lett.*, 2025, **10**, 5474–5484.

125 C. Prehal, C. Koczwara, N. Jäckel, A. Schreiber, M. Burian, H. Amenitsch, M. A. Hartmann, V. Presser and O. Paris, Quantification of ion confinement and desolvation in nanoporous carbon supercapacitors with modelling and in situ X-ray scattering, *Nat. Energy*, 2017, **2**, 16215.

126 A. C. Forse, J. M. Griffin, C. Merlet, J. Carretero-Gonzalez, A.-R. O. Raji, N. M. Trease and C. P. Grey, Direct observation of ion dynamics in supercapacitor electrodes using in situ diffusion NMR spectroscopy, *Nat. Energy*, 2017, **2**, 16216.

127 T. Kress, X. Liu and A. C. Forse, Pore network tortuosity controls fast charging in supercapacitors, *Nat. Mater.*, 2025, 1–7.

128 M. E. Şahin, F. Blaabjerg and A. Sangwongwanich, A comprehensive review on supercapacitor applications and developments, *Energies*, 2022, **15**, 674.

129 H. Guo, M. Elmanzalawy, P. Sivakumar and S. Fleischmann, Unifying electrolyte formulation and electrode nanoconfinement design to enable new ion–solvent cointercalation chemistries, *Energy Environ. Sci.*, 2024, **17**, 2100–2116.

130 R. Subramanian, Electroinitiated polymerization on electrodes. *Electric Phenomena in Polymer Science*, 2005, pp. 33–58.

131 G.-X. Li, V. Koverga, A. Nguyen, R. Kou, M. Ncube, H. Jiang, K. Wang, M. Liao, H. Guo and J. Chen, others Enhancing lithium-metal battery longevity through minimized coordinating diluent, *Nat. Energy*, 2024, **9**, 817–827.

132 M. Nojabaee, D. Kopljar, N. Wagner and K. A. Friedrich, Understanding the Nature of Solid-Electrolyte Interphase on Lithium Metal in Liquid Electrolytes: A Review on Growth, Properties, and Application-Related Challenges, *Rare Met.*, 2021, **4**, 909–922.

133 J.-L. Li, Y.-N. Wang, S.-Y. Sun, Z. Zheng, Y. Gao, P. Shi, Y.-J. Zhao, X. Li, Q. Li and X.-Q. Zhang, others Understanding and regulating the mechanical stability of solid electrolyte interphase in batteries, *Adv. Energy Mater.*, 2025, **15**, 2403845.

134 Y. Gao, Z. Yan, J. L. Gray, X. He, D. Wang, T. Chen, Q. Huang, Y. C. Li, H. Wang and S. H. Kim, others Polymer–inorganic solid–electrolyte interphase for stable lithium metal batteries under lean electrolyte conditions, *Nat. Mater.*, 2019, **18**, 384–389.

135 J. M. Asl, Z. Shafieizadeh, M. Anaraki and J. Sabbaghzadeh, Inspecting The Effect Of Thermal Stress On The Interdiffusion Of Metal Multilayer Produced By Electron-Beam Gun Evaporation, *AIP Conf. Proc.*, 2010, 67–70.

136 D. Peak and J. Corbett, Diffusion-controlled reaction kinetics, *Phys. Rev. B*, 1972, **5**, 1226.

137 A. S. Kulathuvayal and Y. Su, Ionic transport through the solid electrolyte interphase in lithium-ion batteries: A review from first-principles perspectives, *ACS Appl. Energy Mater.*, 2023, **6**, 5628–5645.

138 Y. Chu, Y. Shen, F. Guo, X. Zhao, Q. Dong, Q. Zhang, W. Li, H. Chen, Z. Luo and L. Chen, Advanced characterizations of solid electrolyte interphases in lithium-ion batteries, *Electrochem. Energy Rev.*, 2020, **3**, 187–219.

139 A. Syugaev, R. Zonov, K. Mikheev, A. Maratkanova and G. Mikheev, Electrochemical impedance of laser-induced graphene: Frequency response of porous structure, *J. Phys. Chem. Solids*, 2023, **181**, 111533.

140 H. Zhu, Z. Li, C. Li, H. Jia, H. Fang, L. Qiao, P. Lv and X. Li, Near-in-situ electrochemical impedance spectroscopy analysis based on lithium iron phosphate electrode, *Electrochim. Acta*, 2023, **464**, 142919.

141 M. Levi and D. Aurbach, Impedance spectra of porous, composite intercalation electrodes: The origin of the low-frequency semicircles, *J. Power Sources*, 2005, **146**, 727–731.

142 F. La Mantia, J. Vetter and P. Novák, Impedance spectroscopy on porous materials: A general model and application to graphite electrodes of lithium-ion batteries, *Electrochim. Acta*, 2008, **53**, 4109–4121.

143 A. Plis, P. Połczyński and R. Jurczakowski, Equivalent circuit for assessing pore size distribution in porous electrodes by EIS, *Electrochem. Commun.*, 2024, **164**, 107716.

144 L. Xu, Y. Xiao, Z.-X. Yu, Y. Yang, C. Yan and J.-Q. Huang, Revisiting the Electrochemical Impedance Spectroscopy of Porous Electrodes in Li-ion Batteries by Employing Reference Electrode, *Angew. Chem., Int. Ed.*, 2024, **63**, e202406054.

145 R. Morasch, H. A. Gasteiger and B. Suthar, Li-ion battery material impedance analysis ii: graphite and solid electrolyte interphase kinetics, *J. Electrochem. Soc.*, 2024, **171**, 050548.

146 S. D. Talian, S. Brutti, M. A. Navarra, J. Moškon and M. Gaberscek, Impedance spectroscopy applied to lithium battery materials: Good practices in measurements and analyses, *Energy Storage Mater.*, 2024, **69**, 103413.

147 Z. Sun, J. Yang, H. Xu, C. Jiang, Y. Niu, X. Lian, Y. Liu, R. Su, D. Liu and Y. Long, others Enabling an inorganic-rich interface via cationic surfactant for high-performance lithium metal batteries, *Nano-Micro Lett.*, 2024, **16**, 141.

148 Z. Chen, J. Pan, W. Huang, K. Shi, Z. Yang, H. Wu, S. Wei, G. Jiang, W. Zou and R. Zhang, others Heterogeneity-Segment Charge-Induced-Coupling Catalysis of Component-Selective-Type Covalent Organic Frameworks Interface toward Stabilizing Lithium Metal Anode, *ACS Nano*, 2025, **19**, 13160–13174.

149 C. Xu, J. Mu, T. Zhou, S. Tian, P. Gao, G. Yin, J. Zhou and F. Li, Surface Redox Pseudocapacitance Boosting Vanadium Nitride for High-Power and Ultra-Stable Potassium-Ion Capacitors, *Adv. Funct. Mater.*, 2022, **32**, 2206501.

150 M. Hao, S. Weng, C. Zhong, Y. Li and X. Wang, Structure and evolution of solid electrolyte interphase (SEI) at the electrode-electrolyte interface, *Mater. Today Energy*, 2025, 101998.

151 C. Groher, D. M. Cupid, A. Mautner, E. Rosenberg and J. Kahr, Operando GC/MS for the investigation of different decomposition pathways during solid electrolyte interphase (SEI) formation with SEI forming additives, *J. Power Sources*, 2024, **605**, 234481.

152 Y. Liu, K. Dong, T. Lv, Z. Chen, S. Cao, F. Zheng and T. Chen, Constructing bilayer heterogeneous organogel electrolytes of Lewis acidic/basic polymers to suppress self-discharge of supercapacitors, *Chem. Eng. J.*, 2024, **479**, 147716.

153 Y. Chen, W. Wu, S. Gonzalez-Munoz, L. Forcieri, C. Wells, S. P. Jarvis, F. Wu, R. Young, A. Dey and M. Isaacs, others Nanoarchitecture factors of solid electrolyte interphase formation via 3D nano-rheology microscopy and surface force-distance spectroscopy, *Nat. Commun.*, 2023, **14**, 1321.

154 Y. Liang, N. Song, M. Zhang, X. An, K. Song, W. Chen, J. Feng, S. Xiong and B. Xi, Robust Interfacial Chemistry Induced by B-Doping Enables Rapid, Stable Sodium Storage, *Adv. Energy Mater.*, 2023, **13**, 2302825.

155 J. Chen, X. Rao, F. Zhang, Y. Ein-Eli and D. Q. Tan, Unveiling Activated Carbon Degradation in Supercapacitor Using Liquid Cell Transmission Electron Microscopy, *ACS Appl. Energy Mater.*, 2024, **7**, 9797–9805.

156 K. Machida, S. Suematsu and K. Tamamitsu, Polyfluorene/carbon nanocomposite for electrochemical capacitors, *Electrochemistry*, 2007, **75**, 601–603.

157 S. Kholimatussadiah, C.-L. Hsu, S.-W. Ke, T.-C. Chou, Y.-F. Wu, R. Yakimova, A. Kumatani, K.-H. Chen, L.-C. Chen and H.-Y. Du, In-situ observation of hydrogen nanobubbles formation on graphene surface by AFM-SECM, *Electrochim. Acta*, 2024, **493**, 144425.

158 P. Ruch, D. Cericola, A. Foelske-Schmitz, R. Kötz and A. Wokaun, Aging of electrochemical double layer capacitors with acetonitrile-based electrolyte at elevated voltages, *Electrochim. Acta*, 2010, **55**, 4412–4420.

159 D. Gandla, G. Song, C. Wu, Y. Ein-Eli and D. Q. Tan, Atomic layer deposition (ALD) of alumina over activated carbon electrodes enabling a stable 4 V supercapacitor operation, *ChemistryOpen*, 2021, **10**, 402–407.

160 S. Fleischmann, J. B. Mitchell, R. Wang, C. Zhan, D.-e. Jiang, V. Presser and V. Augustyn, Pseudocapacitance: from fundamental understanding to high power energy storage materials, *Chem. Rev.*, 2020, **120**, 6738–6782.

161 S. Rondinini, A. Minguzzi, E. Achilli, C. Locatelli, G. Agostini, S. Pascarelli, G. Spinolo, A. Vertova and P. Ghigna, The dynamics of pseudocapacitive phenomena studied by Energy Dispersive X-Ray Absorption Spectroscopy on hydrous iridium oxide electrodes in alkaline media, *Electrochim. Acta*, 2016, **212**, 247–253.

162 B. R. P. Yip, C. Chen, Y. Jiang, D. Ohayon, G. C. Bazan and X. Wang, Aqueous asymmetric pseudocapacitor featuring high areal energy and power using conjugated polyelectrolytes and Ti3C2T x MXene, *Nat. Commun.*, 2025, **16**, 7984.

163 A. Slesinski, S. Sroka, K. Fic, E. Frackowiak and J. Menzel, Operando monitoring of local pH value changes at the carbon electrode surface in neutral sulfate-based aqueous electrochemical capacitors, *ACS Appl. Mater. Interfaces*, 2022, **14**, 37782–37792.

164 K. Palanisamy, S. Daboss, J. Romer, D. Schäfer, M. Rohnke, J. K. Flowers, S. Fuchs, H. S. Stein, M. Fichtner and C. Kranz, Microscopic and spectroscopic analysis of the solid electrolyte interphase at hard carbon composite anodes in 1 M NaPF6/diglyme, *Rare Met.*, 2024, **7**, e202300482.

165 Y. Aoki, M. Oda, S. Kojima, Y. Yamaga, T. Ishihama, T. Nagashima, T. Doi and M. Inaba, Effective approach by computational chemical prediction and experimental verification to elucidate SEI formation mechanism in LiPF6-, LiFSI-, and LiBF4-containing electrolyte solutions, *J. Phys. Chem. C*, 2022, **127**, 69–77.

166 Y. Li, F. Bai, C. Li, Y. Wang and T. Li, Understanding the inorganic-rich feature of anion-derived solid electrolyte interphase, *Adv. Energy Mater.*, 2024, **14**, 2304414.

167 Q. Wu, M. T. McDowell and Y. Qi, Effect of the electric double layer (EDL) in multicomponent electrolyte reduction and solid electrolyte interphase (SEI) formation in lithium batteries, *J. Am. Chem. Soc.*, 2023, **145**, 2473–2484.

168 T. Ramachandran, R. K. Raji, S. Palanisamy, N. Renuka and K. Karuppasamy, The role of in situ and operando techniques in unraveling local electrochemical supercapacitor phenomena, *J. Ind. Eng. Chem.*, 2025, **145**, 144–168.

169 F. Capone, J. Sottmann, V. Meunier, L. P. Ramírez, A. Grimaud, A. Iadecola, M. Scardamaglia, J.-P. Rueff and R. Dedryvère, Operando observation of the dynamic SEI formation on a carbonaceous electrode by near-ambient pressure XPS, *Energy Environ. Sci.*, 2024, **17**, 1509–1519.

170 B. Freitas, W. G. Nunes, C. G. Real, C. B. Rodella, G. Doubek, L. M. da Silva, E. H. Thaines, L. A. Pocrifka, R. G. Freitas and H. Zanin, Combining in situ electrochemistry, operando XRD & Raman spectroscopy, and density functional theory to investigate the fundamentals of Li 2 CO 3 formation in supercapacitors, *J. Mater. Chem. A*, 2023, **11**, 20636–20650.

171 D. Diddens, W. A. Appiah, Y. Mabrouk, A. Heuer, T. Vegge and A. Bhowmik, Modeling the solid electrolyte interphase: Machine learning as a game changer?, *Adv. Mater. Interfaces*, 2022, **9**, 2101734.

172 A. G. Shard and M. A. Baker, Practical guides for x-ray photoelectron spectroscopy: Use of argon ion beams for sputter depth profiling and cleaning, *J. Vac. Sci. Technol., A*, 2024, **42**, 050801.

173 S. Yakovlev, J. Zekonyte, C.-H. Solterbeck and M. Es-Souni, Interfacial effects on the electrical properties of multiferroic BiFeO3/Pt/Si thin film heterostructures, *Thin Solid Films*, 2005, **493**, 24–29.

174 A. Andersson, D. Abraham, R. Haasch, S. MacLaren, J. Liu and K. Amine, Surface characterization of electrodes from high power lithium-ion batteries, *J. Electrochem. Soc.*, 2002, **149**, A1358.

175 L.-S. Chang, Y.-C. Lin, C.-Y. Su, H.-C. Wu and J.-P. Pan, Effect of C60 ion sputtering on the compositional depth profiling in XPS for Li (Ni, Co, Mn) O2 electrodes, *Appl. Surf. Sci.*, 2011, **258**, 1279–1281.

176 K. Ridier, D. Aureau, B. Bérini, Y. Dumont, N. Keller, J. Vigneron, A. Etcheberry and A. Fouchet, Enhanced

depth profiling of perovskite oxide: low defect levels induced in SrTiO3 by Argon cluster sputtering, *J. Phys. Chem. C*, 2016, **120**, 21358–21363.

177 Z. D. Schultz, J. M. Marr and H. Wang, Tip enhanced Raman scattering: plasmonic enhancements for nanoscale chemical analysis, *Nanophotonics*, 2014, **3**, 91–104.

178 T. Schmid, L. Opilik, C. Blum and R. Zenobi, Nanoscale chemical imaging using tip-enhanced Raman spectroscopy: a critical review, *Angew. Chem., Int. Ed.*, 2013, **52**, 5940–5954.

179 K. Vilkevičius, I. Ignatjev, A. Selskis, G. Niaura and E. Stankevičius, Tuning SERS performance through the laser-induced morphology changes of gold nanostructures, *Appl. Surf. Sci.*, 2024, **660**, 160003.

180 R. Qin, Y. Wang, Q. Zhao, K. Yang and F. Pan, EQCM for in-depth study of metal anodes for electrochemical energy storage, *Chin. J. Struct. Chem.*, 2020, **39**, 605–614.

181 S. Daboss, T. Philipp, K. Palanisamy, J. Flowers, H. Stein and C. Kranz, Characterization of the solid/electrolyte interphase at hard carbon anodes via scanning (electrochemical) probe microscopy, *Electrochim. Acta*, 2023, **453**, 142345.

182 M. Zhou, Y. Liao, L. Li, R. Xiong, G. Shen, Y. Chen, T. Huang, M. Li, H. Zhou and Y. Zhang, Unraveling the heterogeneity of solid electrolyte interphase kinetically affecting lithium electrodeposition on lithium metal anode, *J. Energy Chem.*, 2023, **85**, 181–190.

183 Q. Zhang, C. Zhou, M. Li, Y. Zhu, X. Wei, S. Shen, Z. Ji, G. Luo, Y. Cheng and X. Yang, others Revealing Structural Insights of Solid Electrolyte Interphase in High-Concentrated Non-Flammable Electrolyte for Li Metal Batteries by Cryo-TEM, *Small*, 2023, **19**, 2300849.

184 S. Izawa, K. Nakano, K. Suzuki, Y. Chen, T. Kikitsu, D. Hashizume, T. Koganezawa, T.-Q. Nguyen and K. Tajima, Crystallization and polymorphism of organic semiconductor in thin film induced by surface segregated monolayers, *Sci. Rep.*, 2018, **8**, 481.

185 Y. Xu, K. Dong, Y. Jie, P. Adelhelm, Y. Chen, L. Xu, P. Yu, J. Kim, Z. Kochovski and Z. Yu, others Promoting mechanistic understanding of lithium deposition and solid-electrolyte interphase (SEI) formation using advanced characterization and simulation methods: recent progress, limitations, and future perspectives, *Adv. Energy Mater.*, 2022, **12**, 2200398.

186 S. Chen, Z. Gong, P. Zhao, Y. Zhang, B. Cheng, J. Hou, J. Song, X. Ding, J. Sun and J. Shi, others Design of nanostructure in solid electrolyte interphase for enhancing the mechanical durability of lithium metal anode by deep-learning approach, *Energy Storage Mater.*, 2024, **65**, 103096.

187 Y. Fan, X. Wang, G. Bo, X. Xu, K. W. See, B. Johannessen and W. K. Pang, Operando Synchrotron X-Ray Absorption Spectroscopy: A Key Tool for Cathode Material Studies in Next-Generation Batteries, *Advanced Science*, 2025, **12**, 2414480.

188 J. W. Gittins, Y. Chen, S. Arnold, V. Augustyn, A. Balducci, T. Brousse, E. Frackowiak, P. Gómez-Romero, A. Kanwade and L. Köps, others Interlaboratory study assessing the analysis of supercapacitor electrochemistry data, *J. Power Sources*, 2023, **585**, 233637.

189 J. P. A. dos Santos, F. C. Rufino, J. I. Y. Ota, R. C. Fernandes, R. Vicentini, C. J. Pagan, L. M. Da Silva and H. Zanin, Best practices for electrochemical characterization of supercapacitors, *J. Energy Chem.*, 2023, **80**, 265–283.

190 C. Shen, S. Wang, Y. Jin and W.-Q. Han, In situ AFM imaging of solid electrolyte interfaces on HOPG with ethylene carbonate and fluoroethylene carbonate-based electrolytes, *ACS Appl. Mater. Interfaces*, 2015, **7**, 25441–25447.

191 H. Zhang, D. Wang and C. Shen, In-situ EC-AFM and ex-situ XPS characterization to investigate the mechanism of SEI formation in highly concentrated aqueous electrolyte for Li-ion batteries, *Appl. Surf. Sci.*, 2020, **507**, 145059.

192 Y. Liang, M. Burton, B. Jagger, H. Guo, J. Ihli and M. Pasta, In situ XPS investigation of the SEI formed on LGPS and LAGP with metallic lithium, *Chem. Commun.*, 2024, **60**, 12597–12600.

193 R. Guo, D. Wang, L. Zuin and B. M. Gallant, Reactivity and Evolution of Ionic Solid-Electrolyte-Interphases in Battery Electrolytes, *ECS Meet. Abstr.*, 2021, **239**, 149.

194 G. C. Mohanty, C. C. Gowda, P. Gakhad, S. Das, M. Sanjay, S. Chowdhury, K. Biswas, A. Singh and C. S. Tiwary, Iron-cobalt-nickel-copper-zinc (FeCoNiCuZn) high entropy alloy as positive electrode for high specific capacitance supercapacitor, *Electrochim. Acta*, 2023, **470**, 143272.

195 X. Guoguang, W. Min, W. Jian, L. Hongzhen, W. Yang, W. Yang and Z. Yuegang, In-situ Electrochemical Characterization Methodology, *Chin. J. Catal.*, 2019, **40**, 187.

196 R. Yuan, H. Jiao, H. Zhu, D. Fang and S. Jiao, In situ characterization techniques and methodologies for high-temperature electrochemistry, *Chem*, 2023, **9**, 2481–2508.

197 Y. Zhou, M. Su, X. Yu, Y. Zhang, J.-G. Wang, X. Ren, R. Cao, W. Xu, D. R. Baer and Y. Du, others Real-time mass spectrometric characterization of the solid–electrolyte interphase of a lithium-ion battery, *Nat. Nanotechnol.*, 2020, **15**, 224–230.

198 W. Zhang, V. Koverga, S. Liu, J. Zhou, J. Wang, P. Bai, S. Tan, N. K. Dandu, Z. Wang and F. Chen, others Single-phase local-high-concentration solid polymer electrolytes for lithium-metal batteries, *Nat. Energy*, 2024, **9**, 386–400.

199 C.-z. Yang, Y. Lou, J. Zhang, X. Xie and B. Xia, *Materials and Working Mechanisms of Secondary Batteries*, Springer, 2023, pp 207–226.

200 L. T. Hess, N. P. Nguyen, A. H. Dee, A. K. Gupta, Z. Kwon and S. Yue, How Surface Functionalization Controls Confined Electrolyte Structure and Dynamics at Graphene Interfaces, *J. Phys. Chem. B*, 2025, 10864–10872.

201 M. Sk, P. Pradhan, B. Patra and A. Guria, Green biomass derived porous carbon materials for electrical double-layer capacitors (EDLCs), *Mater. Today Chem.*, 2023, **30**, 101582.

202 K. Kraiwattanawong, A review on the development of a porous carbon-based as modeling materials for electric double layer capacitors, *Arabian J. Chem.*, 2022, **15**, 103625.
203 Y. Kado, Y. Soneda, H. Hatori and M. Kodama, Advanced carbon electrode for electrochemical capacitors, *J. Solid State Electrochem.*, 2019, **23**, 1061–1081.
204 Y. Wang, H. Zhao, L. Li and B. An, Minimizing the confinement effect of micropores to optimize the capacitive performance of carbon materials, *J. Alloys Compd.*, 2025, **1010**, 177228.
205 M. Li, C. Ma, X. Cai, K. Yue, J. Yue, Y. Wang, J. Luo, H. Yuan, J. Nai and S. Zou, others Structural composite solid electrolyte interphases on lithium metal anodes induced by inorganic/organic activators, *Mater. Today Energy*, 2024, **46**, 101734.
206 S. Shaheen Shah, S. Oladepo, M. Ali Ehsan, W. Iali, A. Alenaizan, M. Nahid Siddiqui, M. Oyama, A.-R. Al-Betar and M. A. Aziz, Recent progress in polyaniline and its composites for supercapacitors, *Chem. Rec.*, 2024, **24**, e202300105.
207 J. Pan, C. Li, Y. Peng, L. Wang, B. Li, G. Zheng and M. Song, Application of transition metal (Ni, Co and Zn) oxides based electrode materials for ion-batteries and supercapacitors, *Int. J. Electrochem. Sci.*, 2023, **18**, 100233.
208 M. Marr, J. Kuhn, C. Metcalfe, J. Harris and O. Kesler, Electrochemical performance of solid oxide fuel cells having electrolytes made by suspension and solution precursor plasma spraying, *J. Power Sources*, 2014, **245**, 398–405.
209 C.-Y. Tseng, Y.-S. Ye, J. Joseph, K.-Y. Kao, J. Rick, S.-L. Huang and B.-J. Hwang, Tuning transport properties by manipulating the phase segregation of tetramethyldisiloxane segments in modified polyimide electrolytes, *J. Power Sources*, 2011, **196**, 3470–3478.
210 L. Yu, J. Li, N. Ahmad, X. He, G. Wan, R. Liu, X. Ma, J. Liang, Z. Jiang and G. Zhang, Recent progress on carbon materials for emerging zinc-ion hybrid capacitors, *J. Mater. Chem. A*, 2024, **12**, 9400–9420.
211 Y. Huang, J. Zhou, N. Gao, Z. Yin, H. Zhou, X. Yang and Y. Kuang, Synthesis of 3D reduced graphene oxide/unzipped carbon nanotubes/polyaniline composite for high-performance supercapacitors, *Electrochim. Acta*, 2018, **269**, 649–656.
212 D. Bedrov, D. Dong and M. Ebrahiminia, Multiscale Modeling of Formation and Properties of Solid-Electrolyte Interphases in Li-Ion Batteries, *ECS Meet. Abstr.*, 2020, **237**, 2754.
213 Y. Wang, J. Zhang, X. Zhao, Z. Ren, M. Tang, R. Han, G. Feng, B. Li, D. Zhou and F. Kang, Electric Field-Guided Ion Orchestration for Multi-Chemistry Zinc Metal Batteries, *Adv. Mater.*, 2025, e11163.
214 Y. Chen, Y. Shi, G. Song, B. Yang and H. Pang, Compositing MXene with organic coordination frameworks (MOFs, COFs, and HOFs) for enhanced electrochemical performance, *Next Mater.*, 2025, **6**, 100323.
215 T. Naren, R. Jiang, Q. Gu, G.-c. Kuang, L. Chen and Q. Zhang, Fluorinated organic compounds as promising materials to protect lithium metal anode: a review, *Mater. Today Energy*, 2024, **40**, 101512.
216 P. Kurzweil, J. Schottenbauer and C. Schell, Past, present and future of electrochemical capacitors: Pseudocapacitance, aging mechanisms and service life estimation, *J. Energy Storage*, 2021, **35**, 102311.
217 N. Ma, D. Yang, S. Riaz, L. Wang and K. Wang, Aging mechanism and models of supercapacitors: A review, *Technologies*, 2023, **11**, 38.
218 S. Mahala, K. Khosravinia and A. Kiani, Unwanted degradation in pseudocapacitors: Challenges and opportunities, *J. Energy Storage*, 2023, **67**, 107558.
219 B. Nishchith, S. Ashoka, M. P. Bhat, M. D. Kurkuri, S. Acharya, R. Kumar and Y. Kalegowda, Reversible surface reconstruction of Na3NiCO3PO4: A battery type electrode for pseudocapacitor applications, *J. Power Sources*, 2022, **520**, 230903.
220 Y. Huang, C. Yang, B. Deng, C. Wang, Q. Li, C. D. V. Thibault, K. Huang, K. Huo and H. Wu, Nanostructured pseudocapacitors with pH-tunable electrolyte for electrochromic smart windows, *Nano Energy*, 2019, **66**, 104200.
221 J. Ahn, Y. Song, Y. J. Kim, D. Nam, T. Kim, K. Kwak, C. H. Kwon, Y. Ko, S. J. Lee and J. Cho, Redox-active ligand-mediated assembly for high-performance transition metal oxide nanoparticle-based pseudocapacitors, *Chem. Eng. J.*, 2023, **455**, 140742.
222 Z.-H. He, J.-F. Gao and L.-B. Kong, Electrolyte effect on electrochemical behaviors of manganese fluoride material for aqueous asymmetric and symmetric supercapacitors, *Rare Met.*, 2024, **43**, 1048–1061.
223 S. Dang, Z. Wang, W. Jia, Y. Cao and J. Zhang, Facile synthesis of rod-like nickel-cobalt oxide nanostructure for supercapacitor with excellent cycling stability, *Mater. Res. Bull.*, 2019, **116**, 117–125.
224 S. Gong, F. Zhao, H. Xu, M. Li, J. Qi, H. Wang, Z. Wang, X. Fan, C. Li and J. Liu, Iodine-functionalized titanium carbide MXene with ultra-stable pseudocapacitor performance, *J. Colloid Interface Sci.*, 2022, **615**, 643–649.
225 J. Kumar, R. A. Soomro, B. Fan, J. Tan, N. Sun and B. Xu, Butanedioic acid unlock shelf-stable Ti3C2Tx (MXene) dispersions and their electrochemical performance in supercapacitor, *J. Alloys Compd.*, 2024, **1009**, 176749.
226 K. Kawai, M. Fujita, R. Iizuka, A. Yamada and M. Okubo, Influence of surface termination groups on electrochemical charge storage of MXene electrodes, *2D Materials*, 2023, **10**, 014012.
227 N. Badawi, M. Bhuyan, M. Luqman, R. S. Alshareef, M. R. Hatshan, A. Al-Warthan and S. F. Adil, MXenes the future of solid-state supercapacitors: Status, challenges, prospects, and applications, *Arabian J. Chem.*, 2024, **17**, 105866.
228 W. Bai, Z. Yong, S. Wang, X. Wang, C. Li, F. Pan, D. Liang, Y. Cui and Z. Wang, Polyaniline-MXene composite electrode with excellent electrochemical properties for all-solid flexible supercapacitors, *J. Energy Storage*, 2023, **71**, 108053.

229 N. Anjum, A. A. Noman, M. M. Rahman, D. Sen, R. A. Lazenby and O. I. Okoli, Electrochemical impedance analysis of Ti3C2Tx MXene for pseudocapacitive charge storage, *J. Compos. Sci.*, 2025, **9**, 139.

230 R. Singh, M. S. Samuel, M. Ravikumar, S. Ethiraj and M. Kumar, Graphene materials in pollution trace detection and environmental improvement, *Environ. Res.*, 2024, **243**, 117830.

231 J. Wang, Y. Li, S. Jin, X. Zheng, J. Yuan, D. Kong, H. Hu, X. Feng and D. Chen, Structural design and solid electrolyte interphase modulation of SiOC-based anodes via N-doping for fast-charging lithium-ion batteries, *Chem. Eng. J.*, 2025, 164661.

232 X. Liu, J. Sun, Y. Ran, X. Liu, J. Chai, Z. Liu, P. Zheng and Y. Zheng, Surface engineering for enhanced cycling performance of nanosilicon-based anodes in lithium-ion batteries, *J. Power Sources*, 2025, **654**, 237893.

233 N. Zheng, C. Yang, Q. Dong, S. Hu, Q. Tang, J. Ou, H. Wang, J. Wang, H. Zhang and J. Ge, others Coupled design of surface chemistry and spatial topology enabling lithiophilic host for stable Li metal batteries, *Chem. Eng. J.*, 2025, 165412.

234 R. Jamil, S. Loomba, M. Kar, G. E. Collis, D. S. Silvester and N. Mahmood, Metal anodes meet ionic liquids: An interfacial perspective, *Applied Physics Reviews*, 2024, **11**, 011307.

235 S. Azmi, A. Klimek and E. Frackowiak, Why electrochemical capacitor electrolytes should not be ignored?, *Electrochim. Acta*, 2023, **452**, 142347.

236 P. Krishnan and V. Biju, Effect of electrolyte concentration on the electrochemical performance of RGO-Na2SO4 supercapacitor, *Mater. Today: Proc.*, 2022, **54**, 958–962.

237 Y. Zhang, Elucidating Solvation Structures and Their Impact on SEI Formation at Electrode-Electrolyte Interfaces, *ECS Meet. Abstr.*, 2022, **241**, 1146.

238 B. Zhu, X. Shi, T. Zheng, J. Xiong, Y.-J. Cheng and Y. Xia, Usefulness of uselessness: Teamwork of wide temperature electrolyte enables LFP/Li cells from-40 °C to 140 °C, *Electrochim. Acta*, 2022, **425**, 140698.

239 D. Chai, Y. Zhu, C. Guan, T. Zhang, S. Tang, H. Zhu, X. Li and Y. Fu, Achieving stable interphases toward lithium metal batteries by a dilute and anion-rich electrolyte, *Energy Storage Mater.*, 2023, **62**, 102957.

240 S. Zhang, Z. Bo, H. Yang, J. Yang, L. Duan, J. Yan and K. Cen, Insights into the effects of solvent properties in graphene based electric double-layer capacitors with organic electrolytes, *J. Power Sources*, 2016, **334**, 162–169.

241 S. Sayah, A. Ghosh, M. Baazizi, R. Amine, M. Dahbi, Y. Amine, F. Ghamouss and K. Amine, How do super concentrated electrolytes push the Li-ion batteries and supercapacitors beyond their thermodynamic and electrochemical limits?, *Nano Energy*, 2022, **98**, 107336.

242 W. Wang, S. Chen, X. Liao, R. Huang, F. Wang, J. Chen, Y. Wang, F. Wang and H. Wang, Regulating interfacial reaction through electrolyte chemistry enables gradient interphase for low-temperature zinc metal batteries, *Nat. Commun.*, 2023, **14**, 5443.

243 E. Rahmanian, A. Sajedi-Moghaddam, M. T. Hoveizavi and S. H. Aboutalebi, Electrolyte Hydration Energy as a Universal Descriptor for Ion-Specific Capacitance: Insights from Interpretable Machine Learning, *Adv. Powder Mater.*, 2025, 100361.

244 L. Kong, M. Cheng, H. Huang, J. Pang, S. Liu, Y. Xu and X.-H. Bu, Metal-organic frameworks for advanced aqueous ion batteries and supercapacitors, *EnergyChem*, 2022, **4**, 100090.

245 X. Li, Y. Zhang, J. Chen, Y. Wang, Z. Cheng, X. Chen and M. Guo, A cellulose-based interpenetrating network hydrogel electrolyte for flexible solid-state supercapacitors, *Cellulose*, 2023, **30**, 2399–2412.

246 Y. Shao, M. F. El-Kady, J. Sun, Y. Li, Q. Zhang, M. Zhu, H. Wang, B. Dunn and R. B. Kaner, Design and mechanisms of asymmetric supercapacitors, *Chem. Rev.*, 2018, **118**, 9233–9280.

247 G. Wang, L. Zhang and J. Zhang, A review of electrode materials for electrochemical supercapacitors, *Chem. Soc. Rev.*, 2012, **41**, 797–828.

248 N. Zhang, M. Wang, Y. Quan, X. Li, X. Hu, J. Yan, Y. Wang, M. Sun and S. Li, A review of binder-free electrodes for advanced supercapacitors, *J. Ind. Eng. Chem.*, 2025, **141**, 1–31.

249 J. Lefebvre, F. Galli, C. L. Bianchi, G. S. Patience and D. C. Boffito, Experimental methods in chemical engineering: X-ray photoelectron spectroscopy-XPS, *Can. J. Chem. Eng.*, 2019, **97**, 2588–2593.

250 L. Matuana, J. Balatinecz, R. Sodhi and C. Park, Surface characterization of esterified cellulosic fibers by XPS and FTIR spectroscopy, *Wood Sci. Technol.*, 2001, **35**, 191–201.

251 K. Liu, C. Yu, W. Guo, L. Ni, J. Yu, Y. Xie, Z. Wang, Y. Ren and J. Qiu, Recent research advances of self-discharge in supercapacitors: Mechanisms and suppressing strategies, *J. Energy Chem.*, 2021, **58**, 94–109.

252 I. E. Rauda, V. Augustyn, B. Dunn and S. H. Tolbert, Enhancing pseudocapacitive charge storage in polymer templated mesoporous materials, *Acc. Chem. Res.*, 2013, **46**, 1113–1124.

253 T. Tevi and A. Takshi, Modeling and simulation study of the self-discharge in supercapacitors in presence of a blocking layer, *J. Power Sources*, 2015, **273**, 857–862.

254 W. Li, X. Yang, Z. Chen, T. Lv, X. Wang and J. Qiu, Synthesis and structure regulation of armor-wearing biomass-based porous carbon: Suppression the leakage current and self-discharge of supercapacitors, *Carbon*, 2022, **196**, 136–145.

255 J. Yao, M. Shi, W. Li, Q. Han, M. Wu, W. Yang, E. Wang and X. Lu, Fluorinated Ether-Based Electrolyte for Supercapacitors with Increased Working Voltage and Suppressed Self-discharge, *ChemElectroChem*, 2022, **9**, e202200223.

256 M. Liu, M. Xia, R. Qi, Q. Ma, M. Zhao, Z. Zhang and X. Lu, Lyotropic liquid crystal as an electrolyte additive for suppressing self-discharge of supercapacitors, *ChemElectroChem*, 2019, **6**, 2531–2535.

257 S. Hamedi, T. Ghanbari, E. Moshksar and Z. Hosseini, Time-varying model of self-discharge in a double layer

supercapacitor with blocking layer, *J. Energy Storage*, 2021, **40**, 102730.
258 R. Tang, Studies on electrochemical degradation reactions in supercapacitors, *TANSO*, 2021, **2021**, 127–128.
259 X. Chen, Y. Wu and R. Holze, Ag (e) ing and degradation of supercapacitors: Causes, mechanisms, models and countermeasures, *Molecules*, 2023, **28**, 5028.
260 M. Thomas, S. Veleva, B. Karamanova, A. Brigandì, N. Rey-Raap, A. Arenillas, A. Stoyanova and F. Lufrano, Highly stable and reliable asymmetric solid-state supercapacitors with low self-discharge rates, *Sustainable Mater. Technol.*, 2023, **38**, e00770.
261 G. Liu, X. Li, C. Li, Q. Zheng, Y. Wang, R. Xiao, F. Huang, H. Tian, C. Wang and X. Chen, others Efficient Fabrication of Disordered Graphene with Improved Ion Accessibility, Ion Conductivity, and Density for High-Performance Compact Capacitive Energy Storage, *Advanced Science*, 2024, **11**, 2405155.
262 K. Sarkar and M. A. Talukder, Effects of Edge Atoms and Channel Width on Charge Storage in Nanoporous Carbon Supercapacitors, *arXiv*, 2026, preprint, arXiv:2601.01601, DOI: 10.48550/arXiv.2601.01601.
263 Y. Li, X. Fan, M. Zhang, L. Cui and T. Jiao, Enhanced electrochemical performance of the activated carbon electrodes with a facile and in-situ phosphoric acid modification, *J. Energy Storage*, 2019, **24**, 100744.
264 I. Hussain, K. Singh, M. N. Naseer, M. Al Mahmud, M. K. Aslam, P. Rosaiah, A. Riza, H. Shahzad, A. Ali and W. U. Arifeen, others MXenes in aqueous electrolytes: integrating computational and experimental insights, *J. Ind. Eng. Chem.*, 2026, in press.
265 K. Shevchuk, K. Matthews, R. Wang and Y. Gogotsi, In Situ Electrochemical Raman Spectroscopy of MXenes in Confined Electrolytes, *ECS Meet. Abstr.*, 2023, **244**, 2668.
266 L. Zhang, Y. Cai, R. Fang, Y. Wang and S. Xu, Construction of fully coated polypyrrole oxygen-barrier film based on MXene nanosheets for high reliability capacitive deionization, *Sep. Purif. Technol.*, 2024, **337**, 126362.
267 X. Li, Z. Huang, C. E. Shuck, G. Liang, Y. Gogotsi and C. Zhi, MXene chemistry, electrochemistry and energy storage applications, *Nat. Rev. Chem.*, 2022, **6**, 389–404.
268 M. Wu, S. Xie, C. Yang, X. Xue, H. Li, C. Zhang and J. Xu, An experimental study on the failure behaviors of hybrid supercapacitors under overdischarge conditions, *Ionics*, 2024, **30**, 1061–1074.
269 L. Jin, X. Guo, C. Shen, N. Qin, J. Zheng, Q. Wu, C. Zhang and J. P. Zheng, A universal matching approach for high power-density and high cycling-stability lithium ion capacitor, *J. Power Sources*, 2019, **441**, 227211.
270 O. G. Rojas and W. Sugimoto, Enhanced cycle life and capacity retention of dual electrolyte Li-ion capacitor through optimization of the solid electrolyte, *J. Power Sources Adv.*, 2025, **33**, 100179.
271 V. Vanpeene, I. Martens, M. Mirolo, A. Benayad, L. Daniel, S. Geniès, Y. Maletin, N. Stryzhakova, S. Zelinskyi and S. Chernukhin, others Quantifying degradation mechanisms in a high-performance parallel hybrid lithium-ion supercapacitor induced by long term cycling at high current rates, *J. Electrochem. Soc.*, 2023, **170**, 060517.
272 Y. Qian, B. Wu, Y. Li, Z. Pan, J. Tian, N. Lin and Y. Qian, Pressure-dependent self-template pyrolysis modulates the porosity and surface chemical configuration of carbon for potassium ion hybrid capacitors, *Chem. Eng. J.*, 2023, **451**, 138579.
273 C. H. Lee, J. A. Dura, A. LeBar and S. C. DeCaluwe, Direct, operando observation of the bilayer solid electrolyte interphase structure: Electrolyte reduction on a non-intercalating electrode, *J. Power Sources*, 2019, **412**, 725–735.
274 D. Qiao, X. Wei, J. Zhu, G. Zhang, S. Yang, X. Wang, B. Jiang, X. Lai, Y. Zheng and H. Dai, Mechanism of battery expansion failure due to excess solid electrolyte interphase growth in lithium-ion batteries, *ETransportation*, 2025, 100450.
275 Q. Zhang, Y. Wang and B. Wei, Distinct Self-Discharge Processes via Manipulating Electrode Pore Size of Carbon-Based Electrochemical Capacitors, *Adv. Energy Mater.*, 2023, **13**, 2301860.
276 B. Uralcan and I. B. Uralcan, Origin of enhanced performance in nanoporous electrical double layer capacitors: insights on micropore structure and electrolyte composition from molecular simulations, *ACS Appl. Mater. Interfaces*, 2022, **14**, 16800–16808.
277 W. Fang, Z. Wen, L. Chen, Z. Qin, J. Li, Z. Zheng, Z. Weng, G. Wu, N. Zhang and X. Liu, others Constructing inorganic-rich solid electrolyte interphase via abundant anionic solvation sheath in commercial carbonate electrolytes, *Nano Energy*, 2022, **104**, 107881.
278 M. C. Santos, G. G. Silva, R. Santamaria, P. F. Ortega and R. L. Lavall, Discussion on operational voltage and efficiencies of ionic-liquid-based electrochemical capacitors, *J. Phys. Chem. C*, 2019, **123**, 8541–8549.
279 M. Hu, L. Chen, Y. Jing, Y. Zhu, J. Dai, A. Meng, C. Sun, J. Jia and Z. Li, Intensifying electrochemical activity of Ti3C2Tx MXene via customized interlayer structure and surface chemistry, *Molecules*, 2023, **28**, 5776.
280 X. Jiang, X. Chu, X. Zhang, Y. Xie, T. Yang, J. Huang, W. Li, W. Deng, H. Zhang and W. Yang, Surplus Charge Injection Enables High-Voltage Stable 2d Polyaniline Supercapacitors, *Electrochim. Acta*, 2023, **445**, 142052.
281 A. Parejo-Tovar, F. Béguin and P. Ratajczak, Comprehensive potentiodynamic analysis of electrodes performance in hybrid capacitors, *Electrochem. Commun.*, 2023, **147**, 107436.
282 Q. Abbas, H. Fitzek, V. Pavlenko and B. Gollas, Towards an optimized hybrid electrochemical capacitor in iodide based aqueous redox-electrolyte: Shift of equilibrium potential by electrodes mass-balancing, *Electrochim. Acta*, 2020, **337**, 135785.
283 W. I. Choi, M. S. Park, Y. Shim, H. S. Lee and J. Shin, Atomistic Simulation of Solid Electrolyte Interphase (SEI) Using Reactive Force Field, *ECS Meet. Abstr.*, 2016, **230**, 572.
284 Z. Zhang and W.-Q. Han, From liquid to solid-state lithium metal batteries: fundamental issues and recent developments, *Nano-Micro Lett.*, 2024, **16**, 24.

285 Y. Wang, J. Hong and F. Hao, Mechanical and Li diffusion properties of interface systems in the solid electrolyte interphase, *JOM*, 2024, **76**, 1153–1161.
286 L. Zeng, J. Peng, J. Zhang, X. Tan, X. Ji, S. Li and G. Feng, Molecular dynamics simulations of electrochemical interfaces, *J. Chem. Phys.*, 2023, **159**, 091001.
287 L. Yu, X. Chen, N. Yao, Y.-C. Gao and Q. Zhang, Constant-potential molecular dynamics simulation and its application in rechargeable batteries, *J. Mater. Chem. A*, 2023, **11**, 11078–11088.
288 O. M. Magnussen and A. Groß, Toward an atomic-scale understanding of electrochemical interface structure and dynamics, *J. Am. Chem. Soc.*, 2019, **141**, 4777–4790.
289 Y. He, J. Deng, K. Wang, Q. Gou, H. Luo, Z. Luogu, Z. Chen, K. Wen, Y. Zheng and M. Li, B io-inspired ion channels for suppressing interfacial parasitic reactions and enabling low-energy ion desolvation in aqueous supercapacitors, *Chem. Sci.*, 2025, 16757–16769.
290 C. Pean, B. Daffos, B. Rotenberg, P. Levitz, M. Haefele, P.-L. Taberna, P. Simon and M. Salanne, Confinement, desolvation, and electrosorption effects on the diffusion of ions in nanoporous carbon electrodes, *J. Am. Chem. Soc.*, 2015, **137**, 12627–12632.
291 X. Tan, M. Chen, J. Zhang, S. Li, H. Zhang, L. Yang, T. Sun, X. Qian and G. Feng, Decoding electrochemical processes of lithium-ion batteries by classical molecular dynamics simulations, *Adv. Energy Mater.*, 2024, **14**, 2400564.
292 P. M. Singer, D. Asthagiri, W. G. Chapman and G. J. Hirasaki, Molecular dynamics simulations of NMR relaxation and diffusion of bulk hydrocarbons and water, *J. Magn. Reson.*, 2017, **277**, 15–24.
293 J. Yang, Z. Bo, H. Yang, H. Qi, J. Kong, J. Yan and K. Cen, Reliability of Constant Charge Method for Molecular Dynamics Simulations on EDLCs in Nanometer and Sub-Nanometer Spaces, *ChemElectroChem*, 2017, **4**, 2486–2493.
294 L. Zeng, X. Tan, X. Ji, S. Li, J. Zhang, J. Peng, S. Bi and G. Feng, Constant charge method or constant potential method: Which is better for molecular modeling of electrical double layers?, *J. Energy Chem.*, 2024, **94**, 54–60.
295 A. Chaudhari, K. Agrawal and A. J. Logsdail, Machine learning generalised DFT+ U projectors in a numerical atom-centred orbital framework, *Digital Discovery*, 2025, 3701–3727.
296 W.-Q. Li, G. Wu, J. M. Arce-Ramos, Y. H. Lau and M.-F. Ng, Enabling accurate modelling of materials for a solid electrolyte interphase in lithium-ion batteries using effective machine learning interatomic potentials, *Mater. Horiz.*, 2025, 10770–10781.
297 J. Dai, X. Li, L. Zhao and H. Sun, Enthalpies of mixing predicted using molecular dynamics simulations and OPLS force field, *Fluid Phase Equilib.*, 2010, **289**, 156–165.
298 S. Riniker, Fixed-charge atomistic force fields for molecular dynamics simulations in the condensed phase: An overview, *J. Chem. Inf. Model.*, 2018, **58**, 565–578.
299 Y. Han, D. Jiang, J. Zhang, W. Li, Z. Gan and J. Gu, Development, applications and challenges of ReaxFF reactive force field in molecular simulations, *Front. Chem. Sci. Eng.*, 2016, **10**, 16–38.
300 M. J. Hossain, G. Pawar, B. Liaw, K. L. Gering, E. J. Dufek and A. C. Van Duin, Lithium-electrolyte solvation and reaction in the electrolyte of a lithium ion battery: A ReaxFF reactive force field study, *J. Chem. Phys.*, 2020, **152**, 184301.
301 O. T. Unke, S. Chmiela, M. Gastegger, K. T. Schütt, H. E. Sauceda and K.-R. Müller, SpookyNet: Learning force fields with electronic degrees of freedom and nonlocal effects, *Nat. Commun.*, 2021, **12**, 7273.
302 M. O. Wilson and D. M. Huang, Anisotropic molecular coarse-graining by force and torque matching with neural networks, *J. Chem. Phys.*, 2023, **159**, 024110.
303 Y. Xu, H. Jia, P. Gao, D. E. Galvez-Aranda, S. P. Beltran, X. Cao, P. M. Le, J. Liu, M. H. Engelhard and S. Li, others Direct in situ measurements of electrical properties of solid–electrolyte interphase on lithium metal anodes, *Nat. Energy*, 2023, **8**, 1345–1354.
304 Y. Zhang, D. Krishnamurthy and V. Viswanathan, Engineering solid electrolyte interphase composition by assessing decomposition pathways of fluorinated organic solvents in lithium metal batteries, *J. Electrochem. Soc.*, 2020, **167**, 070554.
305 V. J. Ovejas and A. Cuadras, Impedance characterization of an LCO-NMC/graphite cell: Ohmic conduction, SEI transport and charge-transfer phenomenon, *Batteries*, 2018, **4**, 43.
306 K. Vishweswariah, N. G. Ningappa, M. D. Bouguern, A. Kumar MR, M. B. Armand and K. Zaghib, Evaluation and Characterization of SEI Composition in Lithium Metal and Anode-Free Lithium Batteries, *Adv. Energy Mater.*, 2025, 2501883.
307 P. Ramadass, B. Haran, R. White and B. N. Popov, Capacity fade of Sony 18650 cells cycled at elevated temperatures: Part I. Cycling performance, *J. Power Sources*, 2002, **112**, 606–613.
308 J. J. Gabriel, N. H. Paulson, T. C. Duong, F. Tavazza, C. A. Becker, S. Chaudhuri and M. Stan, Uncertainty quantification in atomistic modeling of metals and its effect on mesoscale and continuum modeling: A review, *Jom*, 2021, **73**, 149–163.
309 F. Schomburg, B. Heidrich, S. Wennemar, R. Drees, T. Roth, M. Kurrat, H. Heimes, A. Jossen, M. Winter and J. Y. Cheong, others Lithium-ion battery cell formation: status and future directions towards a knowledge-based process design, *Energy Environ. Sci.*, 2024, **17**, 2686–2733.
310 T. Zhang, H. Sun, C. Yin, Y. H. Jung, S. Min, Y. Zhang, C. Zhang, Q. Chen, K. J. Lee and Q. Chi, Recent progress in polymer dielectric energy storage: from film fabrication and modification to capacitor performance and application, *Prog. Mater. Sci.*, 2023, **140**, 101207.
311 R. Weber, M. Genovese, A. Louli, S. Hames, C. Martin, I. G. Hill and J. Dahn, Long cycle life and dendrite-free lithium morphology in anode-free lithium pouch cells enabled by a dual-salt liquid electrolyte, *Nat. Energy*, 2019, **4**, 683–689.

312 T. He, X. Kang, F. Wang, J. Zhang, T. Zhang and F. Ran, Capacitive contribution matters in facilitating high power battery materials toward fast-charging alkali metal ion batteries, *Mater. Sci. Eng., R*, 2023, **154**, 100737.

313 P. J. Weddle, E. W. C. Spotte-Smith, A. Verma, H. D. Patel, K. Fink, B. J. T. de Villers, M. C. Schulze, S. M. Blau, K. A. Smith and K. A. Persson, others Continuum-level modeling of Li-ion battery SEI by upscaling atomistically informed reaction mechanisms, *Electrochim. Acta*, 2023, **468**, 143121.

314 S. C. DeCaluwe, Open software for chemical and electrochemical modeling: Opportunities and challenges, *Electrochem. Soc. Interface*, 2019, **28**, 47.

315 P. Hou, Y. Tian and X. Meng, Improving Molecular-Dynamics Simulations for Solid–Liquid Interfaces with Machine-Learning Interatomic Potentials, *Chem. - Eur. J.*, 2024, **30**, e202401373.

316 Q. Chen, S. Wang and C. Ling, Redefining atomistic simulations of all-solid-state batteries through machine learning interatomic potentials, *J. Energy Chem.*, 2025, 666–687.

317 M. Bin Jassar, C. Michel, S. Abada, T. De Bruin, S. Tant, C. Nieto-Draghi and S. N. Steinmann, A Perspective on the Molecular Modeling of Electrolyte Decomposition Reactions for Solid Electrolyte Interphase Growth in Lithium-Ion Batteries, *Adv. Funct. Mater.*, 2024, **34**, 2313188.

318 S. Rocken and J. Zavadlav, Enhancing machine learning potentials through transfer learning across chemical elements, *J. Chem. Inf. Model.*, 2025, **65**, 7406–7414.

319 V. G. Fletcher, A. P. Bartók and L. B. Pártay, Optimal Autonomous MLIP Dataset Building, *arXiv*, 2025, preprint, arXiv:2508.08864, DOI: 10.48550/arXiv.2508.08864.

320 L.-T. Wu, B. J. Hwang and J.-C. Jiang, Combined machine learning and computational protocols to predict electrolyte behavior and SEI formation in Li-metal batteries, *Chem. Eng. J.*, 2025, 163801.

321 H. Wang, L. Zhang and J. Han, others DeePMD-kit: A deep learning package for many-body potential energy representation and molecular dynamics, *Comput. Phys. Commun.*, 2018, **228**, 178–184.

322 S. Gramatte, V. Turlo and O. Politano, Do we really need machine learning interatomic potentials for modeling amorphous metal oxides? Case study on amorphous alumina by recycling an existing ab initio database, *Modell. Simul. Mater. Sci. Eng.*, 2024, **32**, 045010.

323 T. Maxson, A. Soyemi, X. Zhang, B. W. Chen and T. Szilvási, MS25: materials science-focused benchmark data set for machine learning interatomic potentials, *J. Chem. Inf. Model.*, 2025, **65**, 8097–8112.

324 V. Bihani, S. Mannan, U. Pratiush, T. Du, Z. Chen, S. Miret, M. Micoulaut, M. M. Smedskjaer, S. Ranu and N. A. Krishnan, EGraFFBench: evaluation of equivariant graph neural network force fields for atomistic simulations, *Digital Discovery*, 2024, **3**, 759–768.

325 A. Siddiqui and N. D. Hine, Machine-learned interatomic potentials for transition metal dichalcogenide Mo1- x W x S2- 2 y Se2 y alloys, *npj Comput. Mater.*, 2024, **10**, 169.

326 J. Chen and T. J. Martínez, QTPIE: Charge transfer with polarization current equalization. A fluctuating charge model with correct asymptotics, *Chem. Phys. Lett.*, 2007, **438**, 315–320.

327 V. Zaverkin, D. Holzmüller, H. Christiansen, F. Errica, F. Alesiani, M. Takamoto, M. Niepert and J. Kästner, Uncertainty-biased molecular dynamics for learning uniformly accurate interatomic potentials, *npj Comput. Mater.*, 2024, **10**, 83.

328 J. Wang, D. Yu, X. Sun, H. Wang and J. Li, Anodes for low-temperature rechargeable batteries, *Escience*, 2024, **4**, 100252.

329 Q. Sun, Y. Xiang, Y. Liu, L. Xu, T. Leng, Y. Ye, A. Fortunelli, W. A. Goddard III and T. Cheng, Machine learning predicts the x-ray photoelectron spectroscopy of the solid electrolyte interface of lithium metal battery, *Mater. Today Phys.*, 2022, **13**, 8047–8054.

330 B. Tyler, Interpretation of TOF-SIMS images: multivariate and univariate approaches to image de-noising, image segmentation and compound identification, *Appl. Surf. Sci.*, 2003, **203**, 825–831.

331 S. Chatterjee, B. Singh, A. Diwan, Z. R. Lee, M. H. Engelhard, J. Terry, H. D. Tolley, N. B. Gallagher and M. R. Linford, A perspective on two chemometrics tools: PCA and MCR, and introduction of a new one: Pattern recognition entropy (PRE), as applied to XPS and ToF-SIMS depth profiles of organic and inorganic materials, *Appl. Surf. Sci.*, 2018, **433**, 994–1017.

332 M. Bertz, M. Yanagisawa and T. Homma, Deep Learning Combined with Surface-Enhanced Raman Spectroscopy for Chemical Sensing and Recognition, *ECS Meet. Abstr.*, 2021, **239**, 1311.

333 X. Xu, X. Han, L. Lu, F. Wang, M. Yang, X. Liu, Y. Wu, S. Tang, Y. Hou and J. Hou, others Challenges and opportunities toward long-life lithium-ion batteries, *J. Power Sources*, 2024, **603**, 234445.

334 B. Zhu, K. Kretschmer, N. Schlüter and D. Schröder, Combined Machine Learning and Electrochemical Impedance Spectroscopy to Diagnose and Predict the State-of-Health of Commercial SMD Solid-State Batteries, *ECS Meet. Abstr.*, 2023, **243**, 2469.

335 Y. Zheng, W. Zhang, F. Liu, Q. Liang, W. Li, X. Zhou, N. Yue and W. Zheng, Additive-rejuvenated anions (De) intercalation into graphite cathode enables optimum dual-ion battery, *Energy Storage Mater.*, 2024, **67**, 103326.

336 I. A. Soomro, M. N. Lakhan, A. Hanan, H. Almujibah, A. Hussain, A. H. Pato, M. Ahmed, I. A. Chandio, S. A. Memon and M. Umer, others 2D MXenes as electrode materials for metal-sulfur batteries: A review, *Mater. Today Phys.*, 2024, **45**, 101453.

337 J. Wang, M. Wang, F. Chen, Y. Li, L. Zhang, Y. Zhao and C. Chen, In-situ construction of lithiophilic interphase in vertical micro-channels of 3D copper current collector for

high performance lithium-metal batteries, *Energy Storage Mater.*, 2021, **34**, 22–27.

338 J. Xiao, Q. Dai, X. Shen, X. Xie, J. Dai, J. Lam and K.-W. Kwok, Semi-supervised domain adaptation on graphs with contrastive learning and minimax entropy, *Neurocomputing*, 2024, **580**, 127469.

339 M.-F. Ng, Y. Sun and Z. W. Seh, Machine learning-inspired battery material innovation, *Energy Adv.*, 2023, **2**, 449–464.

340 A. Verma, P. Weddle, A. M. Colclasure, J. Atkins and S. C. DeCaluwe, Multiscale Modeling of Solid Electrolyte Interphase Growth in Silicon Anodes, *ECS Meet. Abstr.*, 2021, **240**, 382.

341 M. Arvani, J. Keskinen, D. Lupo and M. Honkanen, Current collectors for low resistance aqueous flexible printed supercapacitors, *J. Energy Storage*, 2020, **29**, 101384.

342 S. C. Kim, S. T. Oyakhire, C. Athanitis, J. Wang, Z. Zhang, W. Zhang, D. T. Boyle, M. S. Kim, Z. Yu, X. Gao, T. Sogade, E. Wu, J. Qin, Z. Bao, S. F. Bent and Y. Cui, Data-driven electrolyte design for lithium metal anodes, *Proc. Natl. Acad. Sci. U. S. A.*, 2023, **120**, e2214357120.

343 S. Manna, S. S. Manna and B. Pathak, Integrated supervised and unsupervised machine learning approach to map the electrochemical windows over 4500 solvents for battery applications, *ACS Appl. Mater. Interfaces*, 2024, **16**, 42138–42152.

344 B. Reddy, P. Narayana, A. Maurya, U. M. R. Paturi, J. Sung, H.-J. Ahn, K. Cho and N. Reddy, Modeling capacitance of carbon-based supercapacitors by artificial neural networks, *J. Energy Storage*, 2023, **72**, 108537.

345 Y. Chai, W. Jia, Z. Hu, S. Jin, H. Jin, H. Ju, X. Yan, H. Ji and L.-J. Wan, Monitoring the mechanical properties of the solid electrolyte interphase (SEI) using electrochemical quartz crystal microbalance with dissipation, *Chin. Chem. Lett.*, 2021, **32**, 1139–1143.

346 L. Liu, C. Liu, M.-Y. Wang, B. Li, K. Wang, X.-Q. Fan, L.-Y. Wang, H.-Q. Wang, S.-L. Hu and X.-G. Diao, Anti-self-discharge ultrathin all-inorganic electrochromic asymmetric supercapacitors enabling intelligent and effective energy storage: L. Liu et al, *Rare Met.*, 2023, **42**, 2957–2971.

347 W. Guo, Y. Li, Z. Sun, S. B. Vilsen and D. I. Stroe, A digital twin to quantitatively understand aging mechanisms coupled effects of NMC battery using dynamic aging profiles, *Energy Storage Mater.*, 2023, **63**, 102965.

348 H. You, X. Wang, J. Zhu, B. Jiang, G. Han, X. Wei and H. Dai, Investigation of lithium-ion battery nonlinear degradation by experiments and model-based simulation, *Energy Storage Mater.*, 2024, **65**, 103083.

349 X. Wang, Y. Jin, S. Schmitt and M. Olhofer, Recent advances in Bayesian optimization, *ACM Computing Surveys*, 2023, vol. 55, pp. 1–36.

350 H. Li, J. Hao and S.-Z. Qiao, AI-Driven Electrolyte Additive Selection to Boost Aqueous Zn-Ion Batteries Stability, *Adv. Mater.*, 2024, **36**, 2411991.

351 P. Ma, R. Kumar, K.-H. Wang and C. V. Amanchukwu, Active learning accelerates electrolyte solvent screening for anode-free lithium metal batteries, *Nat. Commun.*, 2025, **16**, 8396.

352 P. Yan, M. Fischer, H. Martin, C. Wölke, A. N. Krishnamoorthy, I. Cekic-Laskovic, D. Diddens, M. Winter and A. Heuer, Non-aqueous battery electrolytes: high-throughput experimentation and machine learning-aided optimization of ionic conductivity, *J. Mater. Chem. A*, 2024, **12**, 19123–19136.

353 Q. A. Sial, U. Safder, S. Iqbal and R. B. Ali, Advancement in supercapacitors for IoT applications by using machine learning: current trends and future technology, *Sustainability*, 2024, **16**, 1516.

354 D. Rajagopal, A. Koeppe, M. Esmaeilpour, M. Selzer, W. Wenzel, H. Stein and B. Nestler, Data-Driven Virtual Material Analysis and Synthesis for Solid Electrolyte Interphases, *Adv. Energy Mater.*, 2023, **13**, 2301985.

355 M. G. Nam, H. J. Song, J. K. Koo, G. H. Choi, Y. S. Kim, H. J. Kim, C.-S. Shin, Y. Kim, J. H. Nah and Y.-J. Kim, others Standardized cycle life assessment of batteries using extremely lean electrolytic testing conditions, *Commun. Mater.*, 2024, **5**, 29.

356 X. Zhang, Y. Wang, P. Li and Y. Shang, Physics-based modeling and simulation of the evolution of solid electrolyte interphase film in lithium-ion batteries, *J. Energy Storage*, 2026, **141**, 119329.

357 P. E. Lokhande, U. S. Chavan and A. Pandey, Materials and fabrication methods for electrochemical supercapacitors: overview, *Electrochem. Energy Rev.*, 2020, **3**, 155–186.

358 T. L. Kulova and A. M. Skundin, Electrode/electrolyte interphases of sodium-ion batteries, *Energies*, 2022, **15**, 8615.

359 D. Peyrow Hedayati, G. Singh, M. Kucher, T. D. Keene and R. Böhm, Physicochemical Modeling of Electrochemical Impedance in Solid-State Supercapacitors, *Materials*, 2023, **16**, 1232.

360 F. Single, B. Horstmann and A. Latz, Theory of impedance spectroscopy for lithium batteries, *J. Phys. Chem. C*, 2019, **123**, 27327–27343.

361 L. M. Housel, A. Abraham, G. D. Renderos, K. J. Takeuchi, E. S. Takeuchi and A. C. Marschilok, Surface electrolyte interphase control on magnetite, Fe3O4, electrodes: impact on electrochemistry, *MRS Adv.*, 2018, **3**, 581–586.

362 Y. Liu, K. Dong, T. Lv, Z. Chen, S. Cao, Q. Lu, F. Zheng and T. Chen, Revealing the mechanism of bilayer heterogeneous polyelectrolytes to suppress the self-discharge of symmetric supercapacitors, *Small Struct.*, 2023, **4**, 2300046.

363 K. Crompton, M. Hladky, H. H. Park, S. Prokes, C. Love and B. Landi, Lithium-ion cycling performance of multi-walled carbon nanotube electrodes and current collectors coated with nanometer scale Al2O3 by atomic layer deposition, *Electrochim. Acta*, 2018, **292**, 628–638.

364 D. Gandla, G. Song, C. Wu, Y. Ein-Eli and D. Q. Tan, Cover Feature: Atomic Layer Deposition (ALD) of Alumina over Activated Carbon Electrodes Enabling a Stable 4 V Supercapacitor Operation (4/2021), *ChemistryOpen*, 2021, **10**, 388.

365 C. Zheng, J. Wu, L. Zhang and H. Wang, Vital roles of fluoroethylene carbonate in electrochemical energy storage devices: a review, *J. Mater. Chem. C*, 2023, **11**, 344–363.

366 J. Lee, J.-Y. Jeong, J. Ha, Y.-T. Kim and J. Choi, Understanding solid electrolyte interface formation on graphite and silicon anodes in lithium-ion batteries: Exploring the role of fluoroethylene carbonate, *Electrochem. Commun.*, 2024, **163**, 107708.

367 B. Babu, Self-discharge in rechargeable electrochemical energy storage devices, *Energy Storage Mater.*, 2024, **67**, 103261.

368 P. Przygocki, P. Ratajczak and F. Béguin, Quantification of the Charge Consuming Phenomena under High-Voltage Hold of Carbon/Carbon Supercapacitors by Coupling Operando and Post-Mortem Analyses, *Angew. Chem.*, 2019, **131**, 18137–18145.

369 N. U. H. L. Ali, P. Pazhamalai, A. Sathyaseelan, R. Swaminathan and S.-J. Kim, Sodium polyacrylate hydrogel electrolyte: Flexible rechargeable supercapacitor using thermally reduced graphene oxide nanosheets, *J. Power Sources*, 2025, **625**, 235648.

370 Y. Cao, H. Zhang, Y. Zhang, Z. Yang, D. Liu, H. Fu, Y. Zhang, M. Liu and Q. Li, Epitaxial nanofiber separator enabling folding-resistant coaxial fiber-supercapacitor module, *Energy Storage Mater.*, 2022, **49**, 102–110.

371 J. Wagner-Henke, D. Kuai, M. Gerasimov, F. Röder, P. B. Balbuena and U. Krewer, Knowledge-driven design of solid-electrolyte interphases on lithium metal via multiscale modelling, *Nat. Commun.*, 2023, **14**, 6823.

372 A. Tahmasbi, T. Kadyk and M. Eikerling, Statistical physics-based model of solid electrolyte interphase growth in lithium ion batteries, *J. Electrochem. Soc.*, 2017, **164**, A1307.

373 E. Locorotondc, L. Pugi, L. Berzi, M. Pierini, S. Scavuzzc, A. Ferraris, A. G. Airale and M. Carello, Modeling and simulation of constant phase element for battery electrochemical impedance spectroscopy, *2019 IEEE 5th International Forum on Research and Technology for Society and Industry (RTSI)*, 2019, pp 225–230.

374 J. Moškon and M. Gaberšček, Transmission line models for evaluation of impedance response of insertion battery electrodes and cells, *J. Power Sources Adv.*, 2021, **7**, 100047.

375 U. Tröltzsch and O. Kanoun, Generalization of transmission line models for deriving the impedance of diffusion and porous media, *Electrochim. Acta*, 2012, **75**, 347–356.

376 M. Schalenbach, V. Selmert, A. Kretzschmar, L. Raijmakers, Y. E. Durmus, H. Tempel and R.-A. Eichel, How microstructures, oxide layers, and charge transfer reactions influence double layer capacitances. Part 1: impedance spectroscopy and cyclic voltammetry to estimate electrochemically active surface areas (ECSAs), *Phys. Chem. Chem. Phys.*, 2024, **26**, 14288–14304.

377 M. Pech-Canul and P. Castro, Corrosion measurements of steel reinforcement in concrete exposed to a tropical marine atmosphere, *Cem. Concr. Res.*, 2002, **32**, 491–498.

378 M. Itagaki, S. Suzuki, I. Shitanda, K. Watanabe and H. Nakazawa, Impedance analysis on electric double layer capacitor with transmission line model, *J. Power Sources*, 2007, **164**, 415–424.

379 J. Lin, W. Hu, J. Yang, L. Pan, X. Xia, Y. Wei, Z. Gong and Y. Yang, Revisiting High-Frequency Impedance in Li-Ion Batteries: Decoupling Solid Electrolyte Interphase Resistance from Pore Impedance, *Mater. Today Phys.*, 2025, **16**, 7490–7497.

380 S. Perez Beltran and P. B. Balbuena, Unraveling the Dynamics of Solid-Electrolyte Interphase (SEI) Formation on Lithium Metal: Insights from Multiscale Modeling, *ECS Meet. Abstr.*, 2024, **245**, 157.

381 D. D. Macdonald, Why electrochemical impedance spectroscopy is the ultimate tool in mechanistic analysis, *ECS Trans.*, 2009, **19**(20), 55–79.

382 E.-C. Shin, P.-A. Ahn, H.-H. Seo and J.-S. Lee, others Application of a general gas electrode model to Ni-YSZ symmetric cells: Humidity and current collector effects, *J. Korean Ceram. Soc.*, 2016, **53**, 511–520.

383 S. I. Abdul Halim, C. H. Chan and J. Apotheker, Basics of teaching electrochemical impedance spectroscopy of electrolytes for ion-rechargeable batteries–part 1: a good practice on estimation of bulk resistance of solid polymer electrolytes, *Chem. Teach. Int.*, 2021, **3**, 105–115.

384 X. Wang, M. Salari, D.-e. Jiang, J. Chapman Varela, B. Anasori, D. J. Wesolowski, S. Dai, M. W. Grinstaff and Y. Gogotsi, Electrode material–ionic liquid coupling for electrochemical energy storage, *Nat. Rev. Mater.*, 2020, **5**, 787–808.

385 S. Xiang, L. Zhu, L. Fu, M. Wang, X. Zhang, Y. Tang, D. Sun and H. Wang, Cryogenic and in situ characterization techniques for electrode interphase analysis, *eScience*, 2025, **5**, 100291.

386 D. E. Galvez-Aranda, C. Vicharra, L. Selis, F. Franco-Gallo, T. M. Gamero and J. M. Seminario, Molecular Dynamics Study of Interphase Solid Electrolyte/Electrode in Li-Ion Batteries, *ECS Meet. Abstr.*, 2018, 450.

387 R. Li, L. Bao, L. Chen, C. Zha, J. Dong, N. Qi, R. Tang, Y. Lu, M. Wang and R. Huang, others Accelerated aging of lithium-ion batteries: bridging battery aging analysis and operational lifetime prediction, *Sci. Bull.*, 2023, **68**, 3055–3079.

388 Z. Sheng, X. Lin, H. Wei, Y. Zhang, Z. Tian, C. Wang, D. Xu and Y. Wang, Green synthesis of nitrogen-doped hierarchical porous carbon nanosheets derived from polyvinyl chloride towards high-performance supercapacitor, *J. Power Sources*, 2021, **515**, 230629.

389 S. Liu, Z. Liu, X. Shen, X. Wang, S.-C. Liao, R. Yu, Z. Wang, Z. Hu, C.-T. Chen and X. Yu, others Li–Ti cation mixing enhanced structural and performance stability of Li-rich layered oxide, *Adv. Energy Mater.*, 2019, **9**, 1901530.

390 J. Jin, X. Geng, Q. Chen and T.-L. Ren, A better Zn-ion storage device: recent progress for Zn-ion hybrid supercapacitors, *Nano-Micro Lett.*, 2022, **14**, 64.

391 J. Liang, A. Rawal, M. Yu, K. Xiao, H. Liu, Y. Jiang, A. Lennon and D.-W. Wang, Low-potential solid-solid

interfacial charging on layered polyaniline anode for high voltage pseudocapacitive intercalation Li-ion supercapacitors, *Nano Energy*, 2023, **105**, 108010.

392 Z. Jia, S. Hou, J. Peng, X. Wu, W. Tang, W. Sun, S. Lv, X. Yuan, L. Liu and Y. Wu, Recent advances in aqueous and non-aqueous alkali metal hybrid ion capacitors, *J. Mater. Chem. A*, 2024, **12**, 17835–17895.

393 D. Majumdar, M. Mandal and S. K. Bhattacharya, Journey from supercapacitors to supercapatteries: recent advancements in electrochemical energy storage systems, *Emergent Mater.*, 2020, **3**, 347–367.

394 L. Xia, B. Tang, J. Wei and Z. Zhou, Recent advances in alkali metal-ion hybrid supercapacitors, *Rare Met.*, 2021, **4**, 1108–1121.

395 B. A. Ali and N. K. Allam, A first-principles roadmap and limits to design efficient supercapacitor electrode materials, *Phys. Chem. Chem. Phys.*, 2019, **21**, 17494–17511.

396 L. Jia, J. Zhu, X. Zhang, B. Guo, Y. Du and X. Zhuang, Li–solid electrolyte interfaces/interphases in all-solid-state Li batteries, *Electrochem. Energy Rev.*, 2024, **7**, 12.

397 G. Capson-Tojo, R. Moscoviz, S. Astals, Á. Robles and J.-P. Steyer, Unraveling the literature chaos around free ammonia inhibition in anaerobic digestion, *Renewable Sustainable Energy Rev.*, 2020, **117**, 109487.

398 X. Zhang, Z. Guo, X. Li, Q. Liu, H. Hu, F. Li, Q. Huang, L. Zhang, Y. Tang and J. Huang, Cryo-ultramicrotomy enables TEM characterization of global lithium/polymer interfaces, *Energy Environ. Sci.*, 2024, **17**, 1436–1447.

399 J. Tan, J. Matz, P. Dong, J. Shen and M. Ye, A growing appreciation for the role of LiF in the solid electrolyte interphase, *Adv. Energy Mater.*, 2021, **11**, 2100046.

400 A. M. Miksch, T. Morawietz, J. Kästner, A. Urban and N. Artrith, Strategies for the construction of machine-learning potentials for accurate and efficient atomic-scale simulations, *Nucl. Eng. Technol.*, 2021, **2**, 031001.

401 F. Antonello, J. Buongiorno and E. Zio, Physics informed neural networks for surrogate modeling of accidental scenarios in nuclear power plants, *Nuclear Engineering and Technology*, 2023, **55**, 3409–3416.

402 R. Batra, L. Song and R. Ramprasad, Emerging materials intelligence ecosystems propelled by machine learning, *Nat. Rev. Mater.*, 2021, **6**, 655–678.

403 N. Takenaka, A. Bouibes, Y. Yamada, M. Nagaoka and A. Yamada, Frontiers in theoretical analysis of solid electrolyte interphase formation mechanism, *Adv. Mater.*, 2021, **33**, 2100574.

404 X. Zhou, R. Gao, Z. Hu, W. Zhou, Y. Kwok and G. Chen, Unveiling Electron Transport Properties of Lithium Fluoride/Lithium Oxide Interfaces in Solid Electrolyte Interphase on Lithium Metal Anodes, *J. Power Sources*, 2025, 237946.

405 R. Lin, Y. Jin, Y. Li, M. Fu, Y. Gong, L. Lei, Y. Zhang, J. Xu and Y. Xiong, Decoupling Interfacial Stability and Ion Transport in Solid Polymer Electrolyte by Tailored Ligand Chemistry for Lithium Metal Battery, *Adv. Funct. Mater.*, 2025, **35**, 2421880.